



# Assessment of Offshore Wind Energy Opportunities and Challenges in the U.S. Gulf of Mexico

Rebecca Fuchs,<sup>1</sup> Walt Musial,<sup>1</sup> Gabriel R. Zuckerman,<sup>1</sup> Mayank Chetan,<sup>1</sup> Melinda Marquis,<sup>1</sup> Leonardo Rese,<sup>1</sup> Aubryn Cooperman,<sup>1</sup> Patrick Duffy,<sup>1</sup> Rebecca Green,<sup>1</sup> Philipp Beiter,<sup>1</sup> Daniel Mulas Hernando,<sup>1</sup> James A. Morris, Jr.,<sup>2</sup> Alyssa Randall,<sup>3</sup> Jonathan A. Jossart,<sup>3</sup> Lauren Mudd,<sup>4</sup> and Peter Vickery<sup>4</sup>

*1 National Renewable Energy Laboratory*

*2 National Oceanic and Atmospheric Administration*

*3 CSS*

*4 Applied Research Associates, Inc.*

**NREL is a national laboratory of the U.S. Department of Energy  
Office of Energy Efficiency & Renewable Energy  
Operated by the Alliance for Sustainable Energy, LLC**

**Technical Report  
NREL/TP-5000-88195  
December 2023**

This report is available at no cost from the National Renewable Energy Laboratory (NREL) at [www.nrel.gov/publications](http://www.nrel.gov/publications).

Contract No. DE-AC36-08GO28308



# Assessment of Offshore Wind Energy Opportunities and Challenges in the U.S. Gulf of Mexico

Rebecca Fuchs,<sup>1</sup> Walt Musial,<sup>1</sup> Gabriel R. Zuckerman,<sup>1</sup> Mayank Chetan,<sup>1</sup> Melinda Marquis,<sup>1</sup> Leonardo Rese,<sup>1</sup> Aubryn Cooperman,<sup>1</sup> Patrick Duffy,<sup>1</sup> Rebecca Green,<sup>1</sup> Philipp Beiter,<sup>1</sup> Daniel Mulas Hernando,<sup>1</sup> James A. Morris, Jr.,<sup>2</sup> Alyssa Randall,<sup>3</sup> Jonathan A. Jossart,<sup>3</sup> Lauren Mudd,<sup>4</sup> and Peter Vickery<sup>4</sup>

*1 National Renewable Energy Laboratory*

*2 National Oceanic and Atmospheric Administration*

*3 CSS*

*4 Applied Research Associates, Inc.*

## Suggested Citation

Fuchs, Rebecca, Walt Musial, Gabriel R. Zuckerman, Mayank Chetan, Melinda Marquis, Leonardo Rese, Aubryn Cooperman, Patrick Duffy, Rebecca Green, Philipp Beiter, Daniel Mulas Hernando, James A. Morris Jr., Alyssa Randall, Jonathan A. Jossart, Lauren Mudd, and Peter Vickery. 2023. *Assessment of Offshore Wind Energy Opportunities and Challenges in the U.S. Gulf of Mexico*. Golden, CO: National Renewable Energy Laboratory. NREL/TP-5000-88195. <https://www.nrel.gov/docs/fy24osti/88195.pdf>.

**NREL is a national laboratory of the U.S. Department of Energy  
Office of Energy Efficiency & Renewable Energy  
Operated by the Alliance for Sustainable Energy, LLC**

This report is available at no cost from the National Renewable Energy Laboratory (NREL) at [www.nrel.gov/publications](http://www.nrel.gov/publications).

Contract No. DE-AC36-08GO28308

**Technical Report**  
NREL/TP-5000-88195  
December 2023

National Renewable Energy Laboratory  
15013 Denver West Parkway  
Golden, CO 80401  
303-275-3000 • [www.nrel.gov](http://www.nrel.gov)

## NOTICE

This work was authored in part by the National Renewable Energy Laboratory, operated by Alliance for Sustainable Energy, LLC, for the U.S. Department of Energy (DOE) under Contract No. DE-AC36-08GO28308. Funding provided by the U.S. Department of Energy Office of Energy Efficiency and Renewable Energy Wind Energy Technologies Office. The views expressed herein do not necessarily represent the views of the DOE or the U.S. Government.

This report is available at no cost from the National Renewable Energy Laboratory (NREL) at [www.nrel.gov/publications](http://www.nrel.gov/publications).

U.S. Department of Energy (DOE) reports produced after 1991 and a growing number of pre-1991 documents are available free via [www.OSTI.gov](http://www.OSTI.gov).

*Cover Photo from Getty Images 1253690396.*

NREL prints on paper that contains recycled content.

## Acknowledgments

The authors would like to extend thanks to Tershara Matthews, Dr. Jim Kendall, Mike Celata, Idrissa Boube, Lenny Coats and Bridgette Duplantis from the Bureau of Ocean Energy Management Gulf of Mexico for their leadership and support for this research.

The authors would also like to thank the following reviewers and contributors from the National Renewable Energy Laboratory (NREL): Georgios Deskos, Brian Smith, Amy Robertson, and Paul Veers. Thanks also to Daniel O’Connell from BOEM headquarters as well as the Marsh USA, Renewable Energy & Offshore Wind Practice for their input to this report.

In addition, we would like to acknowledge the technical project management support from NREL staff including Setareh Saadat and Betsy Sara, and document editing by Amy Brice.

## List of Acronyms

AEP	annual energy production
API	American Petroleum Institute
BOEM	Bureau of Ocean Energy Management
COV	Coefficient of Variation
DLC	design load case
ERA-5	5 <sup>th</sup> generation European Centre for Medium-Range Weather Forecasts atmospheric reanalysis of the global climate
ERCOT	Electric Reliability Council of Texas
EWM	extreme wind speed model
GCF	gross capacity factor
GW	gigawatt
GWh	gigawatt-hour
IEA	International Energy Agency
IEC	International Electrotechnical Commission
km	kilometer
LCOE	levelized cost of energy
MCDA	multi-criteria decision analysis
MISO	Midcontinent Independent System Operator
mph	miles per hour
m/s	meters per second
MW	megawatt
MWh	megawatt-hour
NCCOS	National Centers for Coastal Ocean Science
nm	nautical mile
NOAA	National Oceanic and Atmospheric Administration
NREL	National Renewable Energy Laboratory
OCS	Outer Continental Shelf
OEM	original equipment manufacturer
POI	point of interconnection
RWE	RWE Offshore US Gulf, LLC
SP	specific power
W/m <sup>2</sup>	watts per square meter
WEIS	Wind Energy with Integrated Servo-control
WRF	Weather Research and Forecasting Model
WEA	wind energy area

## Executive Summary

Offshore wind energy in the Gulf has the potential to be a viable clean energy option to help the region meet the U.S. goals to achieve carbon neutrality by 2050. Many technical challenges are discussed but most can be resolved with engineering solutions that are available to the industry.

**Background:** This study builds on previous work conducted by the National Renewable Energy Laboratory (NREL) (Musial et al. 2020a; Musial et al. 2020b; Musial and Greco 2020). It was commissioned by the Bureau of Ocean Energy Management (BOEM) under an interagency agreement to carry out a regional assessment of offshore wind energy potential in the Gulf of Mexico and provide an updated assessment of wind resource, siting, hurricanes, and infrastructure considerations associated with future offshore wind energy development. It is intended to inform both federal and Gulf state energy planning and to provide information to other stakeholders from industry and the public sector. In cooperation with another ongoing BOEM-funded study, NREL is performing a national assessment of offshore wind energy costs that will include a complete cost assessment for the U.S. Gulf of Mexico. This study is scheduled to be released in April 2024.

**Objectives:** The objectives of this study are to:

- Describe the regional benefits and challenges for offshore wind energy deployment in the Gulf of Mexico
- Provide a description of the process used to determine site suitability for offshore wind farms and define wind energy areas for commercial leasing,
- Document and evaluate the updated offshore wind energy resource database created by NREL for the Gulf of Mexico,
- Discuss state-of-the-art approach for designing wind turbines in hurricane prone regions and the methods used to mitigate the challenges brought on by hurricanes (e.g. insurance).
- Identify challenges and opportunities with the regional supporting infrastructure in the Gulf of Mexico (e.g., points of interconnection, ports) that could be used in offshore wind turbine deployment.
- Describe other technical challenges such as low wind speed turbine designs and jacket foundations needed for softer soil conditions.

**Site Selection and Leasing:** The Gulf is used by multiple stakeholders, industries, and agencies. Therefore, spatial planning that considers the impacts on other ocean users must be conducted so that wind energy areas (WEAs) can minimize interference with other critical ocean uses. BOEM and National Centers for Coastal Ocean Science (NCCOS) collaborated to create an offshore wind energy siting suitability model for the Gulf of Mexico, which was used to identify optimal areas for WEAs (Randall et al., 2022). Some of the stakeholders that contributed to the input database for the spatial suitability modeling include conservation groups, the U.S. Department of Defense, the National Weather Service, and the Southern Shrimp Alliance. This process informed the location and sizes of the three lease areas, as described in Section 2. These leases were put up for competitive auction on Aug. 29, 2023. The auction results showed significantly lower interest from industry than in previous auctions. No bids were submitted for the two lease areas off the coast of Galveston, Texas, but RWE Offshore US Gulf, LLC (RWE) won the Lake

Charles OCS-G 37334 lease (Figure ES-1). The lower interest likely stems from a combination of the lower wind quality of the lease areas in the Gulf, increased hurricane risk, lack of a clear power offtake mechanism, and the uncertainty surrounding the economic headwinds offshore wind is facing due to rising costs from inflation, higher interest rates, and supply chain bottlenecks, which came to a head in the summer of 2023.

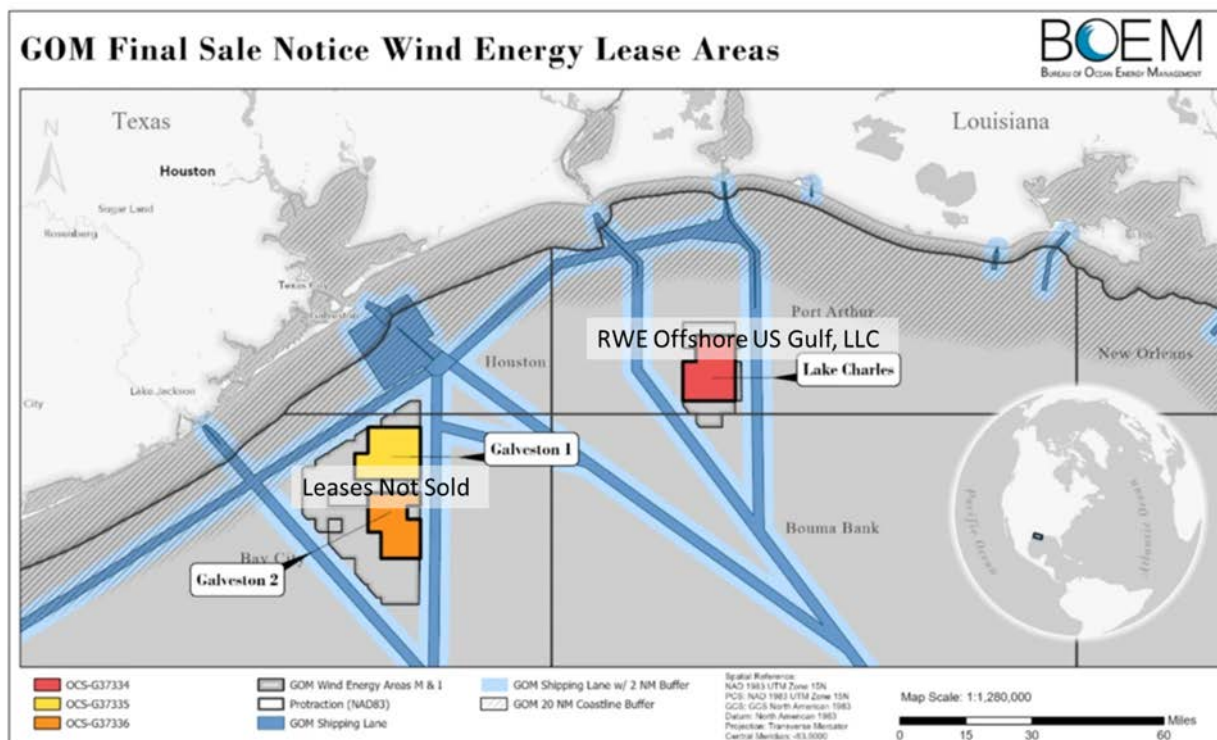


**Figure ES- 1. Three Gulf of Mexico (Gulf) wind energy areas were up for auction on Aug. 29, 2023: Lake Charles (upper left), Galveston I (upper right), and Galveston II (lower center). Only Lake Charles was sold.**  
**Source: BOEM**

**Wind Resource Assessment:** A new wind resource dataset for the Gulf of Mexico that provides wind speeds at a 5-minute resolution over a 21-year period from 2000 to 2020 was developed to replace the previous wind resource dataset that only extended from 2007 to 2013 for an hourly temporal resolution. Within the Gulf of Mexico Call Area, the highest average wind speeds from 2000 to 2020 at 160 meter (m) height were 8.8 meters per second (m/s) found in the western part of the Gulf, near Corpus Christi, Texas, and generally decreased in the eastward direction; the lowest wind speeds were close to 7 m/s on the eastern end of the Gulf of Mexico Call Area, south of New Orleans, Louisiana (Figure ES-2). Unlike most areas of the continental shelf in the United States, wind speed in the Gulf of Mexico does not generally increase with distance from shore. For example, on the western coast of the Gulf, the opposite is true—the highest wind speeds are found near the coast in Texas state waters.

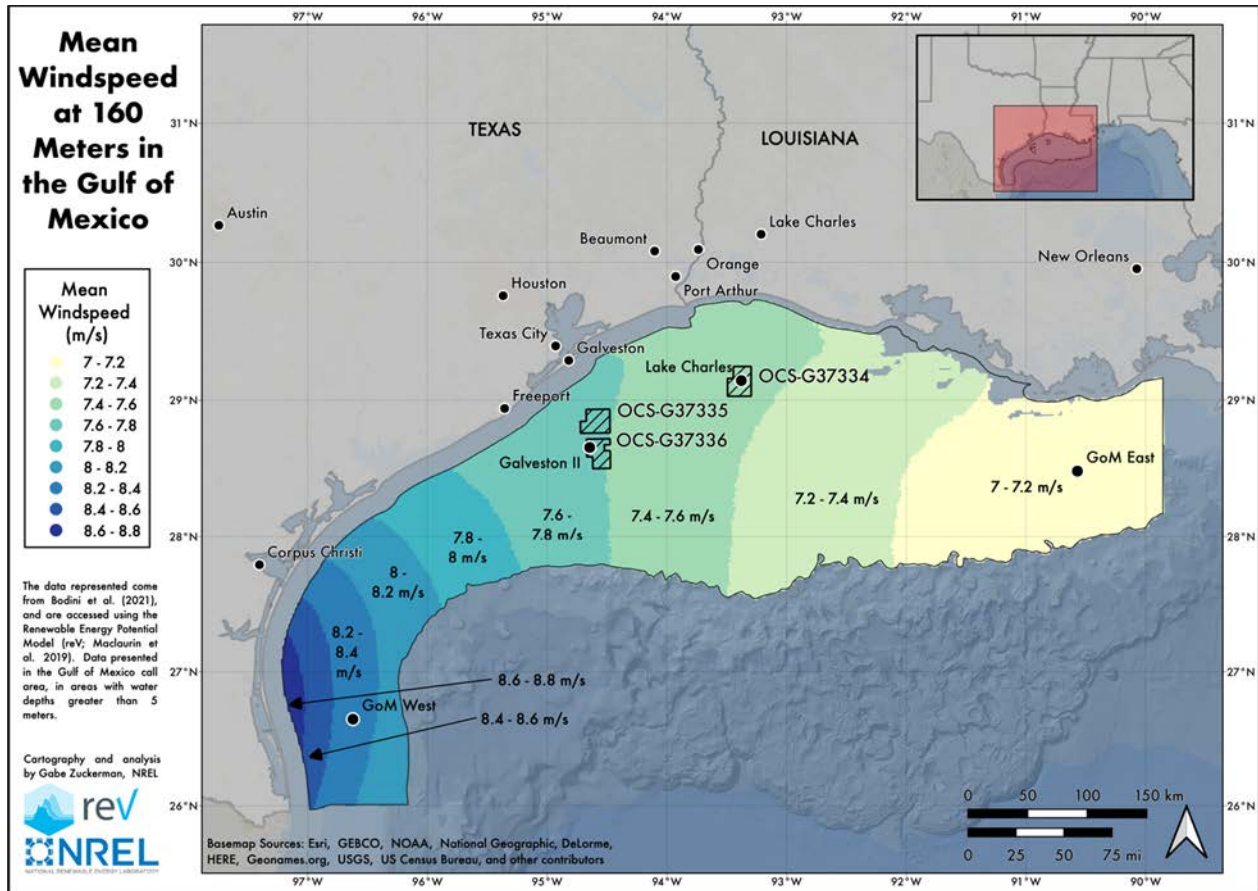


**Figure ES- 2. Mean wind speeds at 160 m elevation over the period 2000-2020. Reference sites (Galveston II, Lake Charles, GoM East, and GoM West) are labeled and analyzed in Figures 9–11.**

*Map by Gabe Zuckerman, NREL*

**Hurricane Design:** The conditions for turbine design in the Gulf of Mexico are challenging because of the competing objectives of maximizing energy capture with low annual average wind speeds and maintaining structural reliability in the presence of major hurricanes (Musial and Greco 2020; Ansari et al. 2021). In this report, the effects of International Electrotechnical Commission (IEC) Class 1 and T-Class winds on the International Energy Agency (IEA) 15-megawatt (MW) reference wind turbine were analyzed for the critical IEC design load cases related to extreme winds on idling offshore wind turbines. The preliminary analysis focused on the tower base loads and tower-top and yaw-bearing loads (Figure ES-3). The study was intended to quantify the benefits of battery back-up systems during loss-of-grid events. It compares the loads experienced by the wind turbine with yaw control - remaining inside the IEC specified  $\pm 15^\circ$  yaw angle region - and the loads when yaw angles were unconstrained over  $\pm 180^\circ$ . Unfortunately, the results did not accurately quantify the loads due to instabilities encountered at high yaw angles and lack of accurate aerodynamic models in existing aeroelastic tools (e.g., OpenFAST). Further analysis and more robust modeling tool development are underway to quantify the magnitude of the loads over  $\pm 180^\circ$  yaw angle to fully assess the benefits of battery back-up for the yaw system. Despite these inconclusive preliminary results, we found that backup power to maintain yaw drive control during grid power loss is a prudent design enhancement in principle because high yaw angles can be avoided where increased extreme loading is expected to occur. In addition, more research is needed to understand the



characteristics of turbulent structures within major hurricanes such as wind shear, veer, high frequency direction changes, and gust factors. Further, corresponding extreme wave conditions need to be coupled with the atmospheric models and incorporated into the design load cases to create more robust wind turbine designs for hurricane prone regions.

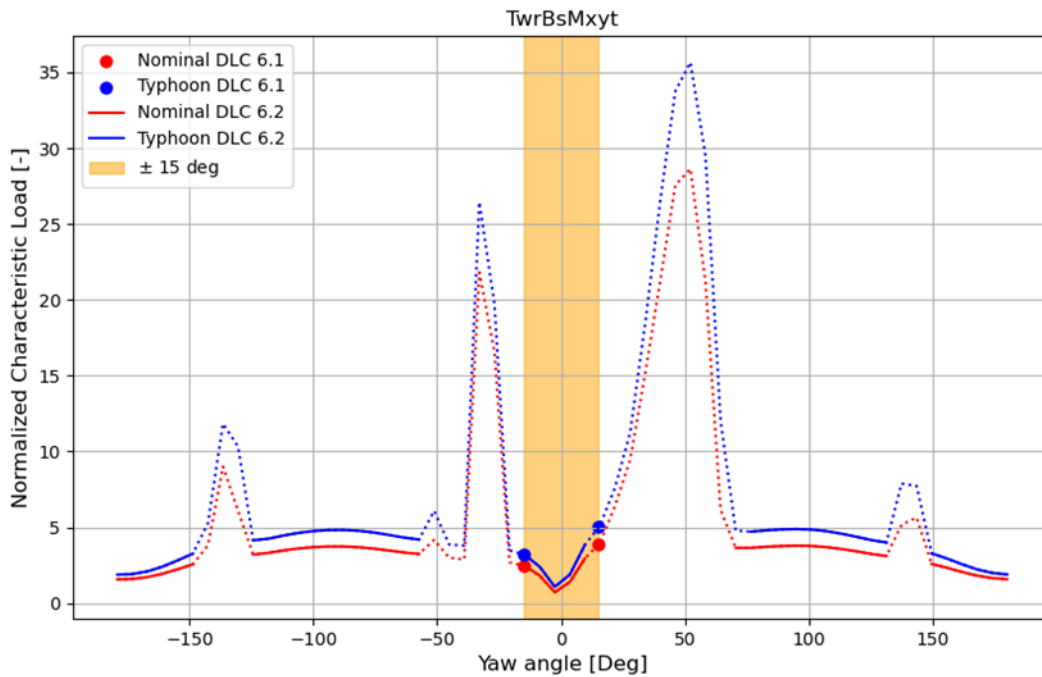


**Figure ES- 3. Tower base combined bending moment shown as a function of yaw angle between the turbine and the incoming wind. The loads are normalized by the load experienced at zero yaw and Class 1 inflow condition. The dotted lines represent areas that are unclear due to model limitations.**

DLC = design load case

**Insurance:** We looked at the question of offshore wind insurance and insurability from the perspective of future projects in the Gulf of Mexico. Insuring for key construction and operational risks is necessary to make offshore wind projects financeable. We found the significance of insurance extends beyond the direct premium costs or “risk transfer.” For a project to obtain debt financing, it would likely also need to reduce the key design risks (which are being actively researched) from hurricanes and obtain insurance before lenders commit funds, but insurance companies have not articulated a comprehensive strategy for design risk mitigation yet. Insurability requires reasonable certainty that the insurance coverage can adequately cover the financial losses from key risks including potential catastrophic damage from major hurricanes and that the turbine systems are sufficiently resilient to withstand the events below a known intensity within the life span of the project. IEC standards require the life

span of a turbine to be at least 20 years and extreme winds to have a 50-year return period<sup>1</sup>. Risk reduction strategies are usually applied in the design stage to mitigate known hazards that may lead to partial or total system failure. Risk reduction may be achieved through the adoption of “best design practices” that make the offshore wind system more resilient to the impacts of major hurricane events. Risk transfer is the more common strategy and involves paying insurance premiums or using collateral to protect against the consequent financial losses from a hurricane event. The increased costs due to risk reduction and risk transfer for wind plants in hurricane-prone regions are not well understood because there is very limited loss data and best practices are still being developed. However, some loss and insurance data are emerging from projects located in the Taiwanese Strait and may be useful in the near term. However, from communication with industry and from NREL cost models, we found that the cost of insurance should not significantly affect the levelized cost of energy; the cost to upgrade a project to make it insurable could be more significant, seen as incremental increases to turbine and substructure costs without making a project unfeasible.

**Infrastructure:** Regional infrastructure for vessels, ports, and electric grid were analyzed. Given the rich history and experience with offshore industrial activities in the Gulf of Mexico, developing offshore wind specific infrastructure could be less of a hurdle compared to other regions, new to offshore construction. Ports in the Gulf of Mexico currently support onshore wind activities and offshore oil and gas activities. We included specific screening criteria for floating and fixed bottom offshore wind energy technologies to identify potential ports in the Gulf of Mexico region. We identified nine ports using the screening criteria that could potentially support offshore wind manufacturing, construction and maintenance activities including the ports of Brownsville, Corpus Christi, Freeport, Houston, Galveston, Port Fourchon, Gulfport, Pascagoula, and Mobile. However, these ports will need further evaluation of their capacity to support offshore wind projects, and possibly certain upgrades or modifications, but the level of upgrade is likely to be less than in other regions where ports were designed for purposes unrelated to offshore energy.

Identifying and developing suitable points of grid interconnection are additional challenges for offshore wind development in the Gulf of Mexico. Electric utility experts were interviewed to understand the feasibility of integrating offshore wind into existing points of interconnection (POIs). We identified 25 plausible POIs and calculated a least-cost path for onshore cable routes. These POIs have one or more transmission lines, one of which is at least 230 kV. The cost of interconnection tends to increase from west to east in our analysis, primarily due to the increasing overland distance to reach the POIs.

**Low-Wind-Speed Turbines:** The relatively lower wind speeds in the Gulf of Mexico (compared to other U.S. regions) result in lower gross capacity factors (GCFs) and less annual energy production (AEP). Four hypothetical turbines were examined (Section 6) to illustrate how the turbine design could improve key performance parameters such as GCF, gross AEP, and wake losses. GCFs were calculated and presented with wake losses from assumed farm layouts over the Gulf of Mexico Call Area. The maximum GCF for the 17-MW low-specific-power (SP) turbine is 55% - 57% on the western end of the Gulf, and generally falls to a range of 37% - 39%

---

<sup>1</sup> A return period is the estimated average time between extreme wind events measured at a given site

on the eastern end. Wake losses were calculated for the same 17-MW low-SP turbine design and ranged from roughly 7% on the western end of the Gulf to 9% on the eastern end of the Gulf. Although there are generally lower wind speeds and greater wake losses on the eastern side of the Gulf, all areas of the Gulf are prone to hurricanes. This technical challenge of low average wind speeds and high extremes does not have a simple engineering solution. However, the analysis showed that the GCF and the AEP increased when the IEA 15-MW reference turbine design was replaced by the 17-MW low-SP turbine.

# Table of Contents

<b>Executive Summary</b> .....	<b>v</b>
<b>1 Introduction</b> .....	<b>1</b>
1.1 Background .....	1
1.2 Project Scope.....	2
<b>2 Wind Energy Area Identification</b> .....	<b>3</b>
2.1 Description of Call Area .....	3
2.2 Suitability of Siting .....	3
<b>3 Wind Resource</b> .....	<b>12</b>
3.1 New Wind Resource Dataset for Gulf of Mexico .....	12
3.2 Overview of Wind Resource in the Gulf of Mexico .....	12
3.3 Vertical Wind Shear .....	13
3.4 Wind Direction.....	14
3.5 Wind Speed Distributions .....	15
3.6 Diurnal Profiles .....	16
<b>4 Hurricane-Specific Challenges</b> .....	<b>18</b>
4.1 State of the Art for Hurricane Design .....	18
4.1.1 Wind Turbine Operating and Survival Conditions.....	18
4.1.2 Design Standards for Offshore Wind Design.....	19
4.1.3 Hurricane Design Standards Provisions .....	21
4.1.4 Assessment of Hurricane Risk and Return Periods.....	22
4.1.5 Offshore Wind Experience in Hurricane-Prone Regions .....	26
4.1.6 Battery Backup Systems for Maintaining Yaw Control.....	26
4.1.7 Insurance for Turbines in Hurricane-Prone Areas .....	35
4.2 Long-Term Hurricane Research Needs .....	39
<b>5 Infrastructure</b> .....	<b>41</b>
5.1 Ports .....	41
5.2 Challenges for Offshore Wind Electric Power Delivery .....	44
5.2.1 Gulf of Mexico Energy Use Profiles .....	44
5.2.2 Points of Interconnect Assessment.....	45
5.2.3 Summary of Findings .....	51
5.2.4 Challenges for Offshore Wind Integration in the Gulf of Mexico .....	51
5.2.5 Limitations to the Findings .....	51
5.2.6 Recommended Next Steps .....	52
<b>6 Other Technology Challenges</b> .....	<b>53</b>
6.1 Low Wind Speeds in Hurricane-Prone Areas .....	53
6.2 Description of Turbine Designs and Associated Power Curves.....	56
6.3 Gross Capacity Factors and Production Profiles .....	59
6.4 Wake Losses.....	60
<b>7 Conclusions</b> .....	<b>64</b>
<b>References</b> .....	<b>67</b>

# List of Figures

Figure ES-1. Three Gulf of Mexico (Gulf) wind energy areas were up for auction on Aug. 29, 2023: Lake Charles (upper left), Galveston I (upper right), and Galveston II (lower center). Only Lake Charles was sold Source: BOEM..... vi

Figure ES-2. Mean wind speeds at 160 m elevation over the period 2000-2020. Reference sites (Galveston II, Lake Charles, GoM East, and GoM West) are labeled and analyzed in Figures 9–11..... vii

Figure ES-3. Tower base combined bending moment shown as a function of yaw angle between the turbine and the incoming wind. The loads are normalized by the load experienced at zero yaw and Class 1 inflow condition. The dotted lines represent areas that are unclear due to model limitations..... viii

Figure 1. Gulf of Mexico Call Area..... 3

Figure 2. Overview of suitability model design and submodel components ..... 5

Figure 3. Suitability modeling results for the Gulf of Mexico Call Area. Green areas show highest relative suitability, while red indicates conflict with ocean activity. .... 6

Figure 4. Wind energy area steps for option identification. 1) High-high clusters overlaid on aliquots. 2) Aliquots with  $\geq 50\%$  area in high-high clusters. 3) Selected lease blocks had  $\geq 50\%$  of selected aliquots. 4) Groups of contiguous lease blocks containing at least seven lease blocks ( $\geq 39,000$  acres)..... 7

Figure 5. Fourteen wind energy areas (WEAs), Options A through N..... 8

Figure 6. Gulf of Mexico Wind Energy Areas..... 9

Figure 7. Three Gulf of Mexico wind energy areas were up for auction on Aug. 29, 2023: Lake Charles (upper left), Galveston I (upper right), and Galveston II (lower center). Only Lake Charles was sold..... 10

Figure 8. Map of mean wind speeds at 160-m elevation over the period 2000–2020 with labeled reference points (black circles): (from east to west) Gulf of Mexico (GoM) East, Lake Charles, Galveston II, and GoM West. BOEM lease areas are also identified. .... 13

Figure 9. Vertical wind shear at the four representative points depicted in Figure 8 over the period 2000–2020..... 14

Figure 10. Wind roses at 160 m at four reference locations shown in Figure 8, clockwise from top left: Gulf of Mexico (GoM) West, Galveston II, Lake Charles, and GoM East..... 15

Figure 11. Hourly wind speed distributions at 160 m at four reference locations shown in Figure 8, clockwise from top left: Gulf of Mexico (GoM) West, Galveston II, Lake Charles, and GoM East..... 16

Figure 12. Diurnal profiles by season at 160 m at four reference locations shown in Figure 8, clockwise from top left: Gulf of Mexico (GoM) West, Galveston II, Lake Charles, and GoM East ..... 17

Figure 13. Wind turbine power curve with extended region of idling out to extreme winds ..... 18

Figure 14. Design standards for turbine and substructure..... 19

Figure 15. Conceptual hazard curves based on 50 and 500-year return periods adapted from API RP-2A. .... 22

Figure 16. Example of modeled hurricane tracks. .... 23

Figure 17. Return period (years) associated with the IEC Class 1A limit-state reference wind speed of 111.9 mph (50 m/s) obtained from a 500,000-year hurricane simulation. .... 24

Figure 18. Return period (years) associated with the IEC T-Class limit-state reference wind speed of 127.5 mph (57 m/s) obtained from a 500,000-year hurricane simulation..... 24

Figure 19. 10-minute sustained wind speed (mph) at 150 m with a return period of 50 years obtained from a 500,000-year hurricane simulation. Note: no isocline for the Class 1A limit state appears since all simulated values of the 50-year wind speed are greater than the Class 1A reference wind speed (111.9 mph, 50 m/s). .... 25

Figure 20. Tower-base combined bending moment shown as a function of yaw angle between the turbine and the incoming wind. The loads are normalized by the load experienced at zero yaw and Class 1 inflow condition. The dotted lines represent areas with higher uncertainty.....	30
Figure 21. Tower-top combined bending moment shown as a function of yaw angle between the turbine and the incoming wind. The loads are normalized by the load experienced at zero yaw and Class I inflow condition. The dotted lines represent areas with higher uncertainty.....	31
Figure 22. Tower-base/yaw-bearing torsion shown as a function of yaw angle between the turbine and the incoming wind. The loads are normalized by the load experienced at zero yaw and IEC Class IB inflow condition. The dotted lines represent areas with higher uncertainty. ....	32
Figure 23. Blade root combined moments shown as a function of yaw angle between the turbine and the incoming wind. The loads are normalized by the load experienced at zero yaw and IEC Class 1B inflow condition. The dotted lines represent areas with higher uncertainty.....	33
Figure 24. Potential staging and integration ports in the Gulf of Mexico.....	43
Figure 25. Energy consumption by end-use sector for 2020. ....	45
Figure 26. Workflow to identify plausible POIs.....	48
Figure 27. Locations and approximate costs and routes for interconnecting to the 25 most plausible POIs in the Gulf of Mexico.....	50
Figure 28. Land-based wind turbine trend toward lower specific power.....	54
Figure 29. Wind turbine rotor diameter vs. rated power for current and announced wind turbine original equipment manufacturer (OEM) offerings.....	55
Figure 30. (a) Wind distribution and power output, (b) wind distribution and gross AEP as a function of wind speed, (c) gross capacity factor, and (d) gross AEP summed over all wind speeds.....	58
Figure 31. Gross capacity factor for the IEA 15-MW turbine across the Gulf of Mexico Call Area. ....	59
Figure 32. Gross capacity factor for the 17-MW low-SP turbine across the Gulf of Mexico Call Area. ...	60
Figure 33. Modeled wake losses for 1-GW wind plants with IEA 15-MW turbines arranged on a square grid, spaced 7 rotor diameters apart. ....	62
Figure 34. Modeled wake losses for 1-GW wind plants with 17-MW low-SP turbines arranged on a square grid, spaced 7 rotor diameters apart.....	63

## List of Tables

Table 1. Gulf of Mexico Proposed Lease Area Generating Capacity Based on 4 MW/km <sup>2</sup> Capacity Density .....	10
Table 2. IEA 15-MW Reference Wind Turbine Parameters.....	28
Table 3. Summary of Parameters for IEC Design Load Cases 6.1 and 6.2 .....	29
Table 4. Strategies To Address Hurricane Risk.....	36
Table 5. Difference in Indicative Insurance Premiums for Offshore Wind Between Regions.....	38
Table 6. Port Types for Offshore Wind Energy.....	42
Table 7. Screening Criteria for Staging and Integration Ports.....	43
Table 8. List of the 25 Most Plausible Points of Interconnect in the Gulf of Mexico Call Area.....	49
Table 9. Comparison of Select Announced Turbines and Specific Power Ratings .....	55
Table 10. Key Turbine Parameters and Performance Metrics .....	56

# 1 Introduction

## 1.1 Background

The offshore energy industry was created in the Gulf of Mexico (Gulf) by the offshore oil and gas industry which has been active there for over 80 years, with the first offshore rig being built in 1947 (American Oil & Gas Historical Society n.d.). Given this long history in the Gulf with offshore oil and gas, this region is particularly well suited in terms of its existing coastal infrastructure and skilled labor workforce to engage with offshore wind when compared to most other U.S. regions.

As a result, there is high motivation to consider offshore wind energy in the Gulf as a major contributor to the region's future energy supply, particularly as the country transitions to a net carbon neutral energy supply by 2050. Locally, offshore wind offers the prospect of high paying jobs that utilize existing industrial infrastructure and work force in the Gulf with minimal cross-training, while providing similar benefits in energy security through locally sourced electricity that the region has grown accustomed to.

The Gulf's potential to support offshore wind energy has prompted interest from federal and state agencies as well as industry participants. An intergovernmental task force was established for the region in June 2021 to coordinate federal, state, local, and tribal governments. The Bureau of Ocean Energy Management (BOEM) initially designated a Call Area in the Gulf of Mexico in November 2021 (BOEM 2021). Within the Gulf Call Area, BOEM subsequently designated two wind energy areas (WEAs) off the coast of Galveston, Texas and Lake Charles, Louisiana (BOEM 2022). In February 2023, BOEM announced the proposed sale of three offshore wind lease areas: two off the Galveston coast and one south of Lake Charles (BOEM 2023a). On Aug. 29, 2023, BOEM held a competitive auction for the three lease areas, which resulted in the sale of the Lake Charles, Louisiana wind energy lease area.

Despite the extensive offshore oil and gas experience, several key challenges exist in the development of an offshore wind energy industry in the Gulf. These challenges include, but are not limited to, hurricanes, low wind speeds, availability of suitable points of interconnection, soft soils, and ocean-use conflicts (Musial et al. 2020). In 2017, the National Renewable Energy Laboratory (NREL) was commissioned by BOEM under an Interagency Agreement to carry out a regional assessment of ocean-based renewable energy in the Gulf and conducted a follow-on study to assess the offshore wind energy potential, technical feasibility, and economic feasibility in the region (Musial et al. 2020a; Musial et al. 2020b; Musial and Greco 2020).

The current report builds on this previous work and provides an updated assessment of several of the technical challenges including lower wind resource, siting, hurricanes, and infrastructure considerations associated with future offshore wind energy development in the Gulf of Mexico. It is intended to inform both federal and Gulf state energy planning, and to provide information to other stakeholders from industry and the public sector. In cooperation with another on-going BOEM-funded study, NREL is performing a national assessment of offshore wind energy costs that will include a complete offshore wind energy cost assessment for the U.S. Gulf of Mexico. This study is scheduled to be released in April 2024.

## 1.2 Project Scope

This report investigates various topics that influence the feasibility and cost of offshore wind energy in the Gulf of Mexico. Each topic covered can be used as a background to inform the inputs of spatial techno-economic cost modeling that will be used to generate the cost analysis for offshore wind in the Gulf of Mexico. The topics include wind energy area identification and site suitability (Section 2), wind resource data (Section 3), hurricane-specific challenges (Section 4), port and grid infrastructure (Section 5), and other technology challenges (Section 6). The content of this report serves as a precursor for a full spatial techno-economic cost analysis for wind energy in the Gulf of Mexico and informs many of the unique regionally specific inputs that will be used in that forthcoming report. It is also part of a companion study by Mudd and Vickery that investigates the hurricane hazards and risks in the Gulf of Mexico Call Area (Mudd et al. 2023).



## 2 Wind Energy Area Identification

### 2.1 Description of Call Area

The geographical scope of this study is the Gulf of Mexico Outer Continental Shelf (OCS) BOEM Call Area outlined in red in Figure 1. The Call Area covers approximately 30 million acres of the OCS extending from the Mexican border with southern Texas to eastern Louisiana's border with Mississippi. The southern edge of the Call Area follows the United States-Mexico maritime boundary out to its intersection with the 400-meter (m) bathymetry contour and follows this contour to the projection just west of the Mississippi River. The 60-m isobath contour is also highlighted in purple and is shown to indicate the approximate depth where fixed-bottom wind turbines are expected to transition to floating wind technology. Floating wind turbines, which are in an earlier stage of development would be the dominant substructure technology deployed between 60 m and 400 m in the Call Area and for the follow-on cost analysis. The Gulf of Mexico waters extend much deeper than 400 m, but these deeper waters are outside the Call Area and therefore outside the scope of this study.

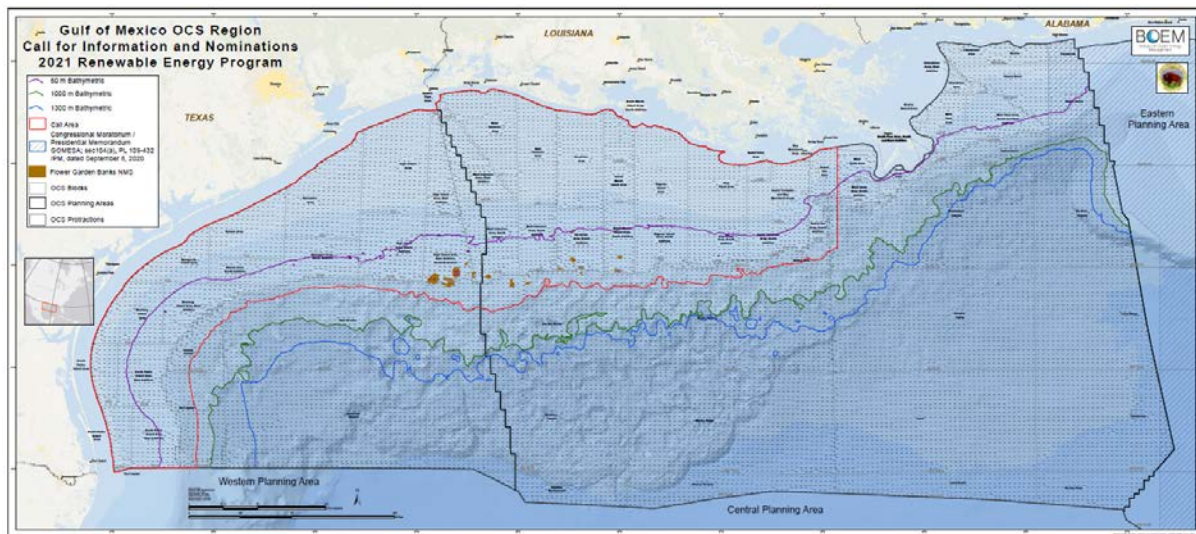


**Figure 1. Gulf of Mexico Call Area**

*Source: BOEM*

Since this study began in early 2022, BOEM engaged in a process to identify wind energy areas from within the Call Area in Figure 1. Although this study considers the entire Call Area, we tried to incorporate new information into the study parameters as it became available from the BOEM site selection process, with a particular focus on the proposed lease areas that resulted from the suitability analysis.

### 2.2 Suitability of Siting

Like other regions, ocean use conflicts are abundant in the Gulf and will need to be addressed through mitigation and avoidance strategies but methods to evaluate siting conflicts have traditionally been manual (Randall et al., 2023). To improve the site selection process, BOEM commissioned the National Oceanographic and Atmospheric Administration's (NOAA's) National Centers for Coastal Ocean Science (NCCOS) to conduct independent spatial suitability

modeling to help identify and avoid ocean use conflicts using their geospatial suitability model, which receives inputs from a wide array of stakeholders and aims to derive an index for where offshore wind farms might fit best. Relevant stakeholders include those involved with national security, fisheries, logistics, industry, and natural and cultural resources. As such, the process by which the original Call Area from 2021 was reduced to the final three lease areas is described herein.

The collaboration between BOEM and the National Centers for Coastal Ocean Science created an offshore wind energy siting suitability model for the Gulf to identify optimal locations for WEAs. A spatial modeling workflow was adapted from Morris et. al (2021) and Riley et. al (2021). Multi-criteria decision analyses are commonly used to site renewable energy projects such as offshore wind farms (Abdel-Basset et al. 2021; Mahdy and Bahaj 2018; Rodriguez-Rodriguez et al. 2016). Multi-criteria decision analyses consider relevant spatial data layers to provide guidance and information for siting, with the ultimate goal providing a model that best represents the most suitable locations for a given project.

For the Gulf WEA siting analysis, a data inventory of all relevant spatial planning data was collected from numerous stakeholders, industries, and agencies. For example, the U.S. Department of Defense, National Weather Service, Southern Shrimp Alliance, and numerous conservation groups all provided comments, and in some cases, data for the spatial planning process. Early conversations with different ocean users allow for conflicts to be represented in the modeling process.

A gridded relative suitability analysis, a type of multi-criteria decision analysis, was used to identify areas suitable for offshore wind energy using a 10-acre hexagonal grid. Relevant data sets from the data inventory were categorized into six different submodels representing various ocean user groups which all received equal weight. These submodels are illustrated in Figure 2.

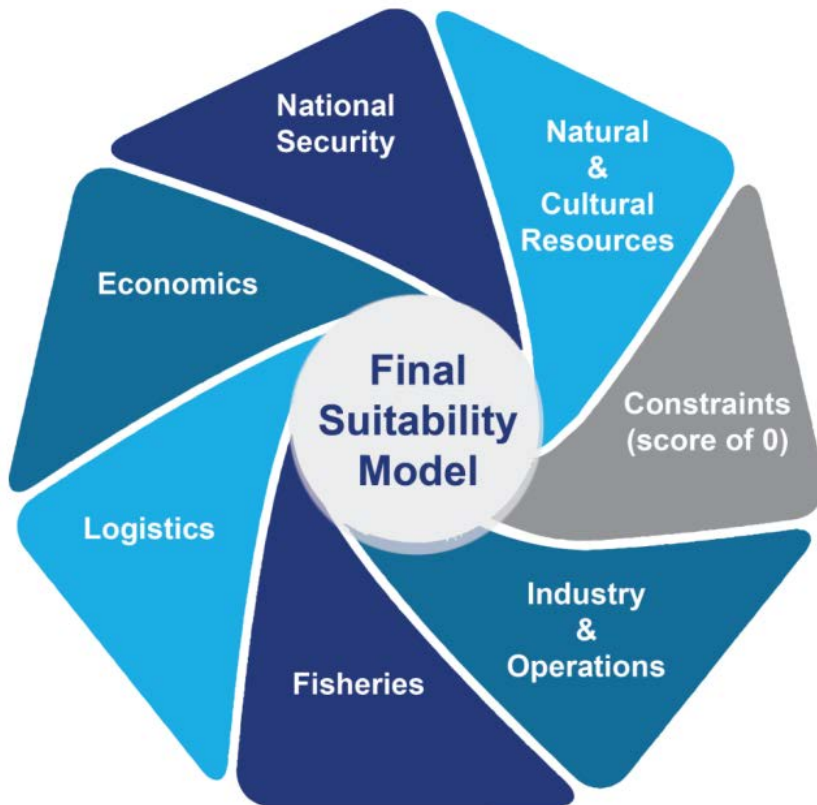


**Figure 2. Overview of suitability model design and submodel components**

Equal weights were used to prevent any one group from dominating the model. Each data set was translated to a grid and assigned a score ranging from 0 to 1, with 0 being unsuitable for offshore wind energy, and 1 being suitable for offshore wind energy. Scores were based on expert opinion or through use of a function (e.g., linear, fuzzy logic membership functions) that best represents a dataset’s relation with wind energy. A combined suitability score for each submodel was then calculated by taking the geometric mean of all datasets within each submodel. A constraints submodel containing all data layers that were completely incompatible (i.e., shipping fairways, existing infrastructure, etc.) was also used, and any grid cell that contained a constraint was considered unsuitable and was therefore not considered in additional analyses. A combined final suitability score was calculated using the geometric mean of the combined scores for each of the six submodels, after removing all grid cells containing constraints (Figure 3). The map shows a gradient from green to red where the green areas have the highest relative suitability, and the red areas indicate constraints that conflict with other ocean activity that would be difficult to avoid.

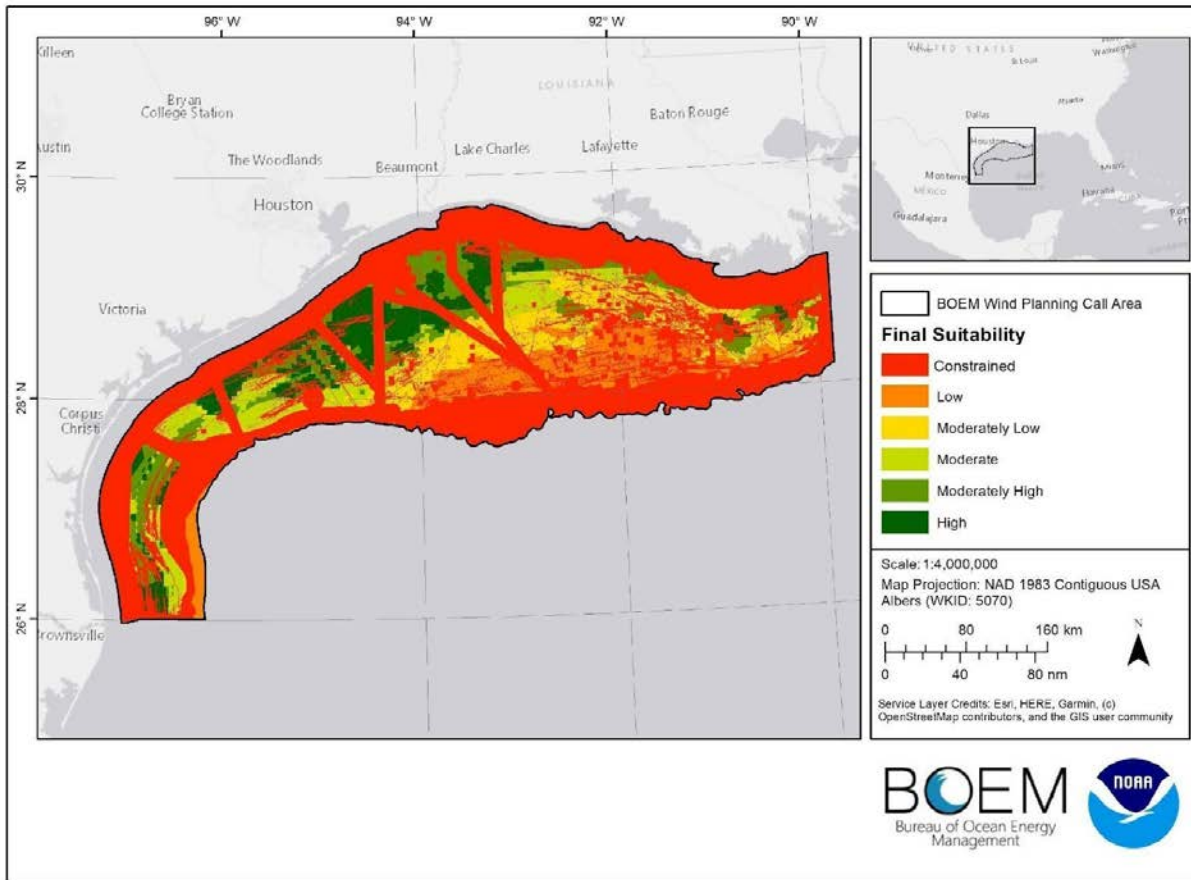


**Figure 3. Suitability modeling results for the Gulf of Mexico Call Area. Green areas show highest relative suitability, while red indicates conflict with ocean activity.**

The most suitable areas were then identified using a local indicator of spatial association analysis, which used the ArcPro Cluster and Outlier Analysis Tool (ArcGIS n.d.). In other words, statistically significant clusters of highly suitable grid cells were identified. BOEM lease blocks and aliquots were then selected based on how much overlap occurred and the highly suitable clusters of grid cells. High-high clusters are statistically significant ( $p < 0.05$ ) highest suitability score areas. WEAs were created from the selected lease blocks based on criteria for inclusion, such as having contiguous cells and at least three neighbors (Figure 4).

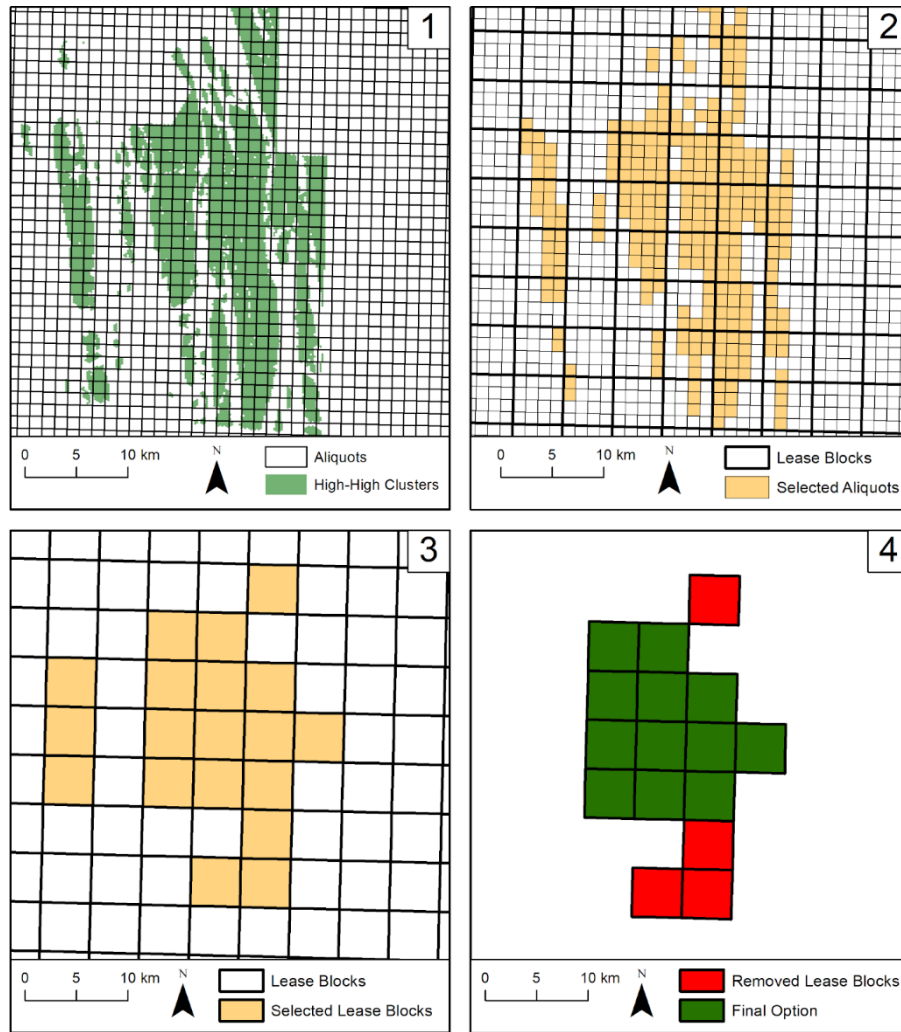


**Figure 4. Wind energy area steps for option identification. 1) High-high clusters overlaid on aliquots. 2) Aliquots with  $\geq 50\%$  area in high-high clusters. 3) Selected lease blocks had  $\geq 50\%$  of selected aliquots. 4) Groups of contiguous lease blocks containing at least seven lease blocks ( $\geq 39,000$  acres).**

The analysis resulted in 14 WEAs being identified (Figure 4). First, high-high clusters were overlaid on aliquots (Figure 4-1); then, those aliquots that had an area greater than or equal to 50% of high-high clusters were selected (Figure 4-2). Next, lease blocks were selected by choosing blocks that had at least 50% of the area containing the selected aliquots (Figure 4-3). Finally, groups of contiguous lease blocks containing at least 7 lease blocks were chosen<sup>2</sup>. Lease blocks were not removed by this logic if removal of the block would reduce a suitable area below 7 lease blocks or roughly 39,000 acres (Figure 4-4). In Figure 5, lease blocks within each

<sup>2</sup> A lease block is a square unit of area defined by BOEM on the outer continental shelf that has a dimension of 4.8 km by 4.8 km with a total area of 23.04 km<sup>2</sup>. Based on average capacity density assumptions of 4 MW/km<sup>2</sup> used by NREL, 7 lease blocks would be able to hold an installed capacity of about 645 MW, or about the size of a small commercial-scale project based on current industry averages. The current proposed lease areas are 17-18 lease blocks in size.

WEA are indicated in yellow and the blue areas (high-high clusters) indicate cells that have the highest suitability determined by the local indicators of spatial association analysis. Next, evaluation and comparison of each WEA option were performed, and further review of areas within each option resulted in the final WEA selections (Figure 6). For more detail, see the full WEA siting analysis report (Randall et al. 2022).

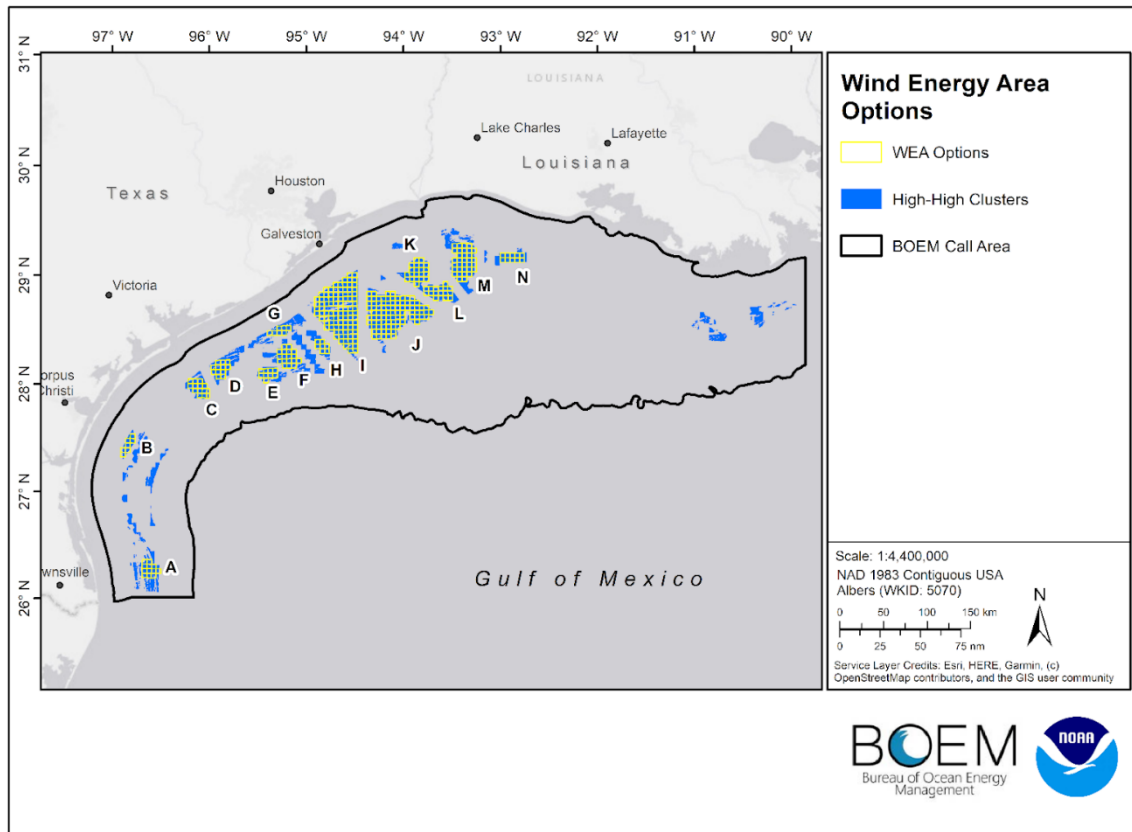


**Figure 5. Fourteen wind energy areas (WEAs), Options A through N.**

*Source: BOEM*

Figure 6 shows the two WEAs: the western Option I in yellow and the eastern Option M in orange. WEA Option I covers 508,265 acres and is approximately 40 nautical miles (nm) from Galveston, Texas. WEA Option M covers 174,275 acres and is approximately 52 nm from Port Arthur, Texas, and 58 nm from Lake Charles, Louisiana. The blue and light blue areas in Figure 6 indicate the primary shipping lanes and a 2-nm buffer to either side, respectively.

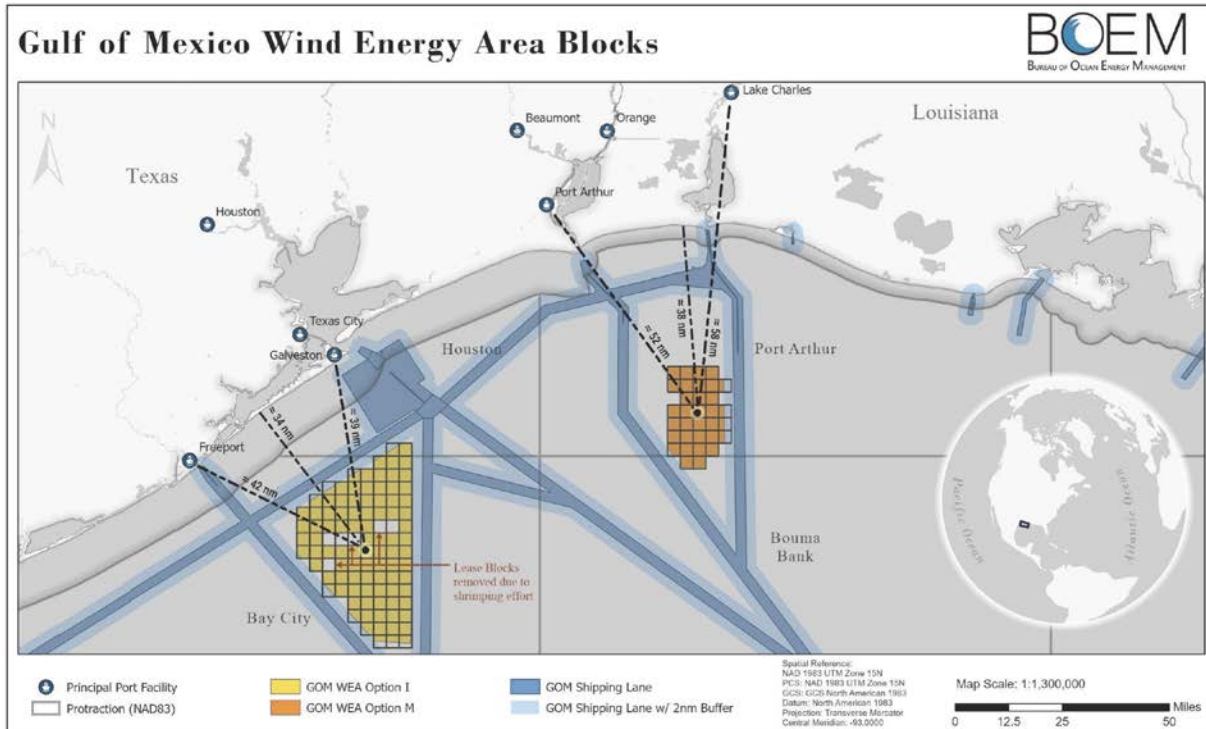


**Figure 6. Gulf of Mexico wind energy areas.**

Source BOEM

Figure 7 shows the location of the three lease areas that went up for auction on Aug. 29, 2023. The amount of offshore wind energy that could potentially be generated from these three sites depends on the specific wind turbine models that are selected and the layout of wind turbines within the lease areas. Table 1 provides a range of estimates for the generating potential of each lease area based on typical capacity densities for offshore wind power plants (Musial et al. 2023; Lopez et al. 2022). The total generating capacity across all three lease areas is about 4.9 gigawatts (GW) based on a nominal 4 MW/km<sup>2</sup> capacity density. This is a conservative average of the projects that are currently under development in the north and mid-Atlantic and is the general default value used by NREL in calculating undeveloped ocean space. Many factors influence the power density (nameplate capacity) of a WEA, but observed capacity densities in European offshore wind plants range between 3 and 19 MW/km<sup>2</sup> (Borrmann et al. 2018).

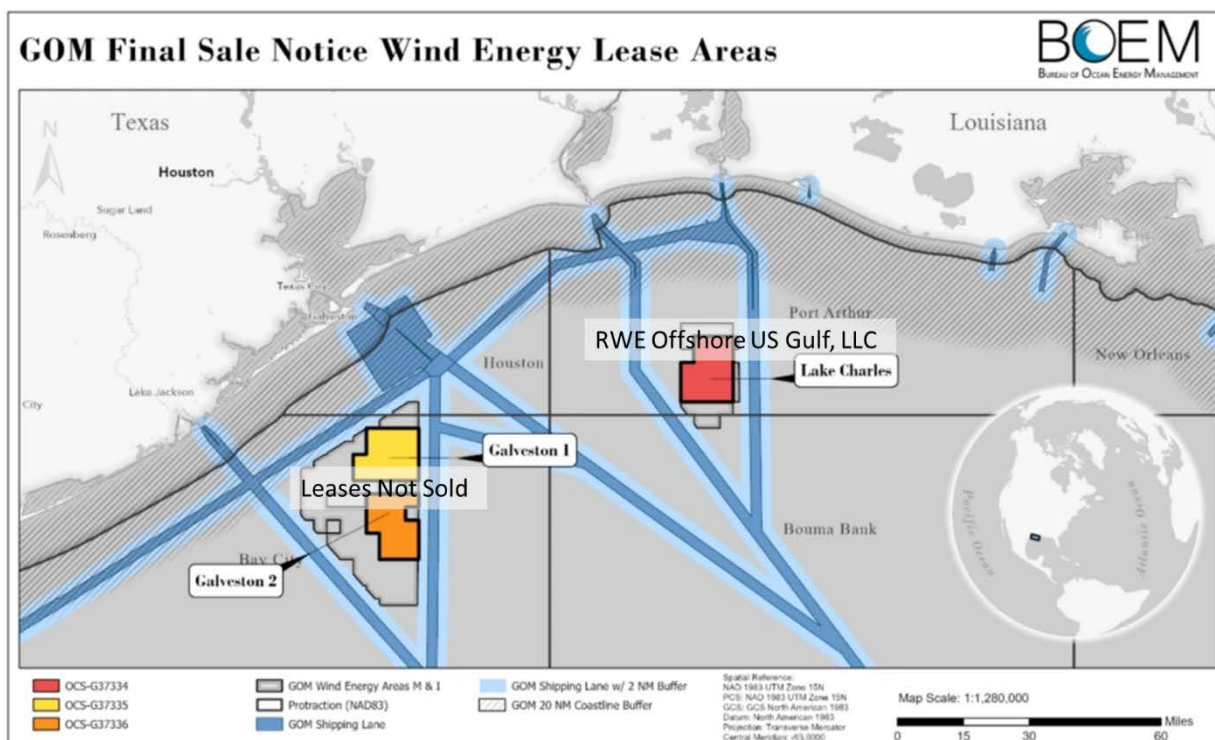


**Figure 7. Three Gulf of Mexico wind energy areas were up for auction on Aug. 29, 2023: Lake Charles (upper left), Galveston I (upper right), and Galveston II (lower center). Only Lake Charles was sold.**

Source: BOEM

**Table 1. Gulf of Mexico Proposed Lease Area Generating Capacity Based on 4 MW/km<sup>2</sup> Capacity Density**

Lease Area ID	Lease Area Size		Generating Potential 4 MW/km <sup>2</sup>
	Acres	km <sup>2</sup>	
Lake Charles OCS-G 37334	102,480	415	1,660
Galveston I OCS-G 37335	102,480	415	1,660
Galveston II OCS-G 37336	96,786	392	1,567
<b>Totals</b>	<b>301,746</b>	<b>1,222</b>	<b>4,887</b>

The Aug. 29, 2023 auction results generated a lower amount of industry interest than previous auctions held in the New York Bight, Carolina Long Bay, and California. There were originally 15 qualified bidders but only two participated, and the auction closed after two rounds. No bids were submitted for the two lease areas off the coast of Galveston, Texas but RWE Offshore US Gulf, LLC (RWE) won lease Lake Charles OCS-G 37334 for a price of \$5.6 million. The lower interest in the Gulf lease areas likely stems from a combination of the lower wind quality of the leases area, increased hurricane risk, lack of a clear power offtake mechanism, and the



uncertainty surrounding economic headwinds from rising costs due to inflation, higher interest rates, and supply chain bottlenecks which came to a head in the summer of 2023. The Lake Charles, Louisiana lease may have been more attractive because Louisiana has a (non-binding) offshore wind target of 5 GW by 2035. Louisiana has also begun talking with developers about possible offshore wind projects in state waters. Texas has made no commitment to offshore wind as of late 2023.

A multiple-factor auction format was used for the Gulf auction, like the California and Carolina Long Bay auctions which earned RWE bidding credits to support workforce training, the development of a local offshore wind supply chain, and a fund to mitigate potential damages to fisheries in the Gulf. The lease agreement will require RWE to engage with potentially affected groups including tribes, ocean users, and local communities (Frank et al. 2023).

## 3 Wind Resource

### 3.1 New Wind Resource Dataset for Gulf of Mexico

The wind resource data used to establish the available potential energy for offshore wind in the Gulf of Mexico are the 2023 National Offshore Wind Dataset, or NOW-23 (Bodini et al. 2021), that were produced using the Weather Research and Forecasting Model (WRF) version 4.2.1 (Skamarock et al. 2021) and validated against observations. NOW-23 is an update to the Wind Integration National Dataset (WIND) Toolkit (Maclaurin et al. 2014; Draxl et al. 2015), which contains wind profile data from 2007 to 2013 on a 2×2-km grid. The WIND Toolkit data showed slightly higher wind speeds (by roughly less than 0.2 m/s) in the Gulf region than the updated dataset used in this study. To generate the updated NOW-23 wind dataset, the European Centre for Medium Range Weather Forecasts 5 Reanalysis (ERA-5) data (Hersbach et al. 2020) were used to initialize the WRF model at a 6-hour refresh rate. The initial horizontal grid spacing was 6 km, with a finer nested internal domain of 2 km. The model was run with 61 vertical levels, 12 of which are in the lower 300 m of the atmosphere, stretching from 5 to 45 m in height in the layer where wind turbines operate. The Yonsei University planetary boundary layer and MM5 surface layer schemes were used in the WRF model runs. The model was run for the years 2000 through 2020. Available outputs are in 5-minute resolution.

### 3.2 Overview of Wind Resource in the Gulf of Mexico

Figure 8 shows the average modeled wind speeds in the Gulf of Mexico at a height of 160 m over the period 2000–2020. Four dark circles mark reference locations where we have investigated the wind resource in greater detail to illustrate how the resource varies across the Gulf of Mexico region. Two of these reference sites are in the Galveston II and Lake Charles lease areas designated by BOEM, and the other two are near the eastern and western ends of the original Call Area. The highest average wind speeds are approximately 8.8 m/s in the west near Corpus Christi, Texas. The lowest wind speeds in the Call Area are roughly 7 m/s and are found south of New Orleans. The 21-year mean wind speeds at 160 m for the representative points in the Galveston II and Lake Charles lease areas are approximately 7.6 m/s and 7.5 m/s, respectively.

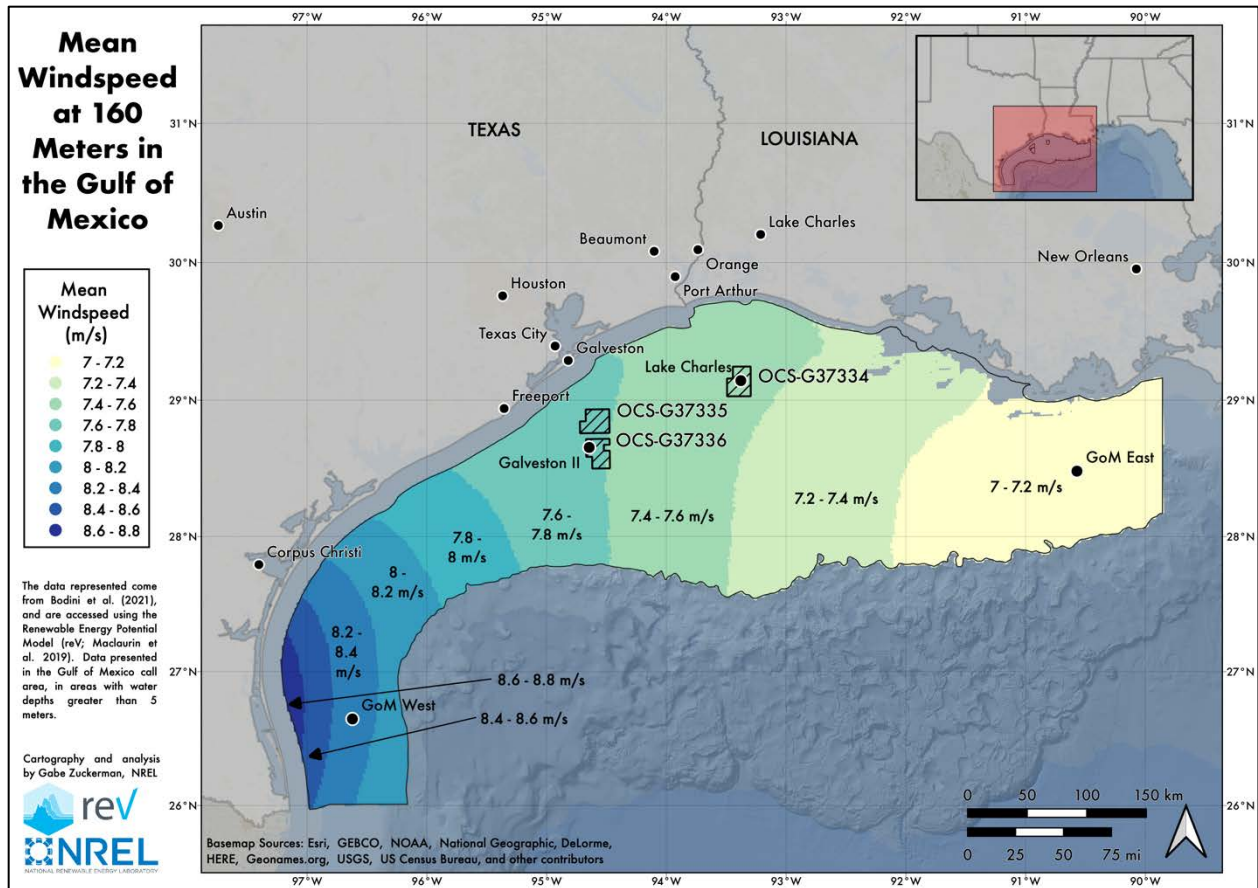


**Figure 8. Map of mean wind speeds at 160-m elevation over the period 2000–2020 with labeled reference points (black circles): (from east to west) Gulf of Mexico (GoM) East, Lake Charles, Galveston II, and GoM West. BOEM lease areas are also identified.**

*Map by Gabe Zuckerman, NREL*

### 3.3 Vertical Wind Shear

Vertical wind shear describes the change in wind speed with height, and vertical wind profiles depend mainly on local atmospheric conditions. Vertical wind shear (increasing wind speed with increasing hub height) tends to have greater benefit for the energy production of land-based wind turbines than for offshore wind turbines. Mean vertical wind shear profiles over the period 2000–2020 are presented in Figure 9 for the four reference locations identified in Figure 8. The trend of increasing mean wind speed from east to west is consistent across all the vertical levels in the profiles. The stronger wind shear in the west means that the wind speed gradient from east to west gets even larger at higher elevations.

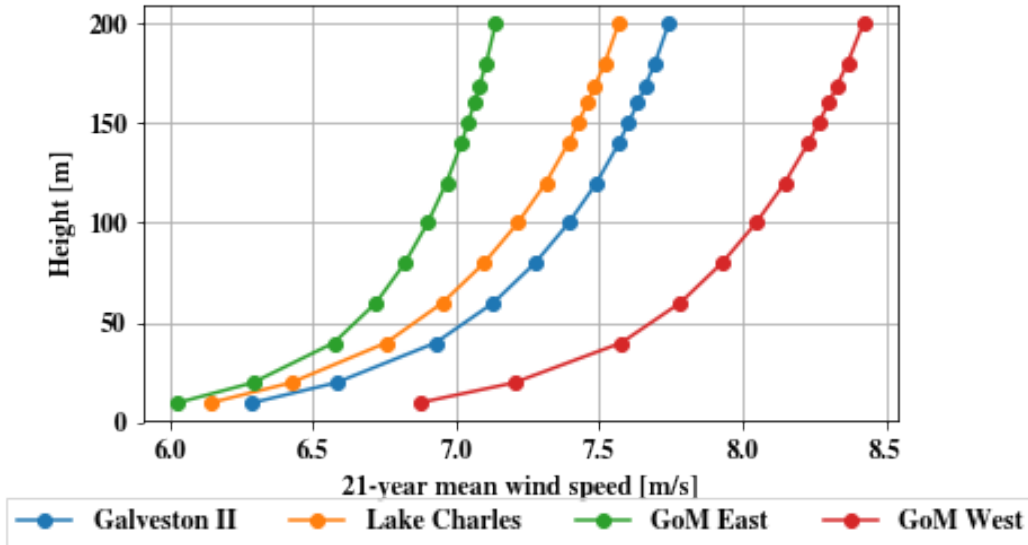


Figure 9. Vertical wind shear at the four representative points depicted in Figure 8 over the period 2000–2020.

### 3.4 Wind Direction

Understanding trends in wind speed and wind direction helps with wind turbine layout optimization to minimize wake losses or maximize annual energy production. Wind roses present the statistical distributions of both wind speed and wind direction. Figure 10 presents wind roses for the four reference locations (black circles) indicated in Figure 8 to show how directionality changes over the original Call Area. For the reference point in the west (GoM\_West), the predominant wind direction is south-southeast, with the most frequent and strongest winds coming from the south-southeast. For the points at Galveston II and Lake Charles, wind speeds are slightly lower and the predominant wind direction is closer to the south compared with the point GoM\_West. Wind speeds are lowest at GoM East, and there is less of a predominant wind direction, though winds most frequently blow from the southeast.

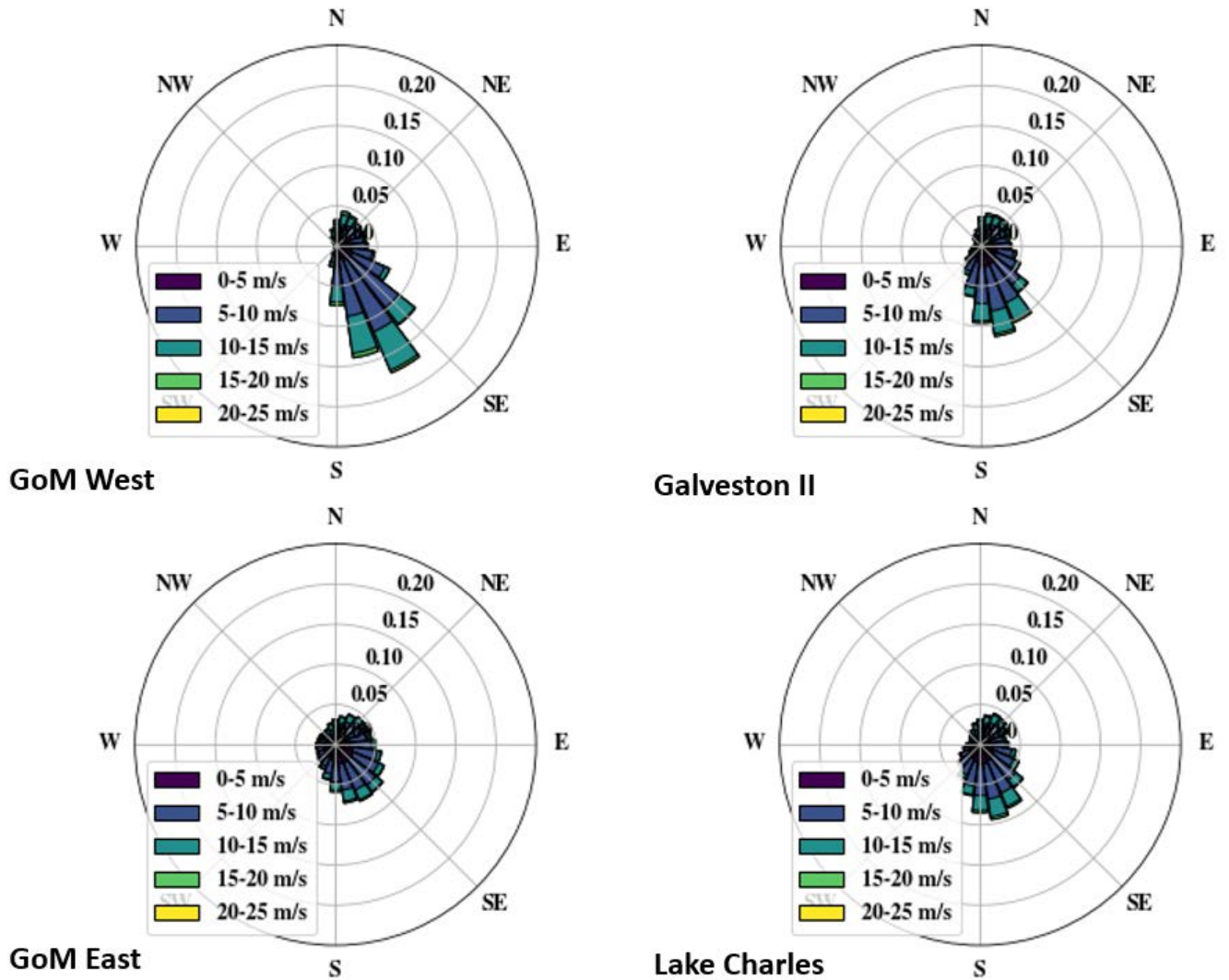


Figure 10. Wind roses at 160 m at four reference locations shown in Figure 8, clockwise from top left: Gulf of Mexico (GoM) West, Galveston II, Lake Charles, and GoM East

### 3.5 Wind Speed Distributions

Figure 11 presents mean hourly wind speed distributions for the four reference locations in Figure 8. The shapes of the distributions are similar across the region, although the peak of the distribution shifts slightly as the mean wind speed changes (higher in the west). The most frequent wind speeds are generally between 5 m/s and 8 m/s, which are in region II (partial load region) of a typical wind turbine power curve where the turbine power output is increasing with wind speed<sup>3</sup>. This is also the region of the power curve where wake losses are more significant. Wake losses are analyzed more in Section 6.4. Mean wind speeds above 20 m/s are uncommon in the Gulf of Mexico. Because the frequency of wind speeds is mostly below the turbine’s rated power, a turbine that performs well in lower wind speeds would be optimal for maximizing energy production and project revenue in the Gulf. Increasing the rotor size for the same

<sup>3</sup> The available power in the wind is proportional to the cube of the wind speed.

generator rating (lowering the turbine’s specific power, measured in watts per square meter [ $\text{W}/\text{m}^2$ ]) will increase the capture area and lead to improved capacity factors, capturing more available energy at lower wind speeds. More information on the design of a low specific power wind turbine for the Gulf is provided in Section 6.

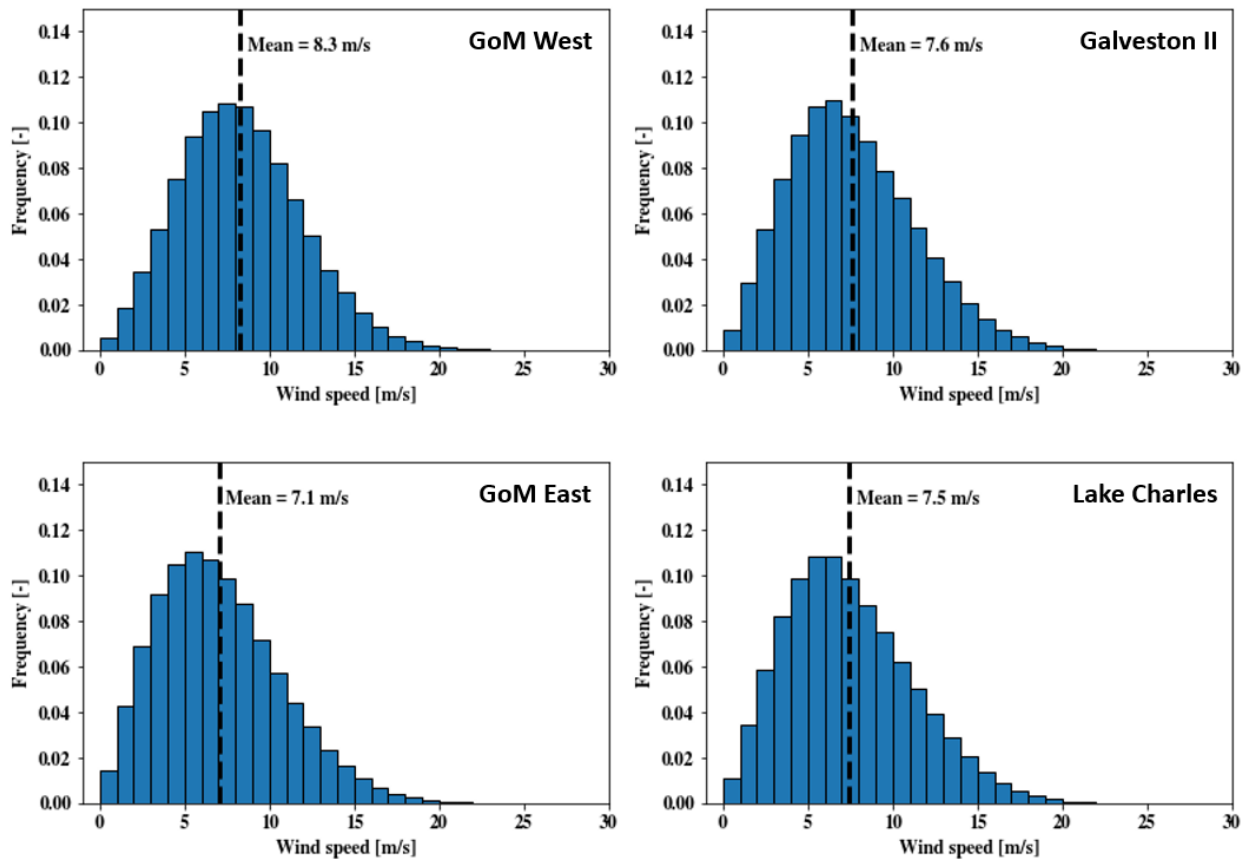
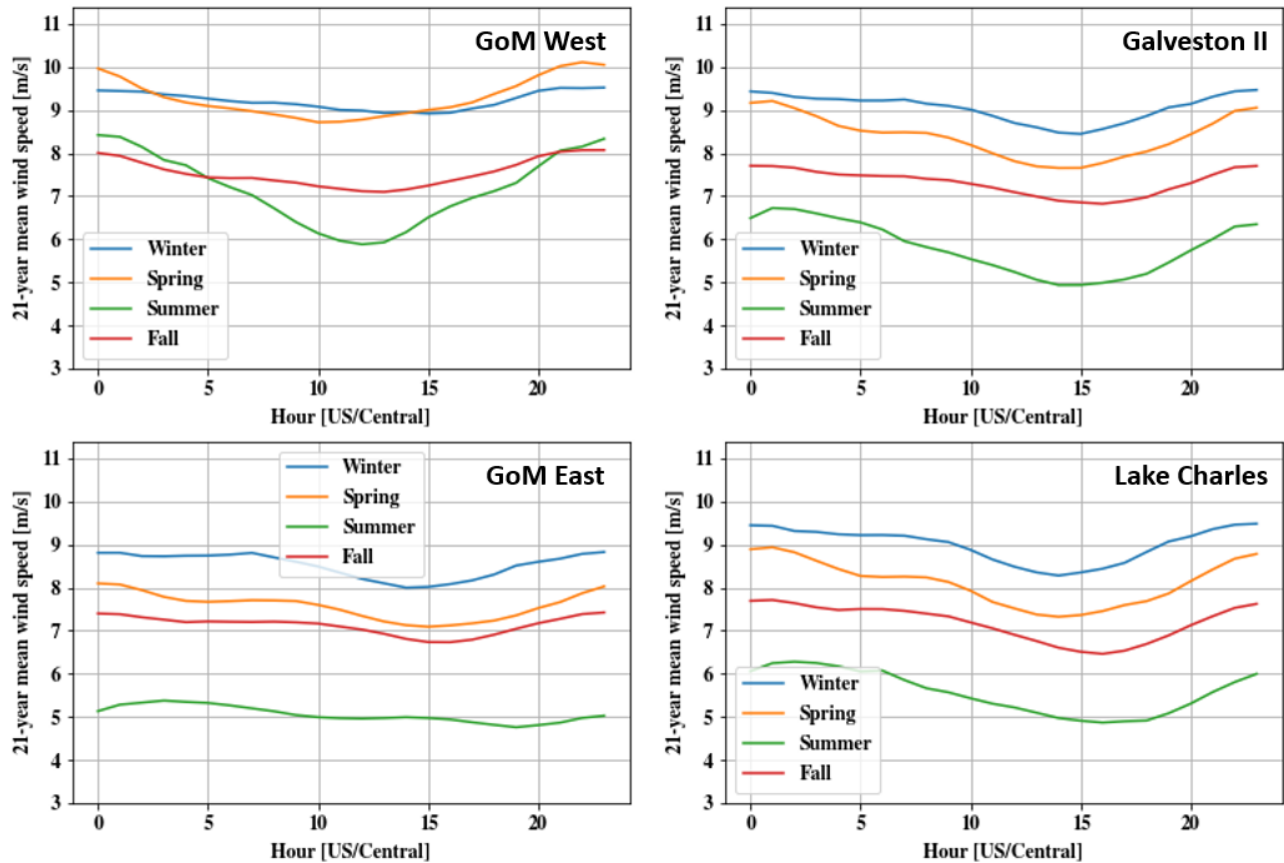


Figure 11. Hourly wind speed distributions at 160 m at four reference locations shown in Figure 8, clockwise from top left: Gulf of Mexico (GoM) West, Galveston II, Lake Charles, and GoM East

### 3.6 Diurnal Profiles

Understanding the expected generation profiles is critical to integrating variable electricity generation resources like wind and solar into the electric grid to ensure electricity demand is met at all hours of the day. Figure 12 shows seasonal and daily variations in the mean wind speed at the four reference locations. Hourly wind speeds are averaged by hour in the day and season. Winter is defined as December, January, and February; spring as March, April, and May; summer as June, July, and August; and fall as September, October, and November.



**Figure 12. Diurnal profiles by season at 160 m at four reference locations shown in Figure 8, clockwise from top left: Gulf of Mexico (GoM) West, Galveston II, Lake Charles, and GoM East**

Based on load forecasts developed by the Electric Reliability Council of Texas (ERCOT), electric loads across ERCOT regions tend to increase throughout the day and peak around 4-5 p.m., especially in the summer when cooling demand is high (ERCOT 2023). Peak electricity demand across the entire ERCOT region is expected to be around 82 GW in 2023 and grow annually to approximately 91 GW by 2032 (ERCOT 2023). Based on a comparison of historical hourly demand forecasts and actual demand for 2022, the South Midcontinent Independent System Operator (MISO) region serving much of Louisiana also has peak demand in summer evenings between 4 and 6 p.m., with a total peak load of over 32 GW (MISO 2023).

Across the entire Call Area, the lowest wind speeds occur during the summer and the highest are generally in the winter, except at GoM\_West, where spring wind speeds can be as high or higher than winter wind speeds. For GoM\_West, summer wind speeds tend to peak in the middle of the night and decrease until noon, when they begin to increase again. While the lower winds likely produce less energy the afternoon ramp-up may be important because it can potentially complement the growing solar generation which decreases in the afternoon and does not produce power at night. Similar afternoon ramping dynamics are present at Galveston II and Lake Charles where the proposed lease areas are located, although the day/night variations of wind speed are lower compared to GoM\_West. In most seasons and locations, the minimum wind speed occurs in the afternoon. Peak wind speeds tend to occur overnight. The range of daily average wind speeds generally remains between 1 and 2 m/s.

## 4 Hurricane-Specific Challenges

### 4.1 State of the Art for Hurricane Design

#### 4.1.1 Wind Turbine Operating and Survival Conditions

The conceptual wind turbine power curve in Figure 13 shows a wide range of wind conditions that extends into the extreme winds that could be produced by a major hurricane. At lower wind speeds, the wind turbine is operating (spinning) and producing power in the region indicated by the green arrow. At a higher wind speed where the probability of occurrence is very small (usually around 25 m/s or 56 miles per hour [mph]), the machine will “cut-out”. This means that the rotor blades are pitched to a feather position and the generator is disconnected. The rotor is no longer able to produce torque or generate power, but the machine can idle or free wheel because no brake is applied to the shaft. In other words, the rotor spins very slowly or remains in one position even in strong winds. This is the normal state of the machine after cut-out, and because the machine is not producing power there are much lower loads on the system.

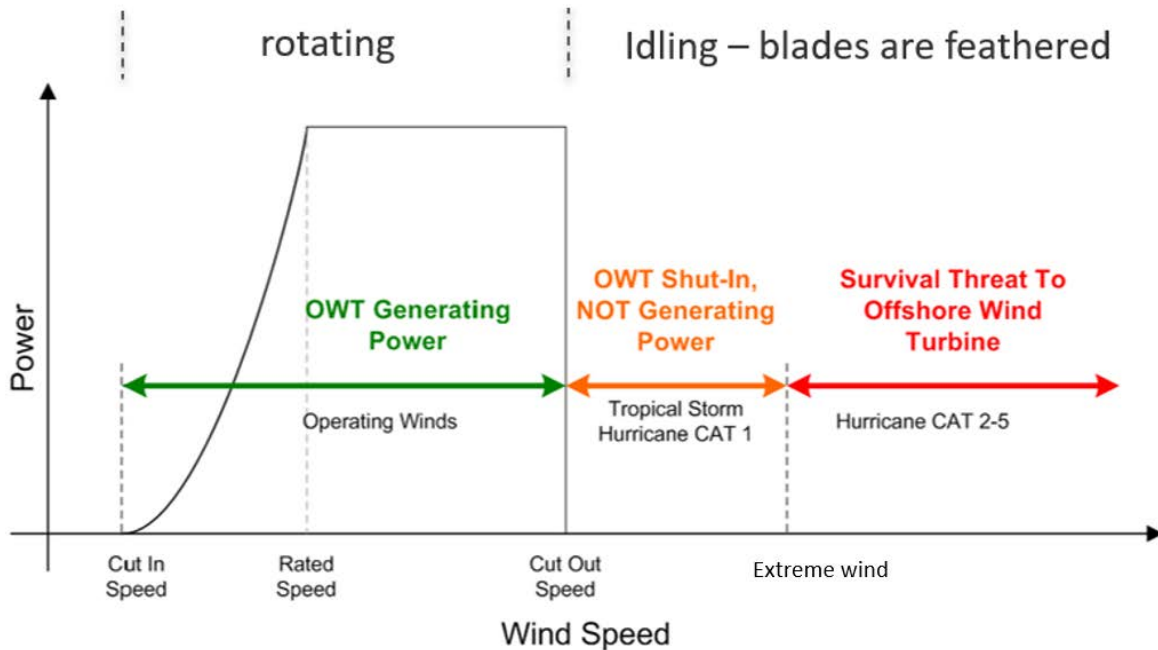


**Figure 13. Wind turbine power curve with extended region of idling out to extreme winds.**

If the turbine shuts down due to high winds from an approaching major hurricane, the turbine will cut-out long before the most extreme damaging winds arrive. As the storm approaches, the winds will continue to increase, and the drag forces on the turbine and support structure (tower and foundation) will also increase. To manage these loads, the standard procedure is to orient the turbine nacelle in a yaw position that is always facing the wind because cross winds can be unpredictable and cause higher loads. To maintain yaw control, the grid connection that powers the yaw system must remain active. If grid power is lost during a storm, the IEC design standards prescribe additional load cases that we discuss later (Sections 4.1.2 and 4.1.6).



#### 4.1.2 Design Standards for Offshore Wind Design

The general approach to wind turbine design is covered by the recently published ANSI/ACP OCRP-1-2022, Offshore Compliance Recommended Practices, Edition 2 (ANSI 2022). This document is a comprehensive consensus-based roadmap for the design of offshore wind plants in the United States. It refers to more than 200 standards and guidelines and covers the basic details for offshore wind system design.

As described in OCRP-1-2022, the support structure and turbine are designed using different standards and methods. The design of the support structure—which comprises the tower, substructure and foundation—evolved from oil and gas standards developed by the American Petroleum Institute (API). The offshore wind turbine design evolved from land-based wind turbine standards developed by the International Electrotechnical Commission (IEC) under IECTC-88. This split is shown in Figure 14.

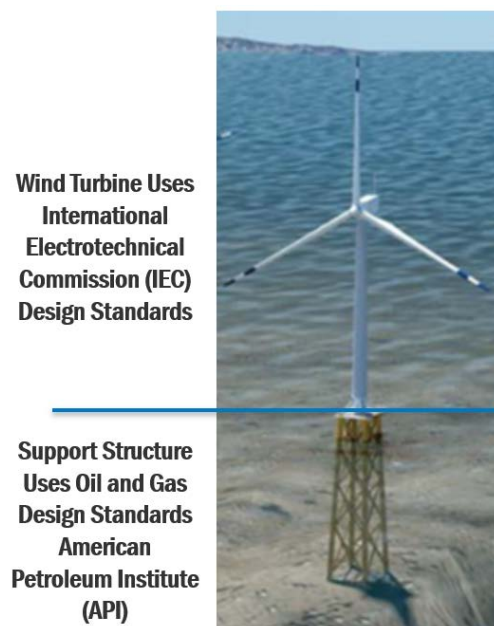


**Figure 14. Design standards for turbine and substructure.**

*Image by NREL*

Initially, the mixing of these two groups of standards to create a single structure that was experiencing the same loading was concerning because there was a risk that this might introduce unequal levels of safety within the wind system. In 2009, this issue was resolved by Jha et al. (2009) when equivalency between API and IEC was established. Generally, the external load conditions and design load cases are set by the design standard IEC 61400-3-1 for fixed bottom offshore wind turbines and the support structure and electrical substation are governed by criteria set in API RP-2A.

The governing international standards for fixed bottom offshore wind turbine design are IEC 61400-1, Edition 4, Wind turbines – Part 1: Design requirements (IEC 2019a), and IEC 61400-3-1 Edition 2 (IEC 2019b), Design requirements for fixed offshore wind turbines. These standards prescribe the design load cases (DLCs) that shall be considered for structural design of the

turbine, towers, and foundations. The critical DLCs relevant to tropical cyclones are DLC 6.1 and DLC 6.2, which require the designer to consider ultimate limit state loading when the rotor is idling. IEC turbine designs are based on design classes to facilitate some site independence to allow turbine mass production and industrialization. As such, each design class covers a range of site conditions that shall not be exceeded. Until the latest edition, IEC Class 1 designs were suited for the most extreme conditions based on a maximum extreme 3-second gust of 70 m/s at hub height for a 50-year return period.<sup>4</sup> The standards use the load and resistance factored design method which prescribes partial safety factors that are designated as either “N” for Normal or “A” for abnormal. The equation below shows the relationship between the characteristic loads which are derived from engineering models and analysis, and the design loads which include the partial safety factors.

$$\text{design loads} = (\text{characteristic load}) \times (\text{partial safety factor})$$

DLC 6.1 is considered a normal condition, with power being provided by the onshore utility grid, which is maintained and operating most of the time. In this case the characteristic loads determined through analysis of the 70 m/s 3-second wind gust are multiplied by a safety factor of 1.35 (because maintaining grid power is considered a normal condition) to determine the maximum allowable design loads that the turbine must withstand.

DLC 6.2 considers the same extreme 70 m/s 3-second wind gust as DLC 6.1 but assumes that the grid providing power to the wind farm and the yaw system is not available (presumably because the storm has damaged the land-based power system). This is considered an “abnormal” condition in the IEC standard because for extratropical storms typical of the North Sea and Baltic Sea, power grid failure is less likely to occur than during a major hurricane in the Gulf. In the DLC 6.2 scenario, operationally the turbine nacelle is locked in the position where it was when the power grid failed and can no longer respond to wind direction changes. In a tropical cyclone, wind direction shifts up to  $\pm 180^\circ$  are expected over the storm’s duration. Wind gusts that strike the machine with large yaw errors (e.g., cross winds greater than  $\pm 15^\circ$ ) can produce much higher characteristic loads than those calculated for DLC 6.1, because the extreme characteristic loading in DLC 6.1 is mitigated by the yaw system’s ability to control favorable yaw positions. For DLC 6.2, IEC 61400-1 requires that yaw errors of  $\pm 180^\circ$  shall be analyzed unless backup power for the yaw system is provided for at least 6 hours. Yaw systems backup power is covered in detail in Section 4.1.6.

All wind turbines are designed to withstand the loads from low category hurricanes based on the well-known Saffir-Simpson hurricane classification system. In the North Atlantic or in the North Sea, extreme winds have historically been limited to wind speeds found in Category 1 or Category 2 storms. When storms produce wind speed gusts and waves that exceed the design conditions for the turbine and support structure, additional design considerations and survival strategies are warranted.

---

<sup>4</sup> Hub height is typically around 150 m above sea level for the new generation of 15 MW-class offshore wind turbines. A return period is the estimated average time between extreme wind events measured at a given site.

### 4.1.3 Hurricane Design Standards Provisions

Although most wind turbines are already designed to withstand wind gusts specified in the IEC DLC 6.1 load case of 70 m/s (156 mph), major hurricanes (Categories 3-5) can produce wind conditions that require more rugged design considerations. State-of-the-art practices for tropical cyclones involve augmentations of conventional turbines and their support structures that increase the strength of components to withstand higher wind and wave conditions, implementation of more robust controls to facilitate storm ride-through, and adaptation of oil and gas experience to engineer adequate structural reliability into the support structures and electric service platforms.

#### 4.1.3.1 Tropical (Typhoon) Class Turbines from IEC

Extreme conditions are defined by IEC standards 61400-1 and 61400-3-1 which prescribe a 50-year return period for the reference wind speed corresponding to the turbine class. The reference wind speed from which the maximum gust is determined, is a 10-minute average wind speed assessed at hub height. Conventional offshore wind turbines are Class 1, which are designed for a reference wind speed of 50 m/s (111.0 mph). The most recent versions of IEC standards have defined a higher Tropical (Typhoon) Class (T-Class) reference wind speed at 57 m/s (127.5 mph). This new T-Class reference wind speed results in a higher extreme gust of 79.8 m/s (180 mph) for IEC DLC 6.1 and 6.2 and correspondingly, longer return periods.

#### 4.1.3.2 Robustness Check for Substructures

The most recent edition of IEC 61400-3-1 added several new annexes, including Annex I, which provides recommendations for alignment of safety levels in tropical cyclone regions (e.g., hurricanes on the U.S. East Coast and Gulf Coast). The new provisions in Annex I were introduced by the U.S. members and are based on the API standards for oil and gas structures that evolved from the proven industry practices founded in the Gulf. Annex I adapts the concept of a robustness check currently used by the offshore oil and gas industry for application to offshore wind support structures. As an annex, the robustness check is optional in the IEC standard but we recommend that it be mandatory in any site subject to hurricanes. It may impact the support structure design at sites where “hazard curves” are relatively steeper than those at other sites, indicating a high coefficient of variation (COV).<sup>5</sup> Offshore wind lease areas along the Atlantic seaboard and in the Gulf of Mexico tend to experience higher COVs than for example in the North Sea, as shown in Figure 15.

---

<sup>5</sup> The coefficient of variation is an indicator of how much greater in severity storms with higher return periods will be.

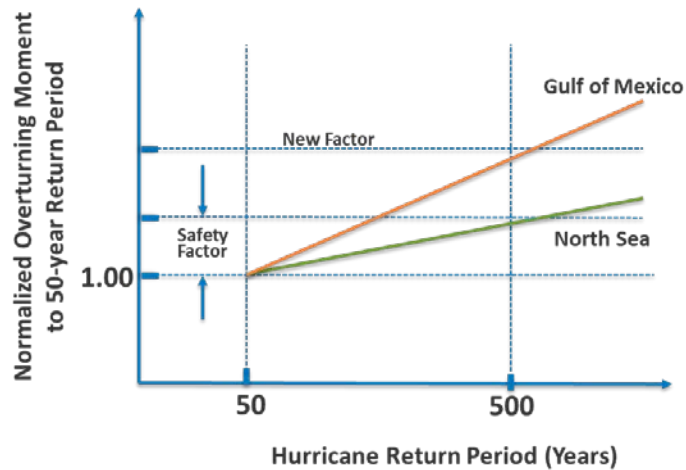


**Figure 15. Conceptual hazard curves based on 50 and 500-year return periods adapted from API RP-2A.**

*Image by NREL*

The turbine support structure design uses site specific data for return periods of 50 years and 500 years as specified by IEC. The limit state design analysis and the robustness check are performed to determine if the support structure has adequate structural reliability to survive in the location where it is installed. The 50-year return period is augmented with the 500-year return period for the extreme gust condition during the robustness check<sup>6</sup>. The unfactored characteristic load corresponding to the 500-year event is applied to the support structure components to demonstrate that structural reliability is maintained at sites where the hazard curves are steeper. Although the 500-year gust is always greater, the degree to which it exceeds the 50-year gust determines if the support structure design must be further strengthened. Figure 15 shows that (hypothetically) in the Gulf, a steeper hazard curve exceeds the design safety factor for the 500-year event, which would indicate that increased strength would be needed in some components.<sup>7</sup>

#### **4.1.4 Assessment of Hurricane Risk and Return Periods**

Hurricane hazard models, such as the one developed by Applied Research Associates (Vickery et al. 2009a; Vickery et al. 2009b) are used to define storm occurrence rates, intensities, storm tracks, and wind fields. The modeling approach is validated by comparing model output against statistics of historical hurricane parameters. These hazard models can be used to estimate return periods or the probability of occurrence for different extreme wind speeds at wind turbine hub height. Accurate knowledge of extreme wind return-periods at a given site is necessary to determine the external design conditions applied to the wind turbine design, making these hazard models necessary for the design of wind energy systems at sites off the US Atlantic Coast or in the Gulf of Mexico.

<sup>6</sup> The 500-year return period is based on the API RP-2A L-2 medium exposure category designated by OCRP-1 for an offshore wind turbine. The electric service platform is designed for an L-1 exposure category which requires a 1000-year return period.

<sup>7</sup> Note that the robustness check does not cover the turbine or any of the rotating components.

The National Hurricane Center has been collecting data on the tracks and severity of hundreds of hurricanes in U.S. waters over many decades. From these public data, synthetic models are developed that can simulate thousands of years of storms and estimate trends into the future, such as storm track changes and storm severity due to climate change as illustrated in Figure 16.

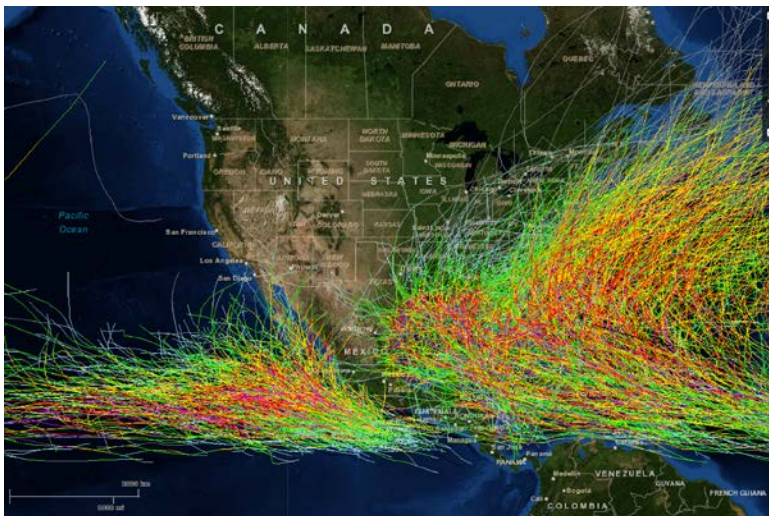


**Figure 16. Example of modeled hurricane tracks.**

*Image from NOAA (2012)*

Past examination of storm tracks from 1900 to 2016 reveal general patterns of extreme wind exposure and frequent tropical cyclones inside the Gulf of Mexico. These wind extremes are analyzed and quantified by Mudd and Vickery in a companion report to this study which completed a 500,000-year hurricane simulation and calculated return periods for the IEC Class 1A and Tropical (Typhoon or T-Class) Class turbines having reference wind speeds of 50 m/s (111.9 mph) and 57 m/s (127.5 mph), respectively<sup>8</sup> (Mudd and Vickery 2023). The study shows that the IEC Class 1A turbine design criteria yield return periods that are shorter than the required 50-year limit state design requirement, making IEC Class 1 designs inadequate for offshore wind in the Gulf of Mexico as shown in Figure 17.

---

<sup>8</sup> Reference wind speeds are calculated at a hub height of 150-m.

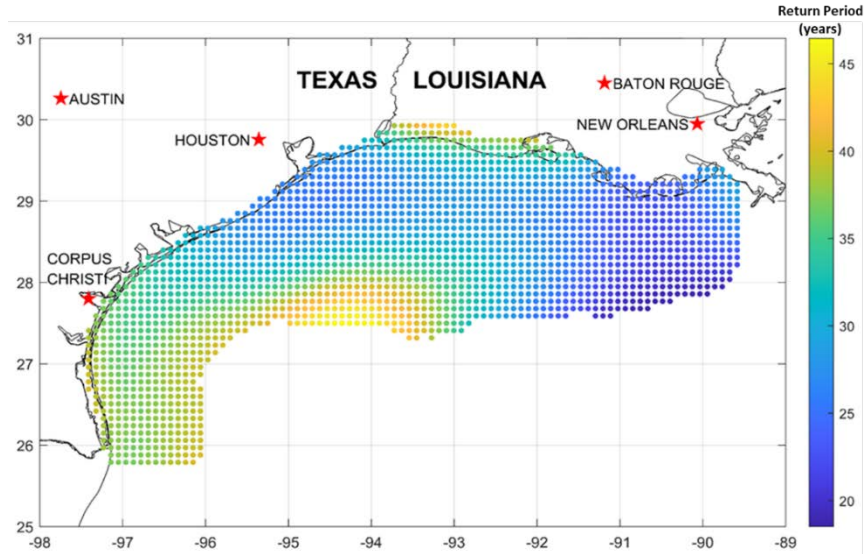


**Figure 17. Return period (years) associated with the IEC Class 1A limit-state reference wind speed of 111.9 mph (50 m/s) obtained from a 500,000-year hurricane simulation.**

*Source: Mudd and Vickery (2023)*

The return periods are shown over the BOEM Call Area using 10-km by 10-km grid cells, with the shortest return periods in dark blue. There were no locations where the IEC Class 1 return periods were greater than 50 years. Therefore, enhanced turbine designs are needed to ensure compliance with IEC standards and to reduce hurricane risk to acceptable levels. The study also looked at the return periods for the enhanced T-Class wind turbine shown in Figure 18.

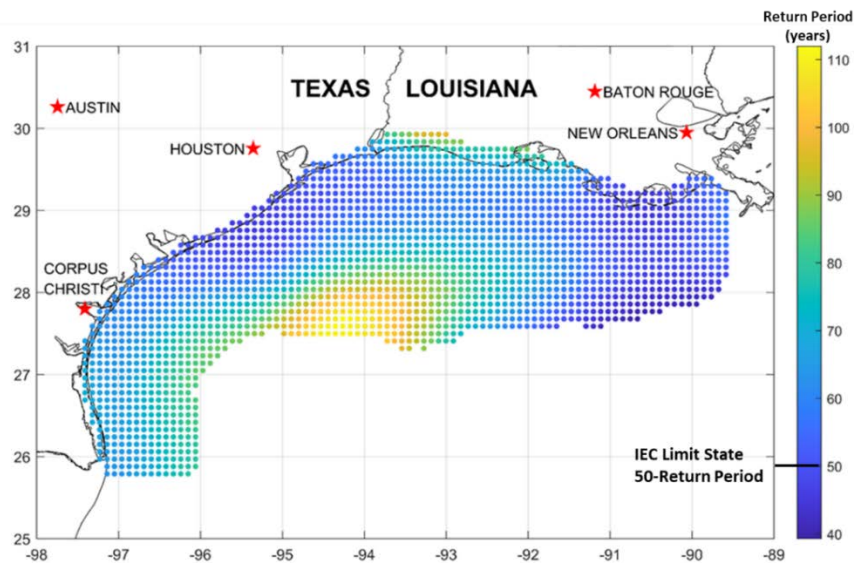


**Figure 18 Return period (years) associated with the IEC T-Class limit-state reference wind speed of 127.5 mph (57 m/s) obtained from a 500,000-year hurricane simulation.**

*Source: Mudd and Vickery (2023)*

The IEC T-Class turbines have a higher reference wind speed of 57 m/s (127.5 mph) leading to longer return periods that are currently compliant with the IEC standards in most regions.

However, it should be noted that these calculations do not account for likely future increases in extreme winds due to climate change. In addition, data (darker blue dots) indicate that some of the return periods may be too close to the 50-year IEC design limit state even with the T-Class turbine design. Specifically, the return periods are roughly 40-60 years near the WEAs of the Gulf, close to the 50-year design requirement. Therefore, although the T-Class turbines have return periods that are mostly above the 50-year threshold there are some areas where a higher S-class turbine might be warranted. This topic is discussed in detail in the companion report by Mudd and Vickery (2023). Regions where the 10-minute sustained wind speeds at a height of 150 m obtained from the study were found to exceed the IEC T-Class reference wind speed of 57 m/s (127.5 mph) are shown in Figure 19.

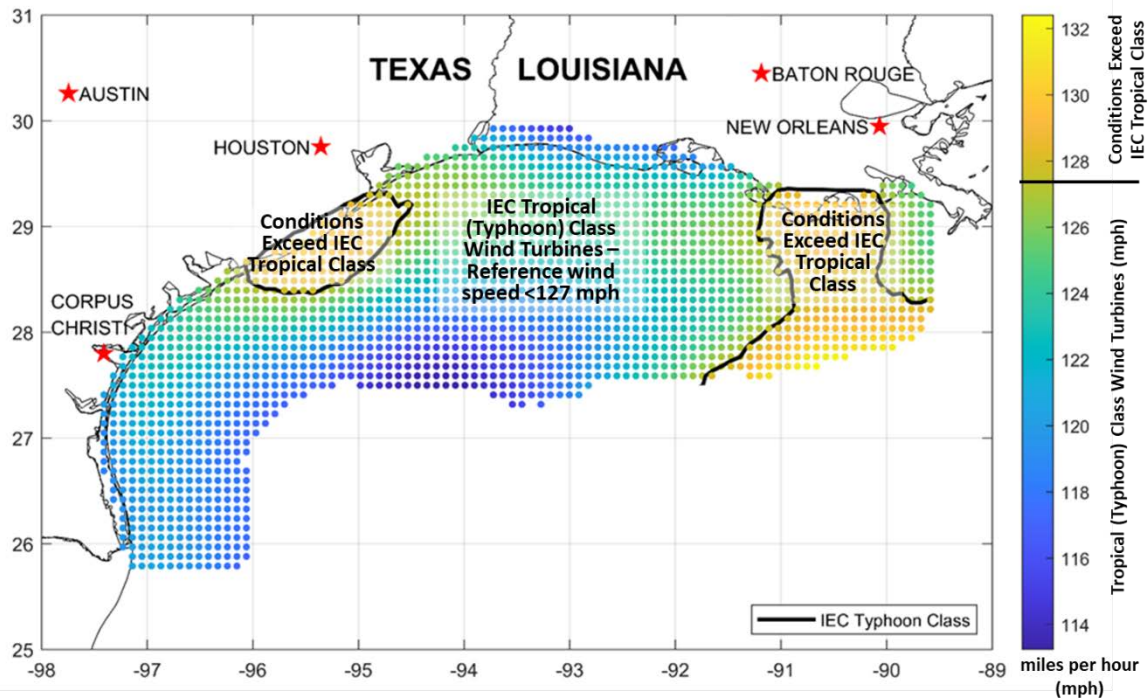


**Figure 19. 10-minute sustained wind speed (mph) at 150 m with a return period of 50 years obtained from a 500,000-year hurricane simulation. Note: no isocline for the Class 1A limit state appears since all simulated values of the 50-year wind speed are greater than the Class 1A reference wind speed (111.9 mph, 50 m/s).**

To help provide insights into the cost impacts of upgrading from Class 1A offshore turbines to T-Class turbines we conducted interviews with some of the major offshore wind turbine original equipment manufacturers (OEMs) (Duffy et al. 2022). Generally, the OEMs indicated that most of the cost difference in upgrading comes from strengthening the tower and foundation, which could lead to an approximately 5%–10% increase in turbine costs, depending on the site. Upgrades to the turbine rotor nacelle assembly were also needed but were estimated to increase turbine costs by less than 1% because most of the strengthening was achieved by adding more laminates to the composite blade structure to strengthen and/or stiffen the blades using the same tooling. Some OEMs indicated that because the incremental costs were minimal, T-Class blades were becoming standard equipment for most machines in the United States going forward.

Some additional design differences include:

- Standard backup power systems to maintain yaw authority during a grid outage.
- Reinforcement of other turbine components including ruggedized speed and direction sensors, and the yaw and pitch systems.

#### **4.1.5 Offshore Wind Experience in Hurricane-Prone Regions**

Wind turbines are already being placed in typhoon-prone regions, such as southeast Asia. In Laos, a 600-MW land-based wind farm has recently begun construction (Monsoon Wind). Mingyang Smart Energy installed a floating 7.25 MW turbine off the hurricane-prone coast of Hainan to support oil and gas extraction activities there. Mingyang claims the turbine can withstand maximum average wind speeds greater than 60 m/s (134 mph) (Jenkinson 2023). GE Renewable Energy has developed the Haliade-X 12-MW and 13-MW offshore wind turbines, the most powerful offshore wind turbine to have a typhoon class certification from DNV as of 2021 (General Electric n.d.). The GE Haliade-X 12-MW turbine is planned for the 1,100 MW wind farm by Ocean Wind, offshore New Jersey (Ocean Wind 1 n.d.). The GE Haliade-X 13-MW turbine is currently under construction at the 800-MW Vineyard Wind project offshore Massachusetts (Vineyard Wind 1 n.d.).

Specialized turbine designs that can withstand hurricanes are already being developed to reduce the risk of turbine loss and damage to the wind farm. Design practices for hurricane-tolerant offshore turbines are still young but are beginning to get increased attention as the offshore wind industry moves into these regions. Some current state-of-the-art solutions for wind turbines in hurricane regions have evolved from successful substructure designs in the offshore oil and gas industry.

#### **4.1.6 Battery Backup Systems for Maintaining Yaw Control**

##### **4.1.6.1 Background**

During extreme high wind events, battery backup systems for maintaining yaw control can be beneficial to prevent major damage to a wind turbine (Kim and Manuel 2014). Such systems are one of the most significant near-term design upgrades for extreme wind load mitigation that is both commercially available and recognized by the existing design standards. It can be applied to either land-based or offshore wind turbines. Earlier yaw system back-up applications envisioned maintaining an independent diesel generator system that would be called on to power the yaw system if grid power was lost, but recent advances in electric vehicles and lithium-ion battery storage have made fossil-fuel back-up systems obsolete (General Electric 2013).

Backup power for the yaw system has not been a common practice for offshore wind turbines thus far, but the newest class of 15-MW turbines which are likely to be deployed in U.S. waters in the north and mid-Atlantic are subject to hurricane conditions and are expected to be outfitted with robust battery backup systems as standard equipment. These battery back-up systems can protect the turbine from excessive loads caused by high misalignment between the wind inflow and the main shaft. According to IEC standards, the battery backup system would also eliminate the need for IEC DLC 6.2 to be considered in the design analysis because uninterruptable yaw tracking would avoid high yaw misalignments during a power grid failure if the wind direction changes were gradual as they would be on average during a hurricane.



The purpose of this section is to provide preliminary analysis to help understand the extent to which battery backup systems can mitigate severe loading conditions during hurricanes in the Gulf. NREL assessed the loading on a representative wind turbine design for the cases with and without battery backup control under extreme hurricane conditions so that comparisons can be made between the two conditions. The analysis was not intended to be used to evaluate turbine specific designs but to help demonstrate the beneficial nature of having a battery back-up control system. The results of the analysis presented herein show promise that the backup systems can mitigate loads, but the study also revealed significant shortcomings in our analysis methods leading to inconclusive results that make the net benefits difficult to quantify. A more rigorous approach is underway at NREL to provide more definitive results and is described later.

#### *4.1.6.2 Methodology and Approach*

The turbine model we selected for this analysis was the IEA 15-MW reference wind turbine which was designed to be representative of the newest 15-MW turbine platform size that is under development by all major turbine manufacturers and that is likely to be deployed at most U.S. offshore wind projects over the next decade. The 15-MW reference offshore wind turbine was developed under IEA Wind Technology Collaboration Programme Task 37 and was a key collaboration between NREL and the Technical University of Denmark, among others (Gaertner et al. 2020). The wind turbine has a rotor diameter of 242 m with a hub height of 150 m. The reference model also enabled coupling with either a monopile or floating platform substructure, depending on the water depth.

In this study it was necessary to make a few simplifying assumptions to achieve better model convergence when running the simulations while staying within the project scope. First, we configured the IEA 15-MW reference turbine model with a stiff, rigid base and ignored the impact of waves and water currents, making it ostensibly a land-based turbine from a modeling point of view. We considered this a reasonable simplification because the backup power system affects mostly the rotor aerodynamic loads. Hydrodynamic loading is important to include in the detailed design, but our objective to gain a preliminary understanding of the relative benefits of yaw battery backup systems was not significantly compromised by using a rigid base.

Another simplification is that the IEA 15-MW reference turbine was designed to the IEC Class 1B turbine criteria and was not intended to withstand major tropical cyclones under T-Class (Category 3+) conditions. In consultation with turbine manufacturers, we agreed that the Class 1B turbine could be used in a comparative loads study and the first order conclusions would be valid for the T-Class turbines that will likely be deployed in the Gulf. Future versions of a T-Class reference wind turbine are under development which will take into consideration hurricane loading conditions. Table 2 summarizes the key parameters of the turbine used in the model.

**Table 2. IEA 15-MW Reference Wind Turbine Parameters**

Parameter	Value
Turbine class	IEC Class I-B
Specific power rating	326 W/m <sup>2</sup>
Rotor diameter	242 m
Tip-speed ratio	9.0
Maximum tip speed	95 m/s
Hub height	150 m
Cut-in wind speed	3 m/s
Cut-out wind speed	25 m/s

For the simulation of the turbine in hurricane conditions, we use NREL’s OpenFAST turbine simulation tool (Jonkman and Sprague 2021). OpenFAST is a state-of-the-art aero-servo-elastic simulation tool for land-based and offshore wind turbines. OpenFAST allows us to run a large number of nonlinear time domain simulations of a turbine under prescribed external conditions. Using OpenFAST, we defined the structure of the IEA 15-MW reference wind turbine, and input wind conditions for IEC T-Class turbines as defined by the IEC 61400-1 Ed. 4 (IEC 2019a). Using these inputs, OpenFAST calculated the aerodynamic loading and the structural response of the turbine and output the load response.

#### 4.1.6.3 Load Analysis Details

This study focuses only on DLC 6.1 and DLC 6.2, described earlier, which are the most relevant load cases for extreme wind conditions because they are prescribed for the idling rotor condition with no power generation. DLC 6.1 is used when the turbine yaw system is active, and DLC 6.2 is used in the case of a loss in electrical grid power and when no backup power to retain yaw authority is available.

The wind conditions for both load cases were considered using an “extreme wind model” (EWM). Based on Section 7.4.7 of IEC 61400-1 Ed. 4, both turbulent and steady inflow EWMs can be used as inputs for the DLC 6.1 and DLC 6.2 simulations for land-based wind turbines. IEC standards require a yaw error of  $\pm 8^\circ$  to be enforced for the turbulent inflow model, but when the steady EWM is used, the allowable yaw error increases to  $\pm 15^\circ$ . For DLC 6.2 (grid loss) a yaw angle of  $\pm 180^\circ$  must be considered because it is assumed that there is no yaw control available to the turbine, and in a tropical cyclone the wind direction would be expected to vary considerably as the storm passes through.

Initially, these simulations were conducted using the *turbulent* EWM, which uses a 50-m/s reference velocity to create a turbulent EWM input spectrum. This is the preferred method by the wind industry because it is more representative of the actual wind input characteristics. Moreover, IEC 61400-3-1 Ed.1 (Design requirements for fixed offshore wind turbines) requires the use of turbulent EWM, as defined in Section 7.4.7. Unfortunately, significant numerical instabilities were encountered in OpenFAST at the higher yaw angles, which prevented us from

obtaining stable outputs during the preliminary runs using turbulent EWM. As such, the results could not be quantified or trusted due to the instabilities, so we shifted to the *steady* EWM.

The steady model is allowed in land-based applications but not for offshore wind turbines. This model estimates turbine loads using a lower-order quasi-steady analysis. It uses the IEC T-Class turbine definition for DLC 6.1 and DLC 6.2 inflow velocity of 79.8 m/s for a steady 3-s gust (gust factor of 1.4). This method enabled us to better control the instabilities at high yaw angles if we allowed the initial dynamically induced oscillations to dissipate. However, this required us to introduce additional (artificial) blade damping, which altered the rotor dynamic properties (e.g., blade stiffness) and increased uncertainty in the calculation of loads in these high yaw angle regions—but it enabled the calculation of loads and thus a comparison with other yaw states. Generally, the steady EWM is less desirable because it is a less realistic representation of the wind conditions but was found to be more conservative than the turbulence model in regions of the yaw azimuth where both models converged.

Table 3 summarizes the key parameters for both extreme wind idling DLCs under IEC Class 1B and T-Class conditions.

**Table 3. Summary of Parameters for IEC Design Load Cases 6.1 and 6.2**

	IEC Class 1 condition		IEC Class-T condition	
	Turbulence	Steady	Turbulence	Steady
EWM $V_{e50}$ [m/s]	50	70	57	79.8
DLC 6.1 Yaw error [deg]	$\pm 8$	$\pm 15$	$\pm 8$	$\pm 15$

The analysis was focused on how loads and moments at the blade root, tower-top yaw bearing, and tower base varied with different yaw misalignment errors. The variation of loads between IEC Class 1 and IEC T-Class conditions are contrasted, and we look at the unfactored characteristic loads experienced by the turbine. The model focuses primarily on the rotor loads, which are the most complex part of the turbine to analyze.

One of the findings was that AeroDyn—the blade aerodynamics model used in OpenFAST, which employs an unsteady aerodynamics model that includes dynamic stall and three-dimensional rotational corrections—was not calibrated for higher angles of attack experienced by the individual blade elements under a  $\pm 180^\circ$  yaw analysis. This was a primary source of increased modeling uncertainty, as the lack of physical damping otherwise afforded by correctly modeling aerodynamic hysteresis during dynamic stall had to be compensated by adding artificial damping. Additionally, the blade structural model in OpenFAST, ElastoDyn, works well for operational conditions, but under structural instabilities, blades may experience extremely high deflections that exceed the theoretical limitations of the ElastoDyn structural model. The extremely high angles of attack experienced by an idling rotor during DLC 6.2 under a  $\pm 180^\circ$  analysis require further model development to gain the required accuracy.

Other than the rotor, the aerodynamic drag loads on the tower were computed and are added to the rotor loads. The tower drag loads are straightforward and have lower uncertainty. However, OpenFAST currently does not include a model to incorporate the aerodynamic drag effects of the

nacelle, which could be significant in determining DLC 6.1 and DLC 6.2, depending on the nacelle geometry. This issue will be corrected in future analysis.

#### 4.1.6.4 Load Analysis Results

Based on the methodology described above, the IEA 15-MW turbine was simulated in OpenFAST for DLC 6.1 and DLC 6.2 under IEC Class 1 and IEC T-Class conditions. The resulting outputs were analyzed to interpret the quasi-steady results considering the uncertainties described above. Only the characteristic loads (unfactored loads experienced by the turbine as computed by OpenFAST) were considered in our analysis.

The combined loading experienced by the turbine at the tower base varies as a function of the yaw angle between the turbine main shaft and the incoming wind, as shown in Figure 20. conditions.

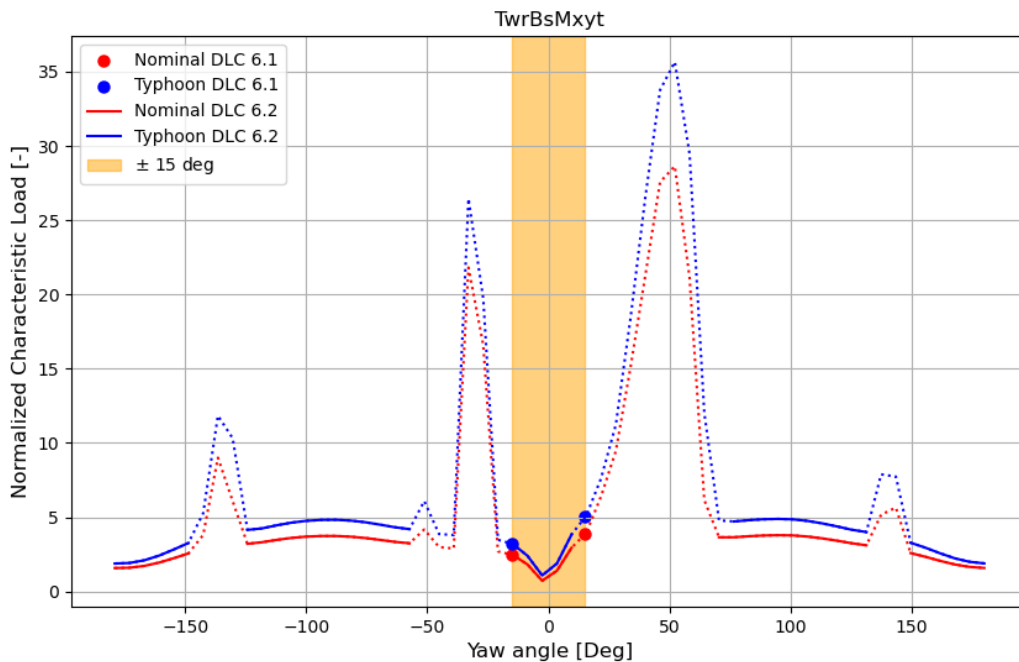


**Figure 20. Tower-base combined bending moment shown as a function of yaw angle between the turbine and the incoming wind. The loads are normalized by the load experienced at zero yaw and Class 1 inflow condition. The dotted lines represent areas with higher uncertainty.**

The combined bending moment at the tower base is the resultant load experienced by the tower in all directions at a given instant. The characteristic loads shown in the figure are normalized by the load experienced by the nacelle at zero yaw angle under IEC Class I inflow. This allows us to compare how the loads behave under IEC T-Class inflow and higher yaw angles. We also plot the loads for both the IEC Class I and T-Class inflow conditions. The yellow shaded region marks a yaw angle range of  $\pm 15^\circ$ . The  $\pm 15^\circ$  region is defined in IEC 61400-1 Ed. 4 for DLC 6.1 as the error the turbine experiences while maintaining yaw authority under steady inflow.

The regions of higher uncertainty due to numerical instabilities in OpenFAST are indicated by the dotted lines on the curves. These areas are generally relevant for DLC 6.2 outside the  $\pm 15^\circ$  region where the yaw drive is not active. These regions are marked with dotted lines on the

curves as a caution that the results generated by forcing the model to converge using excessive damping may not allow a quantitative comparison between DLC 6.1 loads and DLC 6.2 loads due to a high degree of error. Qualitatively, we believe that some of the unstable behavior the model exhibits may be due to extreme blade deflections and high angles of attack that occur at yaw angles greater than  $15^\circ$ . This behavior would likely result in higher loading as these plots indicate, but our confidence is not high enough to estimate the magnitude of this loading. In the regions with higher uncertainty, the load, which is significantly larger, suggests that regions with higher yaw angles should be avoided. This can be achieved through the yaw battery backup system. The results also highlight the necessity of understanding and resolving regions with higher uncertainty to improve turbine designs in hurricane wind conditions at high yaw angles.

The tower-top combined moments close to the yaw bearing (Figure 21) are similar to those of the tower-base loads showing higher loads outside the  $\pm 15^\circ$  yaw-controlled region.

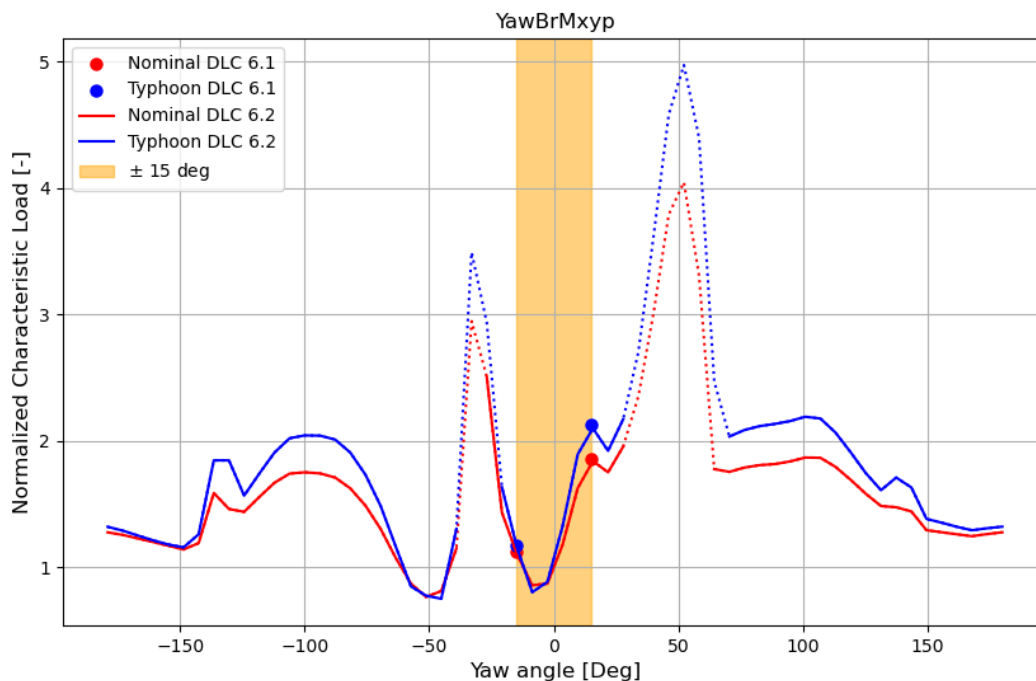


**Figure 21. Tower-top combined bending moment shown as a function of yaw angle between the turbine and the incoming wind. The loads are normalized by the load experienced at zero yaw and Class I inflow condition. The dotted lines represent areas with higher uncertainty.**

The torsional load on the tower top directly influences the yaw bearing and yaw drive (Figure 22). In this plot, the most significant changes in loads are in the  $\pm 15^\circ$  region. The largest design loads occur outside this yaw-controlled region, but the dramatic increase in load at high yaw angles was much less pronounced. Nevertheless, the increased loads beyond the  $\pm 15^\circ$  yaw angle suggest that these high yaw angles should be avoided. This can be achieved through the battery backup system.

One of the most concerning observations from Figure 22 is that within the  $\pm 15^\circ$  region where yaw is actively controlled, the yaw-bearing torsional loading experiences fully reversing loads

across the narrow  $\pm 15^\circ$  band. These reversing loads could potentially generate significant backlash on the yaw drive, which should be avoided if possible and investigated further.

A common trend observed in all the loads analyzed is the asymmetry of the loads across the yaw angles. This is due to the asymmetry of the rotor's geometry with respect to the yaw axis, which includes the blade twist and the asymmetrical airfoils.

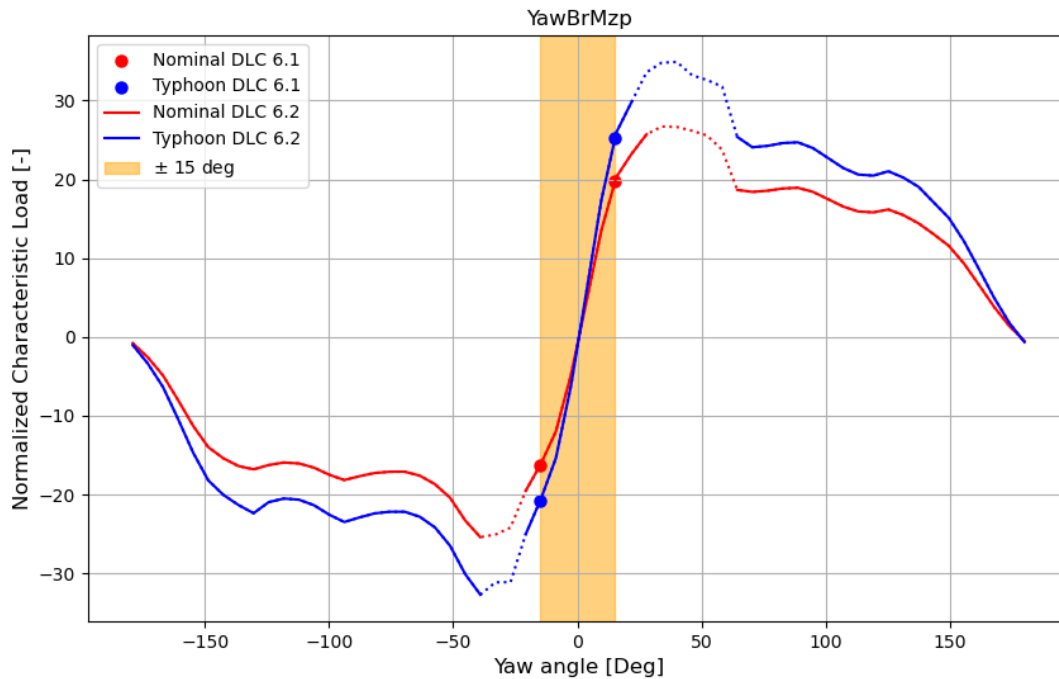


**Figure 22. Tower-base/yaw-bearing torsion shown as a function of yaw angle between the turbine and the incoming wind. The loads are normalized by the load experienced at zero yaw and IEC Class IB inflow condition. The dotted lines represent areas with higher uncertainty.**

Observing the blade root combined loads in Figure 23, we see a similar trend with significant load variation within the  $\pm 15^\circ$  region. Under DLC 6.1 and DLC 6.2 the loads will be primarily driven by the aerodynamic forces on the blade, whereas in operational cases it is a combination of aerodynamic, gravitational, and centrifugal loads on the blade. Though wind turbine blade designs are traditionally driven by operational load cases (DLC 1.1 to DLC 4.2), it is important to understand how the DLC 6.1, and DLC 6.2 loads compare to operational loads.

Another important aspect of the large yaw-angle loading that could be improved upon in this study is to consider the growing physical instabilities that may occur during high angles of attack. These instabilities manifest themselves through large edgewise vibrations characterized by negative aeroelastic damping. Such stall-induced vibrations can rapidly grow, leading to blade failure under idling conditions (DLC 6.1, 6.2). While the introduction of artificial damping to the simulation model managed to suppress such instabilities, allowing for a converged solution to be obtained, it may also have prevented us from identifying potentially more severe dynamic loads associated with these instabilities.

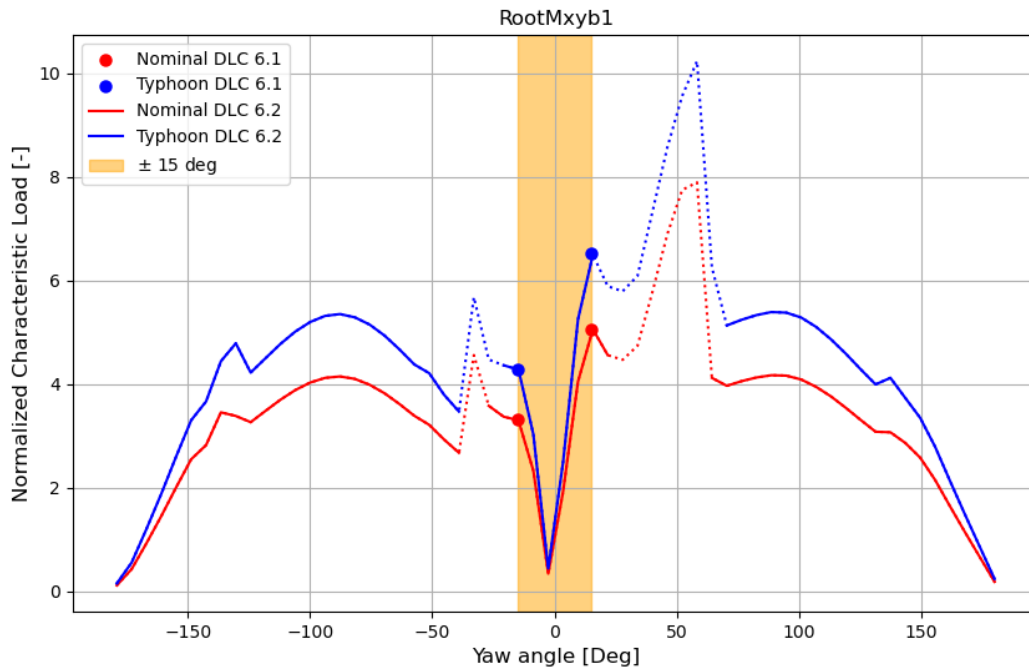


**Figure 23. Blade root combined moments shown as a function of yaw angle between the turbine and the incoming wind. The loads are normalized by the load experienced at zero yaw and IEC Class 1B inflow condition. The dotted lines represent areas with higher uncertainty.**

#### 4.1.6.5 Key Findings, Conclusions, and Limitations for Battery Backup

As a part of this study, the effects of IEC Class I and T-Class winds on the IEA 15-MW reference wind turbine were analyzed for the critical load cases related to extreme winds on idling offshore wind turbines. The scope of this part of the study focused on the largest components like the turbine tower and blade—specifically, the tower-base, tower-top, and yaw-bearing loads. The analysis was intended to quantify the benefits of battery backup systems during loss-of-grid events by comparing the loads experienced by the wind turbine with yaw control and remaining inside the IEC specified  $\pm 15^\circ$  yaw angle region and the loads assessed for unconstrained yaw angles of  $\pm 180^\circ$ .

Our key findings and conclusions are as follows:

- (1) The loads modeling results had an unacceptably high level of uncertainty due to instabilities encountered at high yaw angles, as well as a lack of an accurate dynamic stall model that can predict the correct aerodynamic behavior of the blade at high angles of attack. These effects combined make any quantitative conclusions difficult or impossible.
- (2) The high yaw angle region of instability occurred where higher loads were expected. Further analysis is required to determine the magnitude of the loads over  $\pm 180^\circ$  yaw angle to fully understand the benefits of battery backup for the yaw system.

- (3) Backup power for the yaw drive to maintain a mean yaw error less than  $\pm 15^\circ$  under extreme hurricane wind conditions appears to be a prudent design enhancement to avoid yaw angles where modeling instabilities indicate higher loading.
- (4) The degree to which high-frequency turbulence associated with major hurricanes could generate yaw errors beyond the response time capability of the yaw drive is not known.
- (5) Characteristic loads calculated for DLC 6.2 are identical to the characteristic loads calculated in DCL 6.1 within the  $\pm 15^\circ$  region. Therefore, DLC 6.2 can be waived if battery backup systems and the backup power system have been demonstrated to be reliable. By the same logic, DLC I.2 in Annex I of IEC 61400-3-1 can also be waived.

### *Follow-On Recommendations*

The loads generated in DLC 6.2 may be important to understand because the nature of hurricane turbulence may not be completely understood yet. Rapid changes in the wind direction or wind veer could result in wind gusts that exceed the prescribed  $\pm 15^\circ$  yaw angle region at a rate that the yaw system cannot respond to.

Traditionally, blade designs are driven by operational cases (DLC 1.1 to DLC 4.2), but the effect of hurricane loads compared to operations loads needs to be further studied.

The physics of the extreme wind gust on a large idling wind rotor are not well represented by the normal modeling modules used for operating wind turbines in OpenFAST. Future analysis should incorporate the following enhancement that were not possible in this preliminary assessment:

- To address high angles of attack experienced during extreme cross flow, the aerodynamic model used in OpenFAST, AeroDyn, requires calibration of the dynamic stall model to reflect the unsteady properties of the individual airfoils. The current dynamic stall model was developed for normal operational conditions and therefore lower angles of attack. High-fidelity computational fluid dynamics models, such as Exawind recently developed by NREL, could be used to extract aerodynamic properties under both steady and unsteady inflow conditions and could be used as inputs to calibrate existing dynamic stall models in OpenFAST. Future studies will consider implementing this approach.
- The blade structural model, ElastoDyn, is a reduced-order model based on the Euler-Bernoulli beam theory and does not take into consideration blade torsion or geometric nonlinearities for large blade deflections. BeamDyn, a higher-fidelity structural model within OpenFAST, will be used in future analysis to capture large-angle deflections and torsional deflections that are present under extreme hurricane loading, even though it is more computationally expensive and was out of scope for this project.
- The steady inflow conditions assumed in this study are not representative of realistic hurricane conditions and are not compliant with IEC standards. Future models will only



use the turbulence model or a physics-based turbulence model that captures the temporal and spatial characteristics of microscale (turbine blade scale or smaller) turbulence.

- Also, the current implementation of OpenFAST does not take into consideration nacelle aerodynamic drag loading and nacelle weight, which needs to be included.

It is important to address all these sources of uncertainties in future work. This work is expected to continue under a different project to develop a higher-fidelity dynamic representation of the flow physics of an idling wind turbine rotor under hurricane conditions.

#### **4.1.7 Insurance for Turbines in Hurricane-Prone Areas**

The new risks from extreme weather events such as tropical cyclones (e.g., typhoons and hurricanes) may influence the insurability of offshore wind energy plants. Insuring key construction and operational risks is necessary to render offshore wind projects financeable. The significance of insurance extends beyond the direct premium costs. For a project to obtain debt financing, it must first address the key risks from extreme storms such as hurricanes and obtain insurance before lenders commit funds. Insurability requires reasonable certainty that the insurance coverage can adequately cover the financial losses from key risks—including potential catastrophic damage from major hurricanes—and that the turbine systems are sufficiently resilient to withstand such events.

The risk of a partial or total loss of an offshore wind asset from a hurricane event is typically addressed through two strategies: risk reduction and risk transfer (Table 4):

- Risk reduction strategies are usually applied in the design stage to mitigate known hazards that may lead to partial or total system failure. Risk reduction may be achieved through the adoption of “best design practices” that make the offshore wind system more resilient to the impacts from a major hurricane event. However, the insurance industry has not yet articulated a comprehensive strategy for estimating design risk mitigation.
- Risk transfer involves insurance premiums or collateral to protect against unexpected financial losses from a hurricane event.

The increased costs due to risk reduction and risk transfer for wind plants in hurricane-prone regions are not well understood in the United States because of very limited loss data. Some loss and insurance data are emerging from projects located in the Taiwanese Strait.

**Table 4. Strategies To Address Hurricane Risk***Source: Adapted from Reguero et al. (2020)*

<b>Strategy</b>	<b>Risk Reduction</b>	<b>Risk Transfer</b>
Capital investment to meet more stringent design requirements	Turbine and substations are upgraded to strengthen blades, towers, and sensors, and implement intelligent control systems that enable hurricane ride-through. These measures may be necessary to obtain insurance.	Operational premium payments are lower due to lower failure probability,
Demonstrate resiliency through successful operating experience	Reduced operational uncertainty lowers risk, builds confidence, and caps maximum turbine upgrade costs.	Premiums are reduced when risk reduction is demonstrated. Premiums are reduced from increased competition among insurance providers.
Avoid extreme events through selective siting	Capital investments to upgrade facility for hurricane resiliency will vary depending on site severity.	Premiums may be reduced if risk is demonstrably lower in subregions through weather models.
Reduce uncertainty through advanced research to improve engineering design methods	Advanced high-fidelity computer modeling and design innovations can result in more efficient designs requiring lower up-front investment.	Data from deployed buoys and measurement campaigns to estimate losses and chance of occurrence with higher certainty.

Hurricanes did not initially receive much attention in the offshore wind sector because offshore wind development in European seas was not affected by tropical cyclones. However, several offshore wind projects are now planned in hurricane areas in Asia (e.g., Taiwanese Strait) and North America (Musial et al. 2022). In the United States, most of the lease areas sold on the U.S. OCS are in areas that are exposed to risk from hurricanes (Hallowell et al. 2018). In the North Atlantic, commercial offshore wind farm installations are beginning in 2023 with the 800-MW Vineyard Wind project and the 123-MW South Fork project. Both projects are subject to hurricanes, but the risk profile is considerably lower than comparable projects in the Gulf of Mexico because the external conditions are believed to be within the “normal” design envelope specified by the IEC standards (IEC 2019a; IEC 2019b).

There are very few pricing benchmarks to guide the insurance industry to establish rates for offshore wind premiums in such areas. The lack of hurricane loss records from commercial-scale offshore wind deployment increases the uncertainty of hurricane insurance assessments. This sector also faces limited transferability of experience from related sectors such as offshore oil and gas structures or land-based wind because the design differences and external conditions are pronounced and difficult to compare.

Several of the world’s major energy infrastructure insurance brokers<sup>9</sup> have started to investigate offshore wind hurricane risks and pricing. Despite the nascent knowledge base of the offshore wind insurance industry regarding hurricane risks, we consulted with several insurance experts to understand the impact of hurricane risk on offshore wind insurance premiums in the Gulf of Mexico. We found that hurricane insurance would tend to cover several types of damage, including:

- Physical damage to permanent wind farm property,
- Business interruption and loss of revenue, arising from physical damage to permanent wind farm property
- Contingent business interruption, arising from physical damage to third party owned property (i.e., impacts from damaged assets onto those owned by other parties), such as onshore grid/transmission infrastructure.

These types of hurricane insurance are in addition to the typical risks insured in offshore wind projects, such as property damage during construction and operations, start-up delays, and contractors’ risk (Gatzert and Kosub 2016). In the context of hurricanes, physical damage to permanent wind farm property captures the complete or partial loss of a physical offshore wind asset. Business interruption materializes in the foregone revenue from downtime during and repair of the offshore wind asset after a hurricane event. One major consideration is that the cost to repair physical damage may be affected by replacement times that might be longer for early commercial-stage projects in the United States compared to projects in established offshore wind markets because of supply chain and installation vessel limitations. Contingent business interruption covers damage to the revenue of third parties that results from a hurricane event. Typically, only a fraction of the total offshore wind asset value is insured because a total loss is unlikely, but the maximum loss may not always be easy to determine without loss data. A prior risk assessment typically considers an “attachment” and “exhaustion” point<sup>10</sup> of insurance coverage (Reguero et al. 2020).

Globally, data on turbine system resilience and losses incurred by offshore wind turbines in severe weather and hurricanes is very limited. Most turbines to date are in waters with more benign storm exposure (Swiss Re 2020), and insurance solutions for hurricane- and typhoon-prone areas are only slowly emerging in the Asia-Pacific region (e.g., Taiwan and Japan). U.S. practices for quantifying the risk of hurricanes to offshore wind energy plants are nascent and not yet universally accepted. For quantifying the risk of failure from extreme hurricane-induced wind and waves, a few probabilistic frameworks have been proposed (Hallowell et al. 2018; Wilkie and Galasso 2020). These highlight several challenges, such as a lack of long-term measurements of wind and wave conditions, complexity in modeling spatial-temporal correlations of wind and wave fields from hurricanes, the absence of test data on the structural capacity of full-scale offshore wind components, and the nonlinear structural response of

---

<sup>9</sup> For instance, the insurance brokers Marsh, Aon, or Gallagher.

<sup>10</sup> The “attachment” point refers to the “economic loss at which the insurer would start responding to losses”; the “exhaustion” point defines the “economic loss (and probability) where the insurer would stop covering losses” (Reguero et al. 2020).

offshore wind turbines subjected to hurricane conditions (Hallowell et al. 2018). For practical use, Hallowell et al. (2018) suggest stochastic, numerical models that are oriented toward the Pacific Earthquake Engineering Research Center framework for evaluating earthquake risk (Liu et al. 2012). The model proposed by Hallowell et al. (2018) consists of hazard intensity estimation of wind and wave fields during hurricanes, structural response estimation of offshore wind turbines during hurricane-induced wind and wave, and fragility estimation of axial-flexural loading of offshore wind turbines.

We explored the incremental increase in insurance premiums to account for hurricane risk in the Gulf of Mexico in consultation with industry experts. We found that total insurance expenditures (i.e., encompassing a variety of damages, not just those incurred from hurricanes) for damage to property ranges typically between 1.5% and 3.0% of capital expenditures, and business interruption insurance falls between 15% and 25% of operational expenditures.<sup>11</sup> The insurance premium varies among market regions because of the available claims data, weather data, market maturity, exposure to third party legal liability, number of globally diversified insurers (Gatzert and Kosub 2016), and—relevant in our context—hurricane risk (Table 5).

**Table 5. Difference in Indicative Insurance Premiums for Offshore Wind Between Regions**

Scenario	Damage to Property			Business Interruption		
	UK	US NE	US Gulf	UK	US NE	US Gulf
P60 (moderate)	100%	129%	152%	100%	126%	148%

Note: For a revenue period of 30 years; insurance premiums based on fixed-bottom offshore wind technologies; UK = United Kingdom; US NE = U.S. Northeast.

From our expert consultation, we find that property damage and business interruption insurance rates for projects located in the Gulf of Mexico are nearly 20% higher than for those in the U.S. Northeast, which we conclude is due mostly to the higher risk of major hurricanes that could potentially exceed design conditions. Using these data points, the combined insurance premium for property damage and business interruption from hurricane events amounts to about \$1–\$2/MWh.<sup>12</sup> This is a rather small expense to the project but does not consider the separate capital expenditures for risk reduction to upgrade the offshore wind plant for hurricane resilience. Enhanced natural catastrophe modeling of site-specific environmental conditions and project design parameters can contribute to a better assessment of loss exposure and thereby lower insurance premiums. On the other hand, a growing concentration of projects in regions that are exposed to the same natural catastrophe risk (such as hurricanes in parts of the United States and the Taiwanese Strait) could restrict the capability of a relatively small number of specialist offshore wind insurers to provide such insurance, which might result in higher premium levels.

Beyond these more traditional forms of insurance to cover hurricane risks, some suggest that turbines deployed in natural catastrophe areas can be better covered by parametric insurance,

<sup>11</sup> These estimates exclude insurance premium tax, which typically varies by region.

<sup>12</sup> Assuming indicative capital expenditures of \$3,500 per kilowatt (kW), operational expenditures of \$120/kW-year, a net capacity factor of 40%, and a fixed charge rate of 5.5%.

such as insurance-linked securities and catastrophe bonds (SwissRE 2020). Further, asset owners with a diverse set of generation assets that are exposed to uncorrelated risks might also be better equipped to carry the risk of an offshore wind farm in a hurricane-prone region.

## 4.2 Long-Term Hurricane Research Needs

The design uncertainty and risk posed by major hurricanes is not fully addressed by the design enhancements and strategies described above, but they reflect current best practices that are suitable for the North Atlantic development that is currently underway. Additional investment in hurricane research and commensurate advancements in new design methods and tools are needed to lower project risk and minimize loss probabilities with a goal to achieve the same structural reliability as offshore wind turbines in other regions. The current design approach for hurricane design, based on IEC wind turbine standards, is to use T-Class turbines to survive an extreme 3-s gust with a robust battery back-up for the yaw system. Similarly, combined wave/current design loads on the support structure use basic recommendations from Annex I of IEC 61400-3-1. However, this design approach may oversimplify the complexity of the hurricane event, both in its intensity and duration, leaving the possibility that other damaging DLCs might exist in the form of extreme microscale vorticity, extreme wind updrafts, extreme wave conditions, storm surge, wind/wave misalignment, and low-cycle fatigue due to repeated wind/wave buffeting. To date, the examination of these internal hurricane extreme turbulent structures has been out of reach with the available engineering tools.

Recent advancements in high-fidelity coupled atmospheric-oceanic modeling that can only be done on high-performance computers can now be applied to the analysis tools to simulate extreme hurricanes with high resolution and incorporate detailed physics where necessary. These hurricane simulations can evaluate turbine-scale turbulence features embedded in storms that were previously not detectable. From these learnings, the lower-fidelity engineering tools and design methods can be upgraded to more accurately account for the extreme conditions. The goal would be to develop a lower-fidelity hurricane simulator with the spectral properties of the extreme wind fields across the rotor plane that can be incorporated into our turbine design and analysis tools. By applying the synthetic wind fields to the engineering models, responses of idling offshore wind turbines can be analyzed during various hurricane events to search for conditions that may not be covered by the current design standards and codes. Similarly, irregular waves that occur simultaneously during extreme wind events can be modeled. Extreme hydrodynamic loads may potentially occur from wind/wave misalignment, steep wave crests, or the impact of breaking waves and combinations of these events with extreme winds may lead to new load cases.

This recommended future research could accelerate and enable new wind turbine designs and improve upon the current best practices for offshore wind turbine design in hurricane-prone regions in the United States and, in particular, the Gulf of Mexico. Reducing design uncertainty through advanced hurricane design methods will reduce the probability of catastrophic failures, allow designers and developers to manage financial and project risk at acceptable levels, and ultimately reduce turbine and project costs in hurricane-prone regions. Some of this research has already begun (Sanchez Gomez et al. 2023; NOWRDC n.d.).

Short-term forecasting of weather systems roughly 1–3 days in advance is vastly improving; however, long-term weather system changes happening on a regional (and global) scale of 30

years or more into the future will be very important to understand because turbines installed today will be operating in those conditions. The term “climatology” generally refers to the statistically expected climate regime on a 30-year timescale, but the climatology of most regions is changing rapidly as the planet warms. Notably, climate change models indicate that storm tracks for tropical cyclones in the United States are shifting poleward. Further, the fraction of tropical cyclones expected to reach very intense levels (Categories 4 and 5) is projected to increase over the 21<sup>st</sup> century (Shaw et al. 2016; Intergovernmental Panel on Climate Change 2021). While most offshore wind turbine designs currently assume that climate statistics are static over a project’s lifetime, there is mounting evidence that indicates increasing tropical storm frequency and severity. Therefore, future offshore wind designs in the Gulf need to account for climatological changes due to climate change in the design process.

## 5 Infrastructure

Various types of infrastructure must be in place for successful offshore wind farm installation and operation. Specialized ports, grid infrastructure, and vessels are necessary to support offshore wind development and operations. Although some of this infrastructure may already exist, further investments will be needed to upgrade existing facilities to meet the requirements for component handling, lifting, and throughput. Some ports in the Gulf may be able to avoid the full cost of greenfield or brownfield construction due to their more advanced state in the offshore industrial sector. For example, ports already exist along the Gulf Coast, but they may not meet the offshore wind specifications for upland laydown area for blades and substructures, or they may have overhead air gap constraints that limit tow-out options. Building new ports or adjusting existing ports is very expensive and can potentially influence where the wind farm is going to be installed, because distance from port also increases installation as well as operations and maintenance costs. Section 5.1 identifies different types of ports that are used for various offshore wind activities and discusses which ones show the most promise for supporting offshore wind development in the Gulf of Mexico. The location, quality, and type of grid infrastructure must also be evaluated. The length of export cabling that connects the offshore wind farm to the onshore substation influences the total cost of the wind farm. Further, the rated capacity of the wind farm must be able to safely connect to the grid with points of interconnection that are able to take large power injections. Section 5.2 identifies the challenges for offshore wind energy grid integration in the Gulf of Mexico.

### 5.1 Ports

The Gulf of Mexico has a wind resource that may be tapped by both fixed and floating wind technology. The BOEM Call Area extends from the extensive shallow waters near shore to deeper waters that are delineated by the 400-m isobath. Floating turbines are assumed for depths above 60 m. Fixed and floating technologies have different requirements for port capabilities. The Gulf of Mexico has a diverse array of ports that could potentially support both fixed and floating turbines with some upgrades.

Offshore wind is a nascent industry in the U.S.; however, ports in the Gulf of Mexico also have experience serving two other relevant industries: land-based wind and offshore oil and gas. The state of Texas handles more wind-specific imports than any other state, representing around two-thirds of total U.S. wind component imports in 2021 (Wiser et al. 2022). Although some items enter via land-based points of entry along the Mexican border, the majority of these components are handled by ports in the Gulf of Mexico. The offshore oil and gas industry is supported by a wide range of manufacturing facilities and skilled workforce around the Gulf Coast that could transition to supporting offshore wind (Shields et al. 2023).

Different port types (Table 6) are designated to host a variety of activities during the life cycle of an offshore wind project. The manufacturing ports receive raw materials that are used to construct larger pieces in the supply chain. The staging and integration, or marshaling ports, are used to receive, stage, and store components in the offshore wind supply chain. In the case of floating turbines, the staging and integration ports are also used to assemble the wind turbine and support structure and commission the assembly before towing the system to its operating site. Operations and maintenance (O&M) ports serve as a base for operations, and contain offices, warehouses, storage of spare parts, and facilities that can support O&M vessels.

**Table 6. Port Types for Offshore Wind Energy**

<b>Category</b>	<b>Description of Activities</b>
Manufacturing	Fabrication facilities for any components that will be supplied locally such as support structures, towers, blades, or cables
Staging and Integration (or Marshaling)	Fixed-bottom offshore wind: staging of major components, berthing of wind turbine installation vessels, pre-construction survey vessels, and additional vessels required during construction such as cable lay vessels, heavy lift vessels, etc.  Floating offshore wind: final assembly of wind turbine and support structure, staging of major components, berthing of pre-construction survey vessels, anchor handling tug supply vessels, cable lay vessels, etc., support for major component repairs
Operations and Maintenance	Berthing of crew transfer vessels and service operations vessels, spare parts storage, operations management

The U.S. offshore wind industry has already leveraged capabilities at Gulf ports to support projects along the Atlantic Coast. The jacket foundations used at the Block Island Wind Farm were built in Houma, Louisiana. The first U.S. wind turbine installation vessel is under construction in Brownsville, Texas, and an offshore wind service operations vessel is being built in Houma (Revolution Wind 2023).

The criteria that we used to identify candidate ports for staging and integration are listed in Table 7. The criteria for fixed-bottom offshore wind were adopted from Crown Estate Scotland (2020) and Parkison and Kempton (2022). These ports should be able to provide berths for wind turbine installation vessels, heavy lift vessels, and other specialized vessels for the installation of offshore wind power plants. Land adjacent to the waterfront (upland area) is required to stage wind plant components. Although proximity to offshore wind sites plays an important role in identifying candidate ports, there can also be opportunities for more distant ports to be involved, particularly in component fabrication. In this report, however, we focus on potential staging and integration port locations, which introduce spatial variation in installation costs for offshore wind projects in the Gulf of Mexico.

For floating wind turbines, staging and integration ports provide a sheltered location for the wind turbine and floating substructure to be joined together. Screening criteria for staging and integration ports for floating offshore wind were adopted from Porter and Phillips (2016) and Trowbridge, Lim, and Knipe (2023). These ports must have sufficient upland area (15–25 acres) in which to stage wind turbine components and possibly substructures. Assembly of wind turbines and substructures requires very large cranes capable of lifting the nacelle and rotor (600 tonnes or more) over 150 m (500 ft) above the ground. Completed wind turbine and substructure assemblies require wet storage space, which may also be used to stage substructures before integration. Ports used for staging and integration for floating turbines cannot have air draft restrictions (height limits) that would impede the passage of structures more than 250 m (820 ft) tall. The required water draft (water depth) for ports supporting floating offshore wind depends on the specific substructure design; to identify candidate ports we assume that the required draft will be close to 12 m (38 ft).



**Table 7. Screening Criteria for Staging and Integration Ports**

Port Screening Criteria	Fixed-Bottom Offshore Wind	Floating Offshore Wind
Draft at berth, minimum	10 m (32 ft)	12 m (38 ft)
Air draft, minimum	80 m (260 ft)	Unlimited
Upland area, minimum	6–10 ha (15–25 acres)	12–40 ha (30–100 acres)
Channel width, minimum	25 m (80 ft)	60 m (200 ft)
Wharf length, minimum	400 m (1,300 ft)	460 m (1,500 ft)
Distance to site, maximum	400 km (220 nm)	400 km (220 nm)

The ports of Brownsville, Corpus Christi, Freeport, Houston, Galveston, Port Fourchon, Gulfport, Pascagoula, and Mobile were identified as potential staging and integration ports in the region (Figure 24).

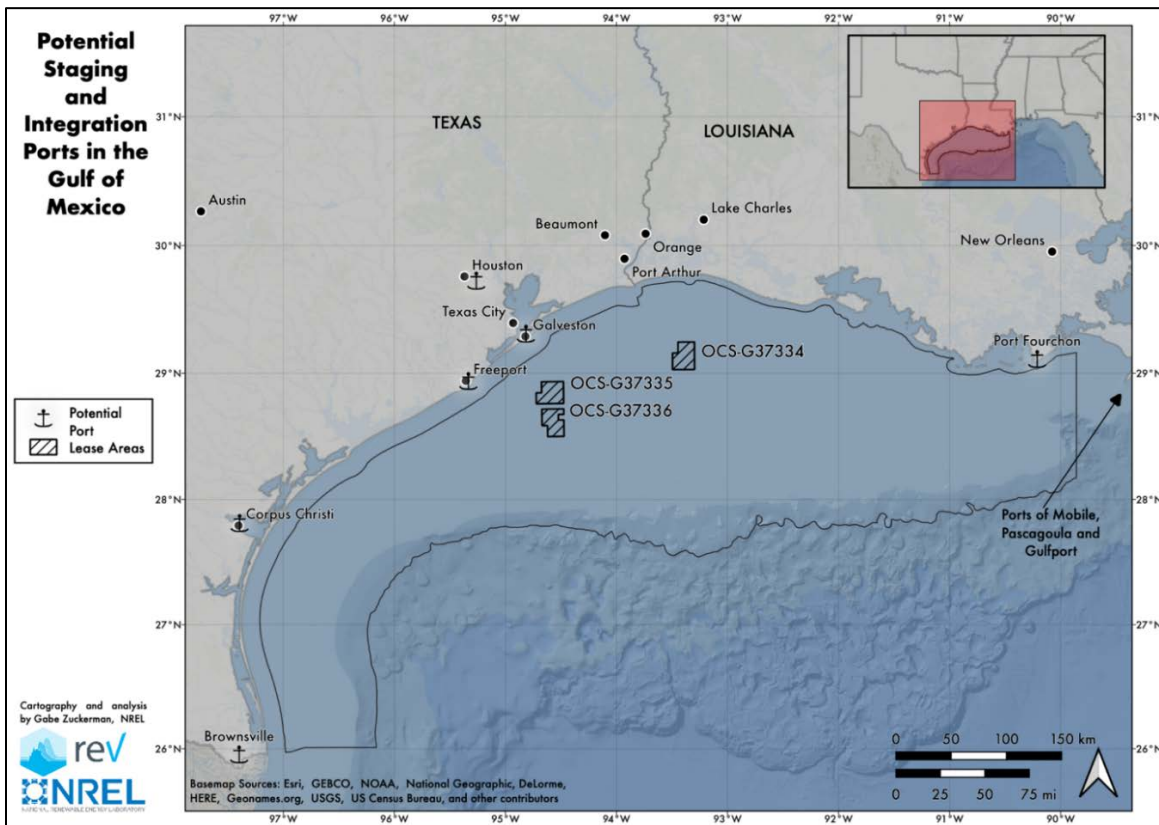


**Figure 24. Potential staging and integration ports in the Gulf of Mexico.**

*Map by Gabriel Zuckerman, NREL*

These ports can serve as input data in an offshore wind energy spatial cost model. More specifically, the location of the ports can be used to calculate the distance from port to the offshore wind site, which provides information about differences in cost when comparing different offshore wind sites. This analysis is part of a forthcoming NREL cost study expected to

be published in April 2024 where the levelized cost of energy for the Gulf of Mexico will be assessed and integrated with cost modeling on a national scale.

## **5.2 Challenges for Offshore Wind Electric Power Delivery**

A major challenge for offshore wind is the deliverability of the electricity produced to a viable offtaker that can purchase the electricity and generate enough revenue for the wind farm to make it profitable. A significant part of the wind farm cost is in the electrical infrastructure to collect the power from the individual turbines and deliver it to a land-based POI, which is typically a substation connected to the larger electricity network with sufficient capacity. Usually, the substation will need to be upgraded at some additional cost, and often the transmission network that it connects to will also need upgrades. When the costs of offshore wind are calculated through our techno-economic models, these additional transmission upgrade costs are not known and are usually not included. Ultimately, they must be accounted for, but it is not usually clear who pays those costs. This cost allocation varies considerably, depending on the policies of the state and local utilities and whether the project qualifies for federal subsidies that may be available.

### **5.2.1 Gulf of Mexico Energy Use Profiles**

Most of the electricity that could be generated in the BOEM Gulf WEAs (Figure 7) would be delivered to either Texas or Louisiana due to their relative proximity. Both states are heavy producers and users of energy from fossil fuels. Louisiana produces about 9% of the country's natural gas and controls about 20% of the nation's oil refining capacity. Louisiana ranks fourth among the states in total energy consumption and ranks second in the nation based on per capita energy consumption. It also has the second highest per capita residential sector electricity consumption in the nation largely because it uses electricity extensively for both heating and air conditioning. Texas is the nation's top crude oil (43%) and natural gas producing (25%) state. In 2021, Texas also produced about 26% of all U.S. wind-powered electricity generation. Texas produces more total electricity than any other state but also uses more energy than any other state across all sectors.

In both Texas and Louisiana, the industrial sector, which includes refineries and petrochemical plants, accounts for over half their energy consumption (Figure 25). In Louisiana the industrial sector makes up over 72% of all energy, which is quite different than the profiles of most Northern states. These massive industrial loads tend to be much more distributed and do not typically depend on electric power from the grid. Therefore, in the Gulf of Mexico, offshore wind power offtakes may not always be an electric utility grid operator. Offtakes may be directed toward other energy users to serve the distributed industrial load directly.

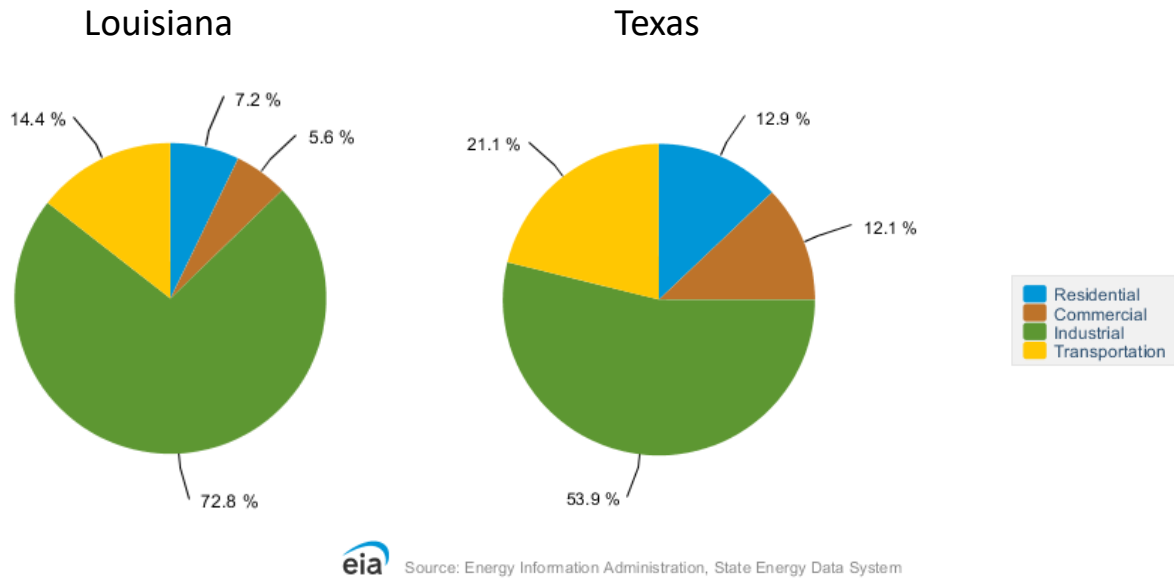


**Figure 25. Energy consumption by end-use sector for 2020.**

Source: Energy Information Administration (EIA) (2023b)

### 5.2.2 Points of Interconnect Assessment

In 2021, the regional intergovernmental renewable energy task force that was formed among the Gulf States of Texas, Louisiana, Mississippi, and Alabama expressed reservations that grid integration of offshore wind could be a potential barrier. In particular, the cable landings and points of interconnect were raised as an area of high uncertainty which motivated this part of the study.

This section describes a first order method used to identify points of interconnect to the electric grid for offshore wind along the coasts of Louisiana and Texas adjacent to the BOEM Call Area. The results inform the export and land-based interconnection cost estimates by providing a clearer breakdown of these additional costs and a first order screening of possible POIs. The possible alternative use of the offshore wind power to serve the region’s large industrial loads is complex and is beyond the scope of this report but we recommend that future studies examine these opportunities more fully.

#### Local Utility Engagement

A top-level literature survey conducted by NREL showed a sparsity of utility planning reports from around the region indicating that the consideration of offshore wind was at a very early stage. In some conversations, it was clear that utility planners were becoming more engaged. As such the best course of action was to seek data directly from subject matter experts involved with regional utility planning or with experience in offshore wind power transmission in the region.

We interviewed technical stakeholders from the following organizations to help develop an understanding of the issues regarding the integration of offshore wind in the gulf:

- American Electric Power

- Entergy Louisiana
- A Louisiana state representative
- Midwest Independent System Operator (MISO)
- Electric Reliability Council of Texas (ERCOT)
- RWE Renewables
- Gulf Wind Technologies
- Louisiana Governor’s Office of Climate Task Force
- Mainstream Renewable Power

Most technical experts expressed a positive interest in offshore wind becoming part of the energy mix in the region because it could potentially help balance energy load in coastal regions where there is currently not much electric generation. They also felt it could add diversity to the electric generation mix while complementing the daytime peaks from future solar energy generation. Some of the experts interviewed felt that the significant thermal generation capacity is unlikely to be fully decommissioned because they believe that the coal plants will eventually be replaced by more efficient natural gas, and methods for carbon capture and sequestration will become available that can compete with renewable sources.

Some of the experts interviewed suggested that Port Fourchon, Cameron liquefied natural gas terminal (LNG), Sabine LNG terminal, Cheniere LNG terminal, and Lower Terrebonne may be possible POIs. However, Port Fourchon and some of these other possible POIs currently lack high voltage transmission lines to move the power to other regions. Therefore, injection of offshore wind at these substations would require upgrades of transmission lines or local industrial electricity offtakers. A full assessment of the energy loads in these regions was not conducted.

In Louisiana, the governor’s state task force is building a consortium to create a pilot project in state or federal waters, using funding from the Infrastructure Investment and Jobs Act (also known as the Bipartisan Infrastructure Law), to demonstrate the feasibility of offshore wind energy to produce green hydrogen<sup>13</sup> as an industry energy source. Louisiana has set a goal of 5 GW of offshore wind energy by 2035 (State of Louisiana 2022).

ERCOT is not including offshore wind in their transmission planning studies yet. ERCOT has a significant amount of installed thermal generation capacity with no plans to have it fully decommissioned. Their current plans are to replace their remaining coal plants with efficient gas-fired generation and have a strong interest in carbon capture and storage technologies.

### *Methods for Identification of POIs*

A comprehensive set of publicly available geographic information system (GIS) data is in the U.S. Energy Atlas which is maintained by the U.S. Energy Information Administration (EIA). These data contain vital information about the locations, characteristics, and capacities of most

---

<sup>13</sup> Green hydrogen is made from renewable energy sources to run electrolyzers that separate H<sub>2</sub> and oxygen from water. Most hydrogen today is made by separating hydrogen from methane which emits carbon dioxide into the atmosphere.

substations, transmission lines, and power plants in the Gulf of Mexico region and were used to screen out unlikely onshore POIs ([EIA 2021](#)).

Data for [electric power transmission lines](#) used a GIS dataset that represents electric power transmission lines from 69 kV to 765 kV. Underground transmission lines are also included where sources were available (EIA 2021).

Data for [electric substations](#) used a GIS dataset that represents electric power substations primarily associated with electric power transmission voltages ranging from 69 kV up to 765 kV. It includes tap locations where two power transmission lines are joined ([HIFLD]).

Data for [power plants](#) used a GIS dataset that represents operable electric generating plants in the United States by energy source. It includes all plants with a combined nameplate capacity of 1 MW or more that are operating, are on standby, or are temporarily or permanently out of service. ([EIA 2023a](#))

We used QGIS, an open-source software tool that allows viewing and analysis of geospatial data, to analyze the databases to identify substations that are most likely to serve as POIs. We assumed that substations that meet the following criteria would be the most likely to be able to support offshore wind electric power injections:

- Multiple transmission lines per substation
- At least one line at 345 kV or higher
- Substation or power plant must be close to shore (modeling judgement based on experience on whether to include)
- Higher apparent power (total current and voltage, including true and reactive power) with zero or one contingency.<sup>14</sup>

Because running power flow and contingency analysis models were not in scope for this project, ranking substations with higher apparent power and either zero or one contingency was the default proxy used to identify plausible POIs. Figure 26 shows the workflow with steps used to prioritize plausible POIs.

---

<sup>14</sup> A contingency is the loss or failure of a small part of a power system, such as a transmission line, or the loss or failure of individual equipment, such as a generator or transformer.

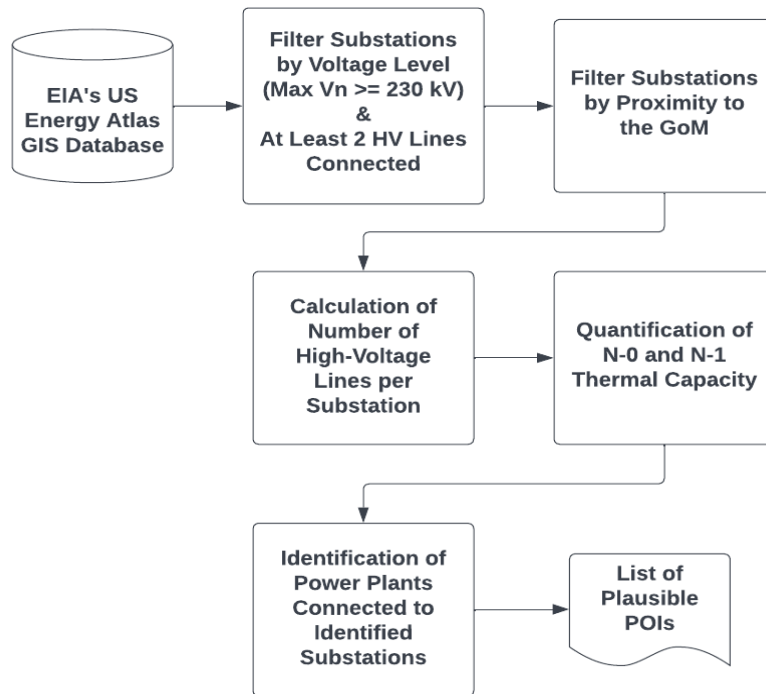


**Figure 26. Workflow to identify plausible POIs**

### 5.2.2.1 Most Plausible POIs and Approximate Costs for Interconnection

The primary purpose of this POI analysis was to provide realistic land-based targets for landing export cables in the techno-economic models that are used to perform the offshore wind cost analysis that will be published in a separate BOEM funded report in April 2024. The levelized cost of energy for offshore wind in the Gulf of Mexico is dependent on the length of the export cable that extends from the offshore substation to the land-based point of interconnect. The cost also varies depending on the route and location of the shore landing that the cables take to get there. To find the approximate cost, we developed a least cost path (LCP) algorithm that traverses a 90-m resolution cost surface from a point on the coastline to the POI and includes the cost to tie into a substation. The cost to traverse a 90-m cell in the cost surface was approximately \$227,000, with multipliers applied to adjust for different land uses (e.g., it is more expensive to move through mountainous terrain than pastureland) with some cells excluded due to the presences of natural or cultural resources (Cole et al. 2021). The algorithm finds all the paths from one point on the coastline to all the POIs, and selects the one with lowest cost, which is not always the shortest path. Cost results are not exact due to the dynamically changing economics of offshore wind and the maturity of the LCP model. Therefore, the primary goal of this analysis was to show relative costs. The cost results also do not include the offshore cable routing, which is a significant cost in offshore wind projects. The onshore cable routing costs, as analyzed here, are not the full costs of cable routing for an offshore wind project. For example, if the least expensive onshore cable path in the Gulf of Mexico is used, it does not necessarily mean the least expensive total cable cost will be realized, and it heavily depends on the cost of the offshore cable, influenced by how far the wind site is from shore.

Table 8 shows 25 most plausible POIs in the Gulf of Mexico offshore wind Call Area, based on the first order methodology described earlier.

**Table 8. List of the 25 Most Plausible Points of Interconnect in the Gulf of Mexico Call Area**

#	ID	Name	Latitude	Longitude	# of Lines	Nominal Voltage [kV]	# 115 or 138 kV Lines	# 230 kV Lines	# 345 kV Lines	# 500 kV Lines	N-0 Capacity [MVA]	N-1 Capacity [MVA]
1	300463	DOW VELASCO	28.99	-95.36	10	345	6		4		6,296	5,058
2	302357	CEDAR BAYOU PLANT	29.75	-94.92	16	345	10		4		7,192	5,954
3	303120	CAVERN	29.03	-95.34	2	345	2		2		2,924	1,686
4	303708	PH ROBINSON	29.49	-94.98	16	345	12		3		6,402	5,164
5	304335	DEER PARK ENERGY CENTER	29.71	-95.14	5	345	1		3		3,938	2,700
6	304795	SOTEX5	28.80	-96.05	15	345	2		9		11,590	10,352
7	304846	CHAMBERS	29.77	-94.90	3	345	1		2		2,700	1,462
8	305373	TAP305373	29.46	-95.26	3	345	2		2		2,924	1,686
9	305725	RIO HONDO	26.28	-97.61	8	345	5		3		4,834	3,596
10	305746	UNKNOWN	26.15	-97.64	2	345			1		1,238	0
11	306047	UNKNOWN	27.85	-97.62	11	345	6		3		5,058	3,820
12	307020	UNKNOWN	28.72	-97.21	6	345	3		2		3,148	1,910
13	307073	UNKNOWN	28.25	-97.34	2	345	1		1		1,462	224
14	309711	UNKNOWN	27.09	-97.77	3	345	1		2		2,700	1,462
15	310370	MEADOW	29.46	-95.26	3	345	2		2		2,924	1,686
16	111779	NELSON	30.28	-93.30	3	500	6	7		2	10,965	8,433
17	149778	RICHARD	30.43	-92.41	13	500	8	1		2	7,507	4,975
18	149836	UNKNOWN	30.26	-91.17	3	500		1		2	5,715	3,183
19	150229	WATERFORD 500KV	29.99	-90.48	2	500		7		1	7,089	4,557
20	151247	WELLS	30.45	-92.14	5	500		2		3	8,898	6,366
21	173166	UNKNOWN	30.21	-93.40	2	500		1		1	3,183	651
22	173167	UNKNOWN	30.28	-93.44	3	500				3	7,596	5,064
24	306010	HARTBURG	30.27	-93.74	6	500		1		4	10,779	8,247
25	307475	CYPRESS	30.30	-94.26	7	500	3	1		1	3,855	1,323
26	300348	UNKNOWN	27.56	-97.67	2	345			2		2,476	1,238

To validate this list, a full power flow analysis would be needed, which was not part of this study. It is likely that this list would be further reduced after conducting such a study. This list, however, narrows down the options that are available for conducting techno-economic analysis

for renewable energy projects connecting to the power grid in the region. If the electric power is being delivered to heavy industry for industrial processes, these criteria may also be different.

We evaluated the POIs suggested earlier in interviews with grid technical experts to our list of the 25 most plausible POIs in Table 8. Based on our filtering criteria:

- Port Fourchon – Waterford 500 kV substation listed on row 19 is on our list of plausible POIs; further investigation is recommended.
- The Cameron LNG POI has only a 69-kV substation which is below our limit of 345 kV limit. Therefore, it is unlikely to be a primary candidate for grid offtake.
- The Sabine LNG POI was eliminated because it’s 220 kV was below our limit of 345 kV.
- The Cheniere LNG POI substation is only 69 kV, which is below our limit of 345 kV.
- The Lower Terrebonne POI has only 115 kV lines connected, which is below our limit of 345 kV; however, the Port Fourchon - Waterford POI is nearby and is on our list.

Figure 27 illustrates the locations and approximate costs and routes for interconnecting to the 25 POIs in Table 8. Onshore interconnection costs tend to increase nearer to New Orleans and farther southwest from the lease areas, because the cable lengths tend to increase to reach the onshore point of interconnection that are located further from the coastline.

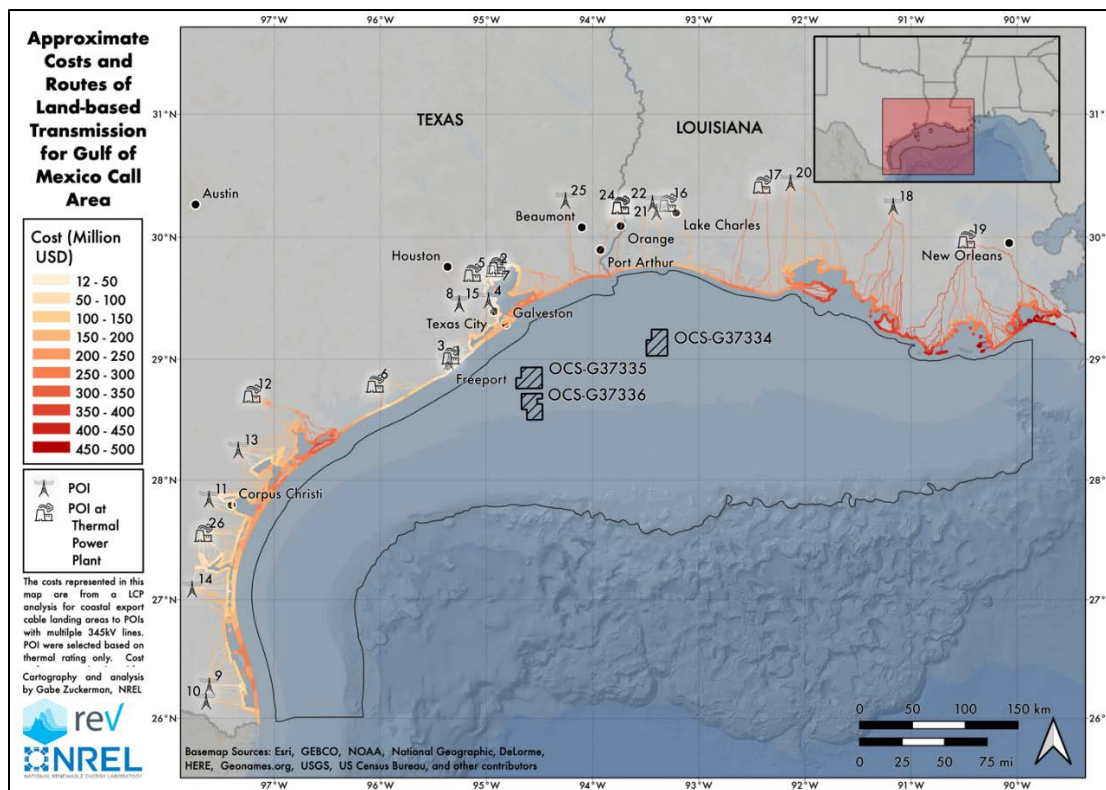


**Figure 27. Locations and approximate costs and routes for interconnecting to the 25 most plausible POIs in the Gulf of Mexico.**

*Map by Gabe Zuckerman, NREL*



### **5.2.3 Summary of Findings**

The Gulf of Mexico is dominated by industrial loads, but many of these loads are in the oil and gas sector, which may be able to use some of the power in the short term, but long-term usage is not clear.

All high-voltage substations in the EIA Energy Atlas were considered in the initial step, and 25 POIs were identified as plausible points of interconnect in the final pass. The 25 selected POIs have at least one 230-kV transmission line and more than one transmission line. They were used as the primary interconnection points for the Gulf of Mexico cost analysis that is forthcoming and will be published in a separated BOEM-funded report by NREL in April 2024.

Interconnecting offshore wind in the Gulf of Mexico appears to be feasible. There are several plausible POIs near the coast with 230-kV or greater high-voltage transmission lines. Although many of these lines would still need to be upgraded to handle gigawatt-scale power injections, the difficulty of making grid connections in the Gulf region is generally not much different than offshore wind development on the Atlantic Coast. The primary difference is that the level of grid planning for offshore wind in the Gulf is at an earlier stage. This has not been the case for land-based wind where Competitive Renewable Energy Zones were developed in Texas in advance of development, which facilitated enormous wind industry growth.

### **5.2.4 Challenges for Offshore Wind Integration in the Gulf of Mexico**

Texas produces more wind energy from land-based wind resources than any other state, which has contributed to wind energy becoming the lowest-cost electric energy source nationally. It is unlikely that the levelized cost of electricity for offshore wind will ever become as low as land-based wind from the Texas panhandle, even though the cost for offshore wind is expected to fall significantly in the coming years. However, additional value for offshore wind may be found in the proximity of the resource to the coastal load centers in southern Louisiana and Texas, which may be difficult to serve with land-based wind electricity. The offshore wind load-matching characteristics may offer some additional grid benefits, but this analysis was not part of the study.

Limited POI headroom capacity is available, as is the case in other regions with high potential for offshore wind deployment. New grid capacity may not become available as rapidly as in other regions because the existing thermal generation may be slower to transition to renewable energy due to plans to retrofit coal plants with more efficient gas-fired generation.

Current long-term transmission expansion plans do not yet account for offshore wind projects in the Gulf of Mexico, but the challenges appear to be similar to other regions, including the availability of idle transmission network capacity to accommodate new offshore wind generation, difficulties in developing new transmission infrastructure, competition for the same transmission resources by other generation resources, and lengthy interconnection queues.

### **5.2.5 Limitations to the Findings**

The headroom capacities of prioritized POIs have not been quantified. We recommend further research to quantify available headroom capacities for prioritized POIs and to identify network reinforcements that would further enable offshore wind integration.

A full cost analysis was not completed for this report but is forthcoming. The cost models used do not include the additional cost to upgrade the land-based transmission system beyond the POI or the integration costs associated with offshore wind. The data from this task provide the necessary inputs to complete the techno-economic levelized cost of energy analysis, but only a qualitative assessment of these additional transmission costs and the feasibility of interconnecting offshore wind energy was done here.

### **5.2.6 Recommended Next Steps**

The following next steps are recommended:

- Refine the list of plausible POIs by considering multiple technical factors, such as likely distance to an offshore platform, voltage levels, and network topology.
- Review existing grid planning studies in the region to better understand the grid constraints and planned actions to reinforce the system, with the goal of refining the selection of plausible POIs.
- Assess the relevant power system simulation models for the region and quantify the headroom capacities by means of power system analyses such as AC power flow, contingency, and system strength.
- In the case of insufficient headroom capacity, identify sets of network reinforcement options to enable the connection of up to the maximum offshore wind potential in the lease areas.
- Assess transmission upgrade costs, based on publicly available transmission cost databases.
- Conduct future energy planning based on scenarios that consider shifting energy use profiles that reflect various deployment levels of offshore wind.

## 6 Other Technology Challenges

In this section, we examine additional technical challenges impacting offshore wind energy development in the Gulf of Mexico. Average hub-height wind speeds in the Gulf range from 7.0 to 8.8 m/s (Figure 8), which are lower than other regions where significant offshore wind development is currently being planned (Draxl et al. 2015; Bodini et al. 2021; Bodini et al. 2023-forthcoming). Lower average wind speeds pose challenges for wind plant economic viability because less kinetic energy is available in the wind, so additional steps must be taken in the turbine design to maximize wind plant performance. A full discussion of customizing turbines for the Gulf of Mexico is outside the scope of this work, but we compare the performance of generic turbine designs (Gaertner et al. 2020) with conceptual turbine designs that follow industry-accepted practices for low-wind-speed regions, which include increasing rotor size relative to the generator size (lower specific power [SP])<sup>15</sup> to capture more incoming wind energy (See Section 6.2). This includes an assessment of the gross capacity factors (GCFs) for four turbines, using the updated wind resource dataset developed for the Gulf region (Section 3).

Additionally, soft soil conditions pose challenges to the deployment of common fixed-bottom substructure designs like monopiles; wider multi-pile designs like jacket substructures may be better suited for the Gulf of Mexico. As such, we developed conceptual jacket substructure designs for each turbine considered, sized according to turbine rating, with higher turbine ratings requiring larger and heavier jackets.

### 6.1 Low Wind Speeds in Hurricane-Prone Areas

Designing for low wind speeds while also designing for hurricane survivability may seem counterintuitive (Section 4). In the Gulf of Mexico, low-SP turbines designed to maximize energy capture at low-wind-speed sites must also be able to survive the extreme high winds of the 50-year return period hurricanes. The complication is that the longer blades required to increase energy capture also require taller towers, and the net result creates higher exposure to the extreme winds. The additional cost to upgrade the turbine's strength for this purpose may be offset by the additional energy that can be produced, but that optimization was not performed in this study. Specific power is expressed in watts per square meter ( $\text{W}/\text{m}^2$ ). Turbines with lower SP ratings (larger rotor-to-generator-rating ratio) capture more energy at low wind speeds, have higher capacity factors, and have lower wake losses for the same turbine spacing.

The more mature land-based wind energy industry has been using this practice of siting low-SP wind turbines in low-wind sites for many years, which has enabled economical wind energy projects in low-wind sites that were dismissed by industry practitioners a couple decades ago (Wiser et al 2023). This trend is shown in Figure 28. The plot, which spans approximately 25 years, shows an almost steady downward trend toward lower-SP machines that largely correlates with siting turbines at lower-wind-speed sites to increase energy production and maximize the financial return of the project. The figure shows that in the late 1990s, when projects would seek only the highest-wind-speed sites, the SP was averaging nearly  $400 \text{ W}/\text{m}^2$ . By 2020, the average SP had reached about  $230 \text{ W}/\text{m}^2$ .

---

<sup>15</sup> Specific power is the ratio of the generator nameplate rating to the rotor-swept area in watts per square meter.

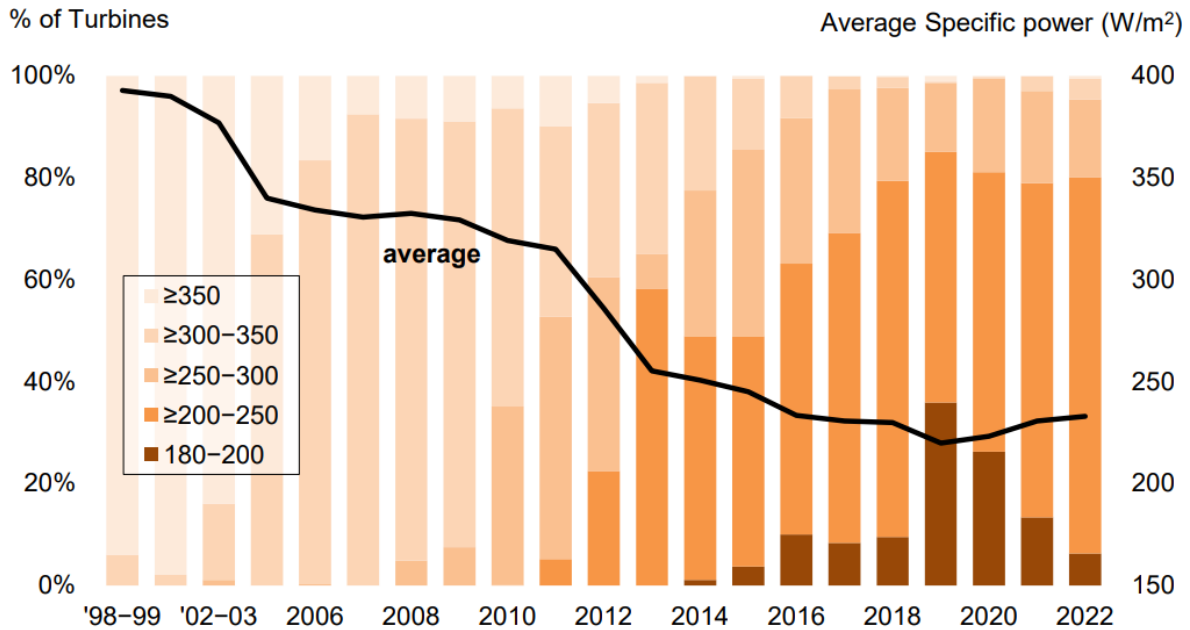


**Figure 28. Land-based wind turbine trend toward lower specific power.**

Source: *Wiser et al. (2023)*

Offshore wind is a younger industry, and developers have focused on higher-wind sites and higher generator ratings like the land-based industry originally did. When the offshore wind energy industry eventually expands into lower-wind-speed sites, like the Gulf of Mexico, lower-SP machines may be necessary to achieve viable project economics. This low-wind-speed optimization has been hindered by the offshore wind industry’s push for turbine upscaling of the generator rating, which tend to drive SP higher, which is suboptimal for low-wind-speed regions.<sup>16</sup>

Most of the newest European-produced offshore wind turbine models are designed for higher average wind speeds than those present in the Gulf of Mexico (e.g., 9 m/s and above) and can operate efficiently in markets like the North Sea with SP ratings of 350 W/m<sup>2</sup> or higher. Turbine manufacturers in China are beginning to offer offshore turbines for lower-wind-speed markets with SP ratings near 300 W/m<sup>2</sup>, but these turbines are not yet being considered for U.S. markets. Table 9 presents SP data for announced turbines from the largest OEMs, sorted from lowest to highest SP. The table shows that available offshore wind turbines have a power rating ranging from 14 to 18 MW, and SP ranging from 292 to 368 W/m<sup>2</sup>. The NREL conceptual design that we will use to assess cost in the Gulf of Mexico is at the bottom of this range, at 17-MW and 280 W/m<sup>2</sup>. Figure 29 plots the SP values of both current and announced wind turbines.

<sup>16</sup> For offshore wind turbines in particular, the current trend toward higher generator ratings may stem from the relative difficulty of engineering turbines with larger rotors versus upscaling generator rating. The massive offshore wind direct-drive generators on the current machines are easier to upsize for power rating than to modify for rotor diameter increases because the latter requires a reduction in rotational speed, which increases the number of poles the generator must have and therefore necessitates a complete drivetrain redesign.

**Table 9. Comparison of Select Announced Turbines and Specific Power Ratings**

Original Equipment Manufacturer	Turbine Model	Specific Power [W/m <sup>2</sup> ]	Power Rating [MW]	Rotor Diameter [m]
Multi-party Conceptual Design	NREL Reference Turbine	326	15	242
NREL Conceptual Design described in Section 6.2	17-MW Low-SP	280	17	278
Mingyang	MySE 18.X-28X	292	18	280
Mingyang	MySE16.0-260	301	16	260
Siemens	SG 14-236 DD	320	14	236
CTG/Goldwind	252-16-MW	321	16	252
GE	Haliade-X 18-MW	339	18	260
China State Shipbuilding Corporation	H260-18-MW	339	18	260
Vestas	V236-15.0-MW	343	15	236
Mingyang	MySE16.0-242	348	16	242
Siemens	SG 14-222 DD	362	14	222
GE	Haliade-X 14-MW	368	14	220

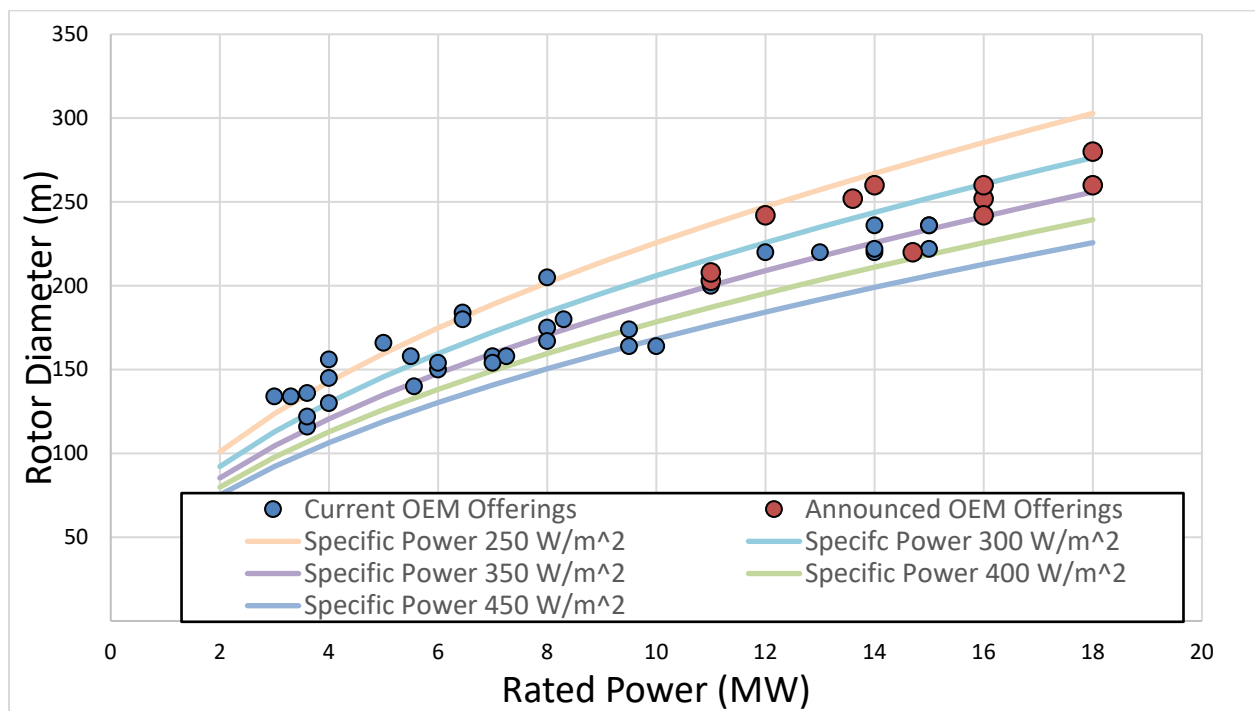


**Figure 29. Wind turbine rotor diameter vs. rated power for current and announced wind turbine original equipment manufacturer (OEM) offerings**

Note: Current and announced OEM offerings are compiled from the largest OEMs in the offshore market, including Siemens Gamesa, Vestas, GE, GoldWind, Shanghai Electric, Mingyang, China State Shipbuilding Corporation, Doosan Heavy Industries. Current offerings must have either operational machines or product brochures and an operational prototype. Data are current as of January 2023. The set of offshore turbines compiled from Asian suppliers may not contain all their respective offshore offerings. *Data collected by NREL*

## 6.2 Description of Turbine Designs and Associated Power Curves

To illustrate the impacts of SP on performance in the Gulf of Mexico, we calculate the performance in terms of GCF for four offshore wind turbines that represent a range of turbine technologies that could be deployed in offshore wind development in the Gulf. Note that most of these reference turbines, which are based on currently available designs, are not optimized for low-wind sites. However, the NREL conceptual design with SP of 280 W/m<sup>2</sup> was included to show how low SP can improve low-wind-speed performance.

Globally, offshore wind turbines have grown steadily in size and rated capacity. The average capacity of offshore wind turbines installed in 2022 was 7.7 MW, and that figure is expected to exceed 12 MW by 2025, according to NREL’s offshore wind database (Musial et al. 2023). In the period of 2030 to 2040, we expect offshore wind turbines with ratings of 15 MW to 17 MW to be commercially available in the United States, growing incrementally within the new technology platform, which has yielded 12-MW to 15-MW prototypes over the past few years (Manget et al.2022). For future deployments into 2035, we project incremental growth of the turbine power rating to 17-MW or slightly higher. This rating could be conservative given the recent pace of offshore wind turbine growth, but as the industry matures, OEMs may begin to optimize their offshore wind turbines and offer lower-SP options rather than just larger generators.

We use the following four turbines to compare energy performance and other metrics:

- a) IEA 15-MW reference turbine (242-m rotor diameter)
- b) A 17-MW, upscaled IEA 15-MW generator with same 242-m rotor diameter,
- c) IEA reference scaled to 17-MW, and
- d) A 17-MW and low specific power turbine described below.

The key parameters for each of these turbines are provided in Table 10.

**Table 10. Key Turbine Parameters and Performance Metrics**

	<b>(1) IEA 15-MW</b>	<b>(2) 17-MW Upscaling of Generator Only From IEA 15-MW</b>	<b>(3) 17-MW Upscaled from IEA 15-MW</b>	<b>(4) 17-MW Low Specific Power</b>
Power rating [MW]	15.0	17.0	17.0	17.0
Wind speed rating [m/s]	10.9	11.3	10.9	10.3
Gross capacity factor	40.2	37.5	40.2	43.6
Gross AEP [GWh]	52.8	55.8	59.9	64.9
Specific power [W/m <sup>2</sup> ]	326	370	325	280
Turbine class	1B	1B	1B	1B
Rotor diameter [m]	242	242	258	278
Hub height [m]	150	150	160	168

Note that in Table 10, the performance metrics Gross AEP and GCF were calculated for each of the turbines based on the wind distribution for the Lake Charles lease area (BOEM lease OCS-G-37334), which was provisionally awarded to RWE for \$5.6 million on August 29, 2023. This lease location is considered a representative Gulf of Mexico site with an average annual wind speed of about 7.5 m/s.

The IEA 15-MW turbine (column 1) is the reference wind turbine developed under IEA Wind Task 37 (Gaertner et al. 2020), which was also used in previous sections. It is a state-of-the-art, open-source, IEC Class 1B turbine reference model. We consider it to be representative of state-of-the-art technology that will likely be deployed in the 2030 timeframe. It has a rotor diameter of 242-m, SP rating of 326 W/m<sup>2</sup>, and a hub height of 150-m. Note that IEC Class 1B will not be sufficiently strong to survive in the Gulf of Mexico, as reported by Mudd and Vickery in a companion report that is part of this study (Mudd and Vickery 2023). The adaptation of this turbine to sustain hurricane loads is not in the scope of the study, but the general behavior of the turbine is expected to be representative of the more extreme conditions.

A 17-MW turbine (column 2) was designed by upscaling only the generator from the 15-MW reference turbine to 17-MW but keeping the rotor diameter (242-m) the same as the reference turbine. This results in an increase in SP from 326 W/m<sup>2</sup> to 370 W/m<sup>2</sup>. This type of upscaling is very common in offshore wind turbines currently because OEMs can implement more rapid changes to increase their generator nameplate rating without making major changes to the blades, hub, rotational speed, or generator footprint. However, it results in less optimal designs with respect to capacity factor and gross energy production, especially in low-wind-speed regions. Upscaling the generator from 15 MW to 17 MW without increasing the rotor diameter leads to a decrease in capacity factor by roughly 3% and an increase in gross AEP from 52.8 GWh to 55.8 GWh—about 3 GWh or about 5.7%.

Another 17-MW turbine (column 3) was developed based on the IEA 15-MW design. The turbine rotor was scaled from 15 MW to 17 MW while maintaining an SP rating of 326 W/m<sup>2</sup>. This type of scaling is less common but results in machines that have similar capacity factors. Upscaling a turbine from 15 MW to 17 MW while increasing rotor diameter to maintain constant SP results in an increase in the gross AEP of roughly 7.1 GWh per turbine, or 13.4%.

Finally, a low-SP version of the 17-MW turbine (column 4) is designed for better energy capture from the low mean wind speeds present in the Gulf of Mexico. The turbine is designed for a lower SP of 280 W/m<sup>2</sup>, requiring a rotor diameter of 278-m. The lower-SP turbines are advantageous because they can extract more energy in areas that have lower mean wind speeds. However, they are more difficult for the turbine manufacturers to adapt from current designs because they require longer blades, slower rotational speeds, and more comprehensive drivetrain redesigns. The 17-MW low-SP turbine has a gross AEP roughly 12.1 GWh higher than the IEA 15-MW turbine, or roughly 22.9% more energy per turbine. The 17-MW low-SP turbine also has the lowest rated wind speed of 10.3 m/s compared to 11.3 m/s for the 17-MW turbine where only the generator was scaled up. Lower rated wind speeds translate to lower maximum operating thrust loads and lower wake losses, which can be advantageous to lower structural loads and increase energy capture.

In Figure 30, panels (a) and (b) show power curves and the power output (respectively) versus the wind speed at hub height for each wind turbine model described in Table 10.

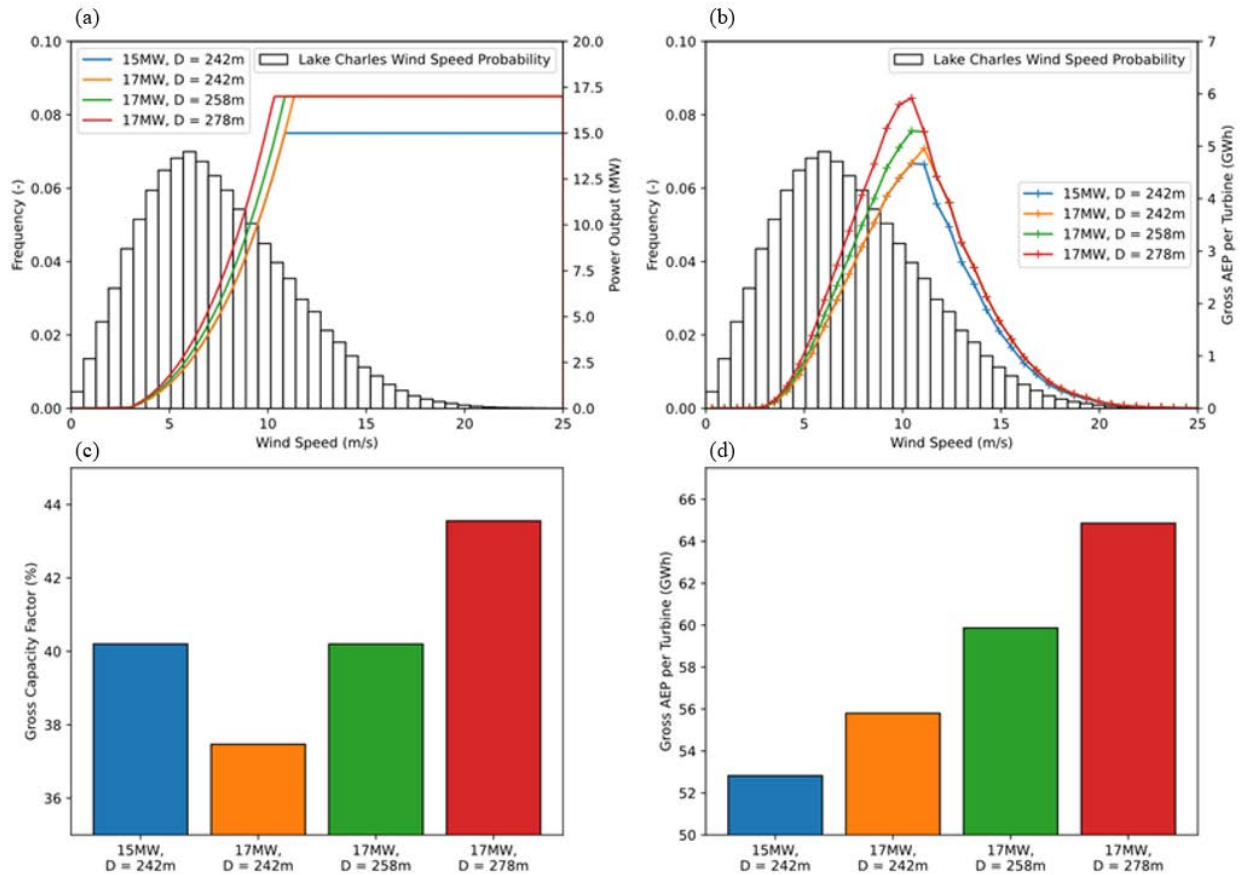


**Figure 30. (a) Wind distribution and power output, (b) wind distribution and gross AEP as a function of wind speed, (c) gross capacity factor, and (d) gross AEP summed over all wind speeds**

Figure 30 c,d show the GCF and the gross AEP that would be generated at that site for each of the turbines. As expected, the results show that the 17-MW low SP turbine performs significantly better than the other turbine designs in terms of energy production and capacity factor.

All turbines in Table 10 are assumed to be installed on jacket substructures. The Wind Plant Integrated System Design and Engineering Model (WISDEM<sup>®</sup>) toolset used for designing the jacket structures is a Python-based wind turbine systems engineering and optimization tool developed at NREL. We used the IEA 15-MW reference turbine with the specified T-Class turbine conditions from the IEC 61400-1 Edition 4 standards to design the jacket foundation. The jacket design is suited for T-Class wind conditions given structural constraints such as stress and shell buckling. It is a four-leg configuration extending 5-m above the mean sea level. The design variables include turbine thrust, the diameter and thickness of the struts, the water depth, and tower height. The jacket structures for these turbines are designed for water depths ranging from 10-m to 60-m.



### 6.3 Gross Capacity Factors and Production Profiles

We represent the geospatial energy production of the Gulf Call Area in terms of GCF (Figures 31 and 32), which represents the total generation as a percentage of the energy that would be generated if the wind turbine is always operating at its rated capacity (no losses). In the Lake Charles lease area, the mean GCF for the IEA 15-MW turbine is 40.2% and the mean GCF for the 17-MW low SP turbine is 43.6% (Table 10). We found that mean wind speeds differ less than 0.4 m/s between the three lease areas, but the Texas lease areas would have slightly higher GCF values.

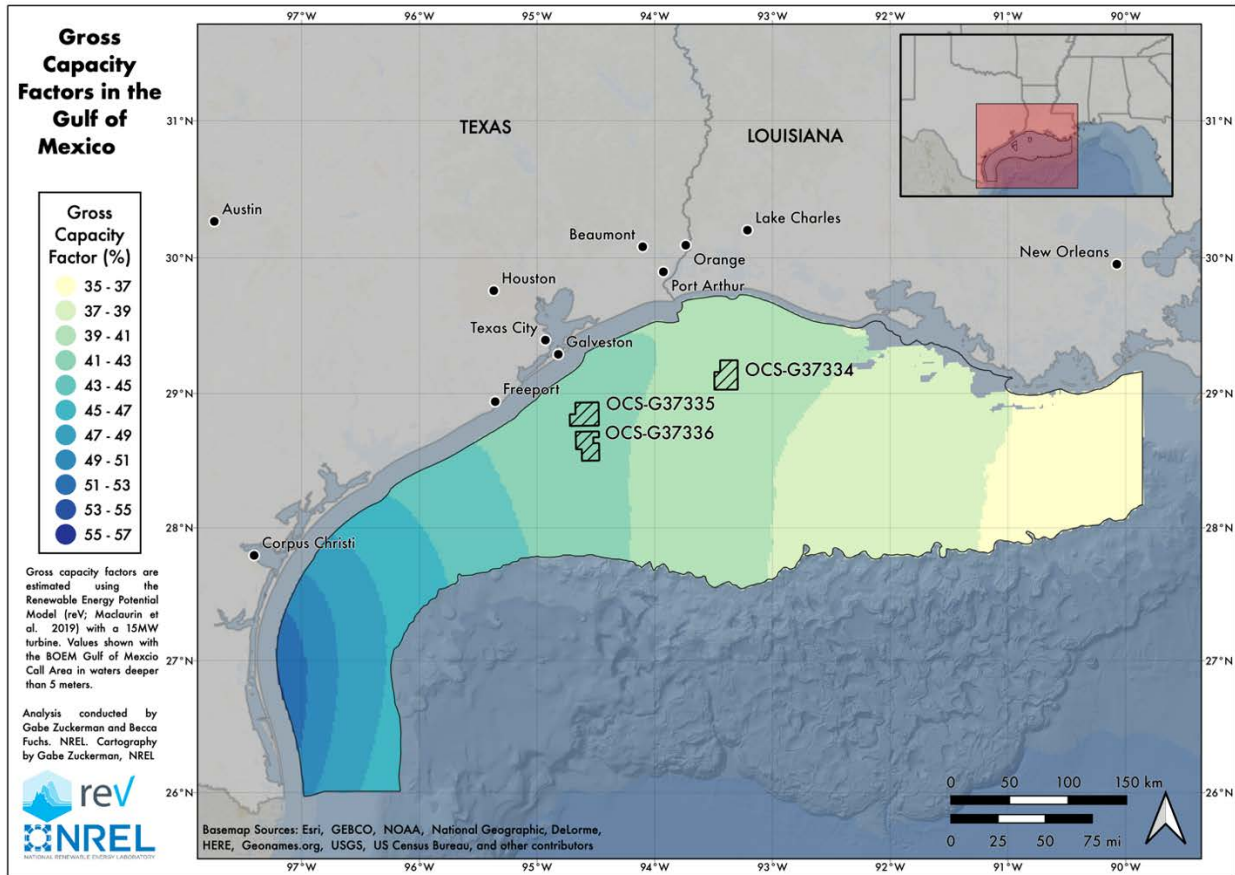
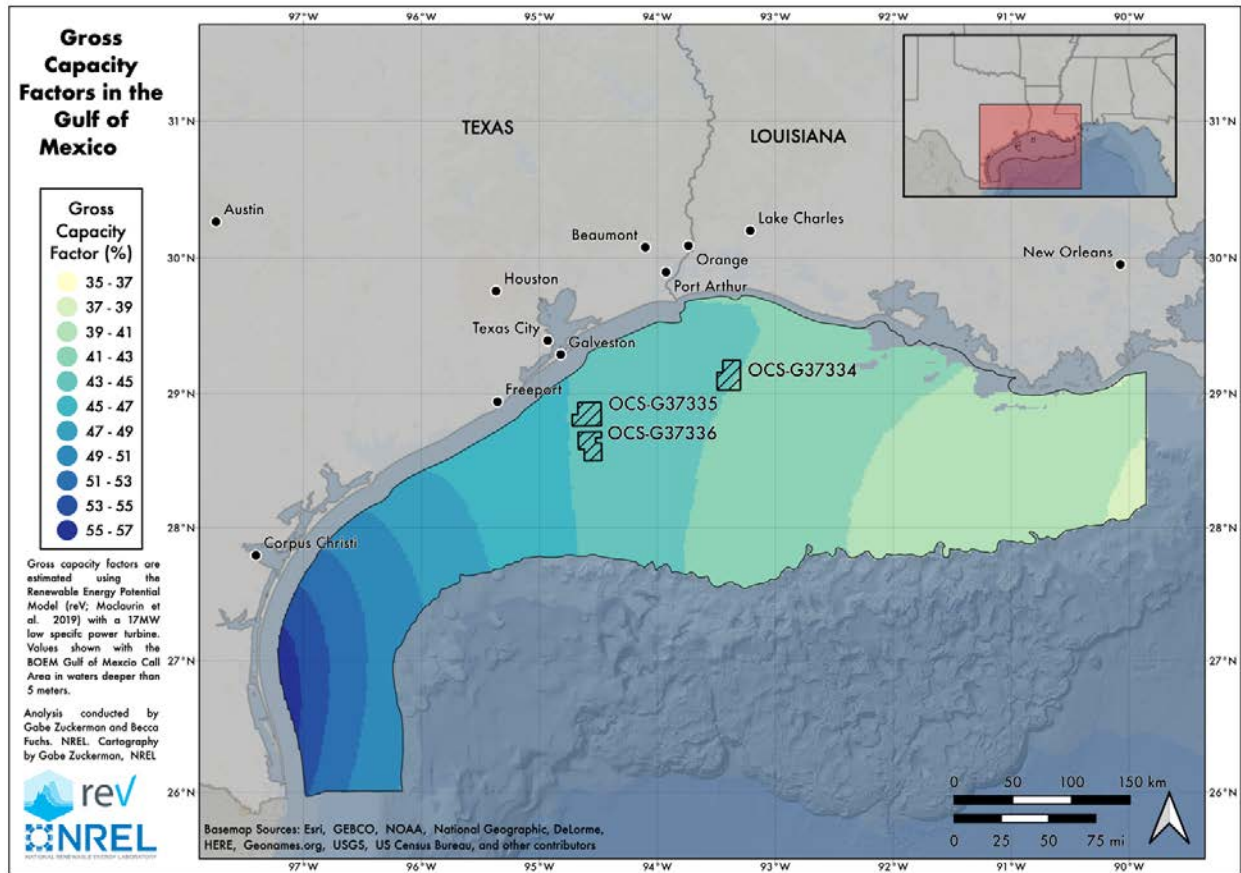


Figure 31. Gross capacity factor for the IEA 15-MW turbine across the Gulf of Mexico Call Area.

Map by Gabe Zuckerman, NREL



**Figure 32. Gross capacity factor for the 17-MW low-SP turbine across the Gulf of Mexico Call Area.**

*Map by Gabe Zuckerman, NREL*

The mean wind speed at 160-m (near hub height) generally increases from about 7 m/s in the eastern part of the Call Area to a maximum of about 8.6 m/s near the southern coast of Texas near the Mexican border (Figure 8). Not surprisingly, the GCFs also follow the same general trend. Across all turbine designs, the highest GCF values are in the southwestern portion of the Gulf of Mexico (55%–57%) and the lowest GCF values (35%–39%) are on the northeastern side of the Gulf (Figures 31 and 32).

## 6.4 Wake Losses

All the results presented in Sections 6.2 and 6.3 relate to gross energy production from single turbines only without considering losses that inevitably occur due to turbine-to-turbine interference, electric energy conversion and transmission, blade fouling, etc. In this section we assess wake losses for both the IEA 15-MW reference turbine and the 17-MW low-SP turbine using the newest NREL wind resource data presented in Section 3. As wind turbines extract momentum from the wind, wakes form and propagate downwind—the severity and persistence of the wake can vary depending on local atmospheric conditions (Schneemann et al. 2020; Hasager et al. 2015; Pryor, Barthelmie, and Shepherd 2021). A turbine operating in the wake of another turbine generates less power output due to reduced kinetic energy available in the wind and experiences higher mechanical loads due to increased wind-farm-generated turbulence.

Wakes eventually dissipate, and the wind flow recovers its kinetic energy through turbulent mixing with the freestream winds outside the wake boundaries, but the impacts of wake losses on the annual energy production (and revenue) of a wind plant can be significant (Lundquist et al. 2019).

Offshore wind developers generally want to maximize the energy yield of a given lease, which can be done by increasing the total capacity of turbines in the lease area. The higher the turbine rating, the fewer turbines needed to achieve the same generating capacity (Fleming et al. 2023). As the capacity density increases, so do the wake losses for a given turbine model.

In this analysis we compare the difference in wake losses between two turbine types. The analysis evaluates the geospatial wake losses for a generic 1-GW wind plant using the IEA 15-MW reference turbine and 17-MW low-SP wind turbine as described in Table 10. To enable comparisons of wake losses between the two turbines, we chose a generic wind plant layout with turbines on a square grid (columns aligned north-south) and turbines spaced seven rotor diameters (7D) apart. This approach provides insight into how wake losses vary across the Call Area based on the variation in wind speed and wind direction distributions.

To model the wake losses, we used the Gauss curl hybrid wake model in NREL's FLOW Redirection and Induction in Steady State (FLORIS) modeling toolbox (NREL 2022). The choices of wake model and tuning parameters are informed by the FLORIS team at NREL. Turbulence intensity is assumed to be 6%, which is a conservative estimate for a general offshore environment when no local measurements are available. Turbulence intensity impacts how far the wakes propagate downstream before mixing with freestream winds to replenish the kinetic energy. Higher turbulence intensities lead to more mixing and faster wake recovery.

Wind farm flow models and engineering models have inherent uncertainty, which must be considered when calculating the net energy production (delivered electricity) to obtain financing for offshore wind energy projects (Walker et al. 2016; Murcia 2017). Nygaard (2020) developed a methodology for quantifying wake model uncertainty by comparing against measurement campaigns in existing offshore wind farms (Nygaard et al. 2022). They show that the wake model uncertainty of their TurbOPark and Park wake models to be less than 10% of the estimated wake loss.

Note that the present analysis does not include cluster wake effects from other wind farms (Pryor, Barthelmie, and Shepherd 2021) or blockage effects (Bleeg et al. 2018; Nygaard et al. 2022). These dynamics may contribute to higher wake losses. We also do not consider the impacts of wind plant control strategies like "wake steering," which have the potential to reduce wake losses and boost revenues of wind energy projects. King et al. (2021) demonstrate AEP improvements of 0.7% to 2.2% from wind plant control in a large, modeled wind farm, depending on turbulence conditions and the choice of wake model. Fleming et al. (2023) show that wind plant control at offshore wind farms in the United States could potentially see a net gain in annual energy production of 1.3% to 2.3% after optimizing plant layouts. They also show that the impact on revenue may be higher than what is predicted from annual energy production averages, depending on the local electricity price dynamics.

Figures 33 and 34 present the results from the wake loss analysis with FLORIS across the entire Gulf of Mexico Call Area.

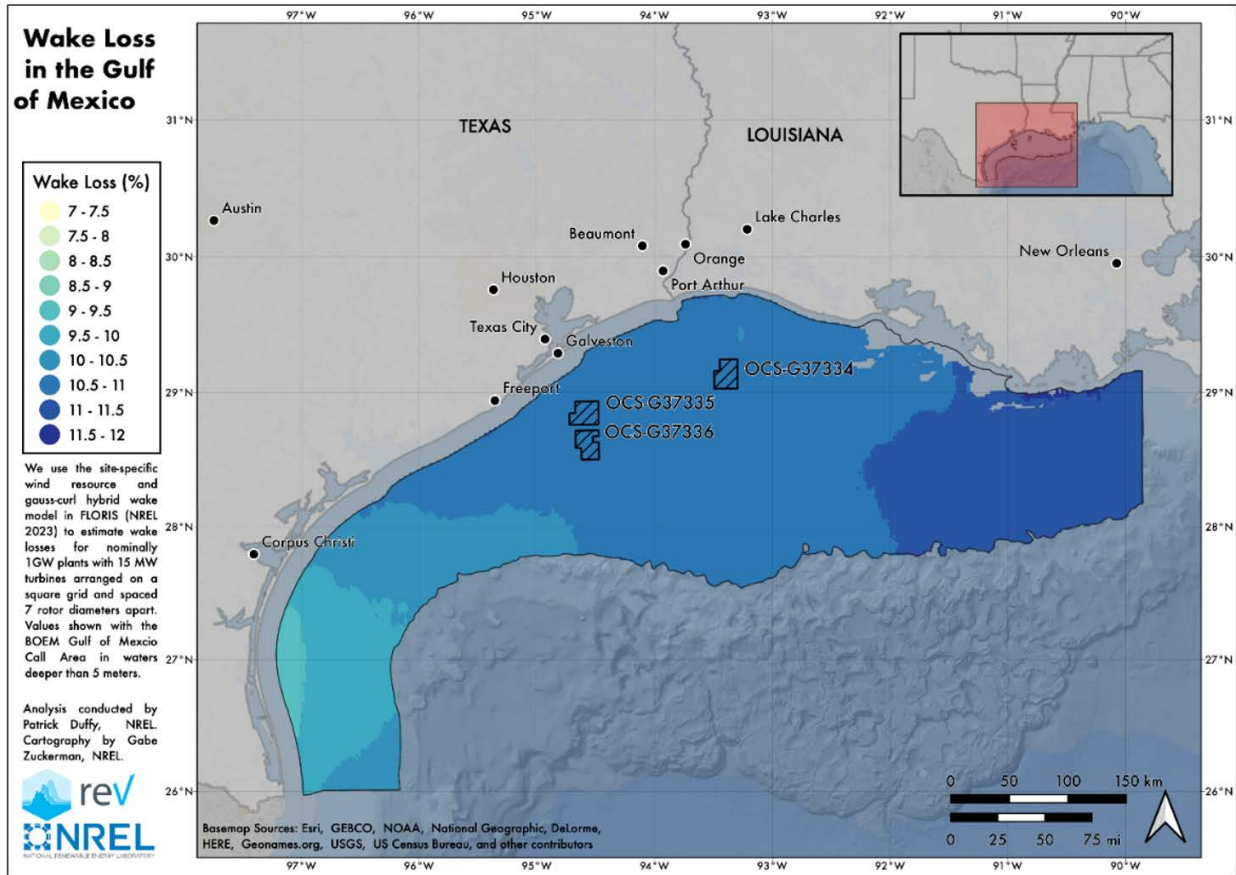


**Figure 33. Modeled wake losses for 1-GW wind plants with IEA 15-MW turbines arranged on a square grid, spaced 7 rotor diameters apart.**

*Map by Gabe Zuckerman, NREL*

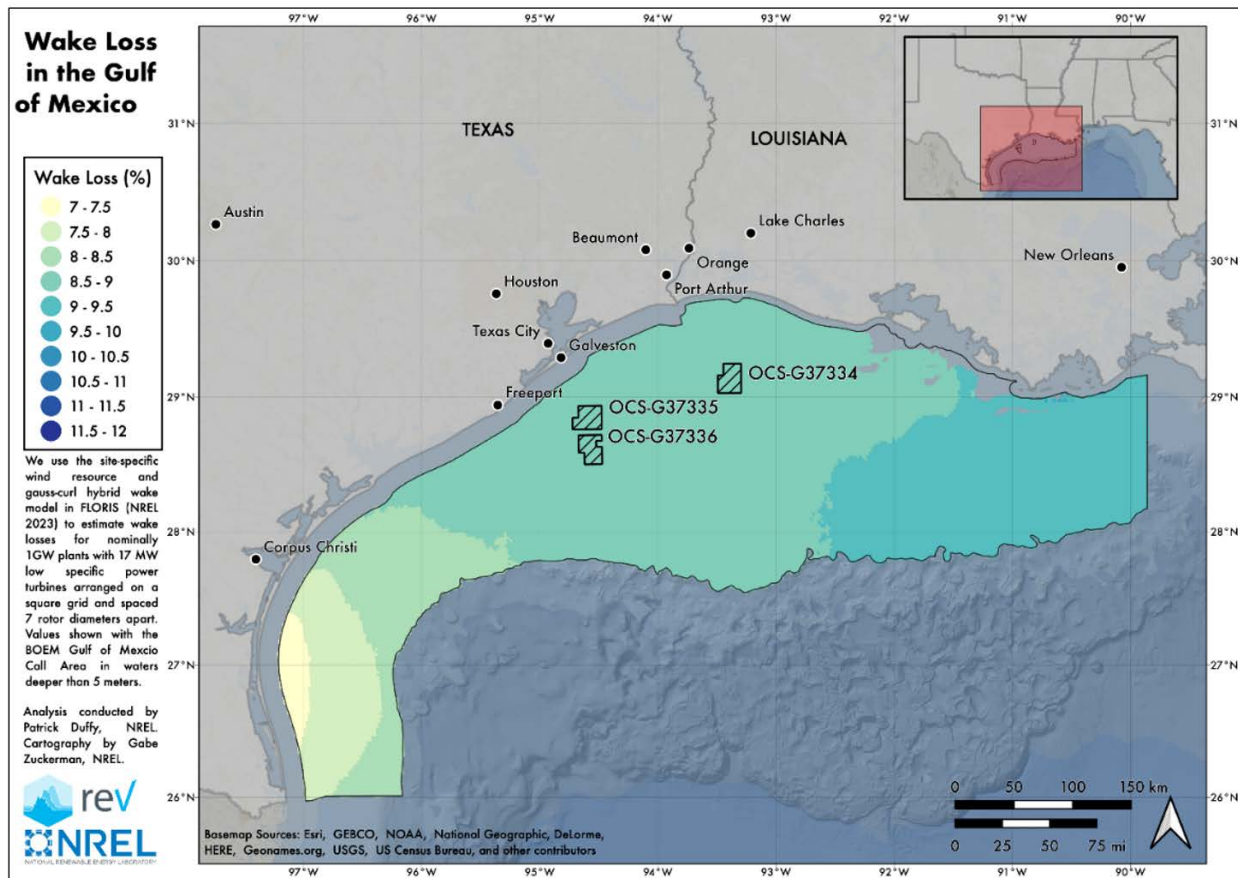


**Figure 34. Modeled wake losses for 1-GW wind plants with 17-MW low-SP turbines arranged on a square grid, spaced 7 rotor diameters apart.**

*Map by Gabe Zuckerman, NREL*

Modeled wake losses range from 7.1% to 11.6% across the domain and across turbine choice. Spatial variation in wake losses across the domain is primarily due to site-specific wind speed and wind direction distributions. Lower wind speed distributions generally lead to higher wake losses. However, in comparing the wake losses between the IEA 15-MW turbine (Figure 33) and the wake losses for the 17-MW low-SP turbine, we observe significantly higher wake losses for the IEA 15-MW turbine across the Call Area. Lower wake losses are generally expected for the 17-MW low-SP turbine because its lower rated wind speed allows it to spend more operating hours above rated power where wake losses are not significant. But it is also because the larger rotor increases the absolute spacing between turbines. While the relative turbine spacing is maintained at 7D, the absolute turbine spacing increases with the larger turbine rotors, and the larger turbine rating reduces the number of turbines in the plant. As such, caution should be used in making assumptions about the source of this reduction in wake losses because the different SP ratings of these two turbines results in approximately 15% lower capacity density for the 17-MW low-SP turbine using the identical 7D spacing.

## 7 Conclusions

This report documents some of the unique physical, technological, and infrastructure-dependent characteristics of the Gulf of Mexico that should be considered for offshore wind development. The key aspects that differentiate the Gulf from other regions in the United States are highlighted here, but this report is not an exhaustive study. Several issues regarding geopolitical constraints, stakeholder and community engagement, conflicts with other ocean users, integration with power-to-grid solutions, and interactions with the environment are not fully covered. The cost and economics of offshore wind in the Gulf will be covered in an NREL report that is forthcoming, expected in April 2024.

The following are the primary summaries and conclusions of this study:

### *Site selection and leasing:*

- Section 2 describes the approach of NOAA that used a new multifactor site suitability model to identify the wind energy areas associated with the Aug. 29, 2023 auction. The section documents the approach and validates the use of this tool, which is an improvement over previous methods that were less rigorous. We recommend that the site suitability model development continue, and new layers added to better represent the technology constraints, including economics, grid information, interarray wind farm spacing, etc.
- The lease auction that was held on Aug. 29, 2023, showed lower-than-expected interest in offshore wind in the Gulf, but the coincidence of the auction timing with increased market and cost uncertainty that came to light during the summer of 2023 likely dampened developer interest. The Louisiana state commitment to set a 5-GW target by 2035 likely made the Lake Charles lease area more attractive and may have led to the RWE purchase of that lease for \$5.6 million.

### *Wind resource assessment:*

- Wind site characteristics were evaluated using a new dataset updated for the Gulf region (Bodini et al. 2021) that was introduced in Section 3. We provide details for several characteristics such as wind speed, wind direction, wind shear, and diurnal variability. Wind speeds vary from 7.0 m/s to 8.5 m/s across the Call Area, but within the lease areas the annual wind speed averages were approximately 7.5 m/s.

### *Hurricane Design:*

- The state-of-the-art hurricane resiliency and design methods were documented. Offshore wind turbine manufacturers and developers are already installing wind turbines in typhoon-prone regions in Asia using current methods, which include upgrading the turbine design class set by the IEC standards to (Tropical) T-Class, taking additional precautions to install battery backup systems for the yaw drive, and implementing the robustness check for the support structure that is suggested in Annex I of the 2019 edition of IEC 61400-03-1.

- The companion report developed during this study by Mudd and Vickery examines the severity and probabilities of major hurricanes in the Gulf with respect to Saffir-Simpson criteria and IEC limit-state return periods (Mudd and Vickery 2023). The general conclusion is that all sites in the Gulf will require at least a T-Class turbine, and some sites may require an even more enhanced version that can withstand wind speeds higher than specified in that class. The general approach for a T-Class turbine upgrade is to strengthen components such as the tower, foundation, blades, sensors, and yaw and pitch systems to withstand a higher-speed extreme wind gust for both fixed and floating technologies.
- Battery backup systems to keep the yaw system energized during grid outages were examined in terms of the governing IEC design load cases, DLC 6.1, DLC 6.2, I.1, and I.2. The quantitative analysis that we performed was inconclusive because the physics governing the turbine interactions under extreme wind loading at high angles of attack were not well represented with the modeling tools used but more rigorous analysis is underway. The general conclusions are that battery backup systems would be beneficial to include in new turbine designs installed in hurricane-prone regions, but more research is needed to quantify the benefits.
- Additional research is needed to evaluate both the wind and wave characteristics of major hurricanes in terms of their potential to harbor extreme turbulent structures that may cause ultimate or fatigue load cases that exceed the present design load envelope. Future work to address design uncertainty should also include long-term, high-fidelity weather and climate modeling to understand future design requirements.

*Insurance:*

- Insurance rates and insurability were considered as informed by the limited information available from industry. Generally, our conclusion is that insurance premiums will likely be higher in hurricane-prone regions relative to sites in more northern latitudes, but these higher rates are not likely to have a significant impact on the total project cost. The more important issue may be the insurability of the project. The insurance industry has not evaluated the risks yet or articulated a strategy to address hurricane design risk, but it is likely that certain steps must be taken in the project design to mitigate hurricane risk to make a project insurable, which may include turbine upgrades to T-Class or greater and the implementation of battery backup systems.

*Infrastructure:*

- The investigation of the port infrastructure in the Gulf found significant opportunity with the current infrastructure. These ports already serve land-based wind and offshore oil and gas activities. Floating and fixed-bottom turbine technologies can be supported by nine ports identified using screening criteria for each of these technologies. These ports are Brownsville, Corpus Christi, Freeport, Houston, Galveston, Port Fourchon, Gulfport, Pascagoula, and Mobile. Although some upgrades or modifications may be necessary these ports may require fewer upgrades than ports in other regions because on-going oil and gas activities may provide a higher level of workforce skills and similarities.

- The study examined the interconnect of offshore wind projects to the existing utility grid. A full grid integration study was not performed, but a first-order screening of possible interconnection points resulted in the identification of 25 possible POIs along the coast of the Call Area with at least one 230-kV transmission line and more than one transmission line.
- NREL performed a new least-cost path analysis for land-based routing cables that shows the cost of transmission generally increases from the western part of the Gulf to the eastern side near New Orleans. This is due to the potential POIs being located further from shore.
- Major challenges for grid integration in the Gulf region include lack of long-term transmission planning for offshore wind by utilities in the region. The grids are completely separated between ERCOT in Texas and MISO in the Louisiana region. Some early-stage planning has been done in Louisiana, but there was no evidence of planning in Texas despite their large presence in the land-based wind market.
- The need for alternative offtake mechanisms to serve greater industrial loads in the region is a dominant theme that needs more attention.

*Low-wind speed turbines:*

- Low annual average wind speeds in the Gulf present a major challenge to project economics because expected energy production is lower. The available offshore wind turbine technology that is being planned for deployment in the northeast is suboptimal for most sites in the Gulf Call Area. Ideally, turbines with larger rotors relative to the generator rating (low specific power) are needed for deployment in the Gulf.
- Soft seabed conditions will likely steer Gulf offshore wind development toward jackets or multi-pile support structures that do not rely on lateral soil stiffness. This technology is very common in the Gulf oil industry and is synergistic with local content and local jobs.
- Generally, wake losses increase as wind speed decreases. Therefore, due to lower wind speeds, the percentage of total energy lost to wakes in the Gulf Call Area is greater relative to higher wind sites. Wake losses can be mitigated to some degree through turbine optimization strategies such as low-specific-power turbines.

Despite the flat response to the Aug. 29, 2023 auction, there remains significant optimism that the offshore wind industry can address all the challenges for successful deployment in the Gulf of Mexico. Although it is unlikely that we will see offshore wind deployment in the Gulf before 2030, long-term opportunities may emerge as the larger global industry matures and costs come down. The vision for offshore wind in the Gulf is motivated by the strong head-start the Gulf has in supply chain development and by a huge opportunity to leverage oil and gas infrastructure and skilled labor to capitalize on the energy transition that is underway. The results indicate that offshore wind energy has the potential to be a viable clean energy option to help the region meet U.S. goals to achieve carbon neutrality by 2050.



## References

- Abdel-Basset, M., A. Gamal, R. K. Chakraborty, and M. Ryan. 2021. “A New Hybrid Multi-Criteria Decision-Making Approach for Location Selection of Sustainable Offshore Wind Energy Stations: A Case Study.” *Journal of Cleaner Production* 280: 124462. <https://doi.org/10.1016/j.jclepro.2020.124462>.
- American Oil & Gas Historical Society. No date. “Offshore Oil & Gas History.” AOGHS.org. <https://aoghs.org/offshore-oil-history/>.
- Ansari, A. H., M. A. Olyaei, and Z. Heydari. 2021. “Ensemble Generation for Hurricane Hazard Assessment Along the United States’ Atlantic Coast.” *Coastal Engineering* 169: 103956. <https://doi.org/10.1016/j.coastaleng.2021.103956>.
- ANSI. 2022. Standard: ANSI/ACP OCRP-1-2022 “Offshore Compliance Recommended Practices, Edition 2.”
- Bleeg, James, Mark Purcell, Renzo Ruisi, and Elizabeth Traiger. 2018. “Wind Farm Blockage and the Consequences of Neglecting Its Impact on Energy Production.” *Energies* 11(6): 1609. <https://www.mdpi.com/1996-1073/11/6/1609>.
- Bodini, N., M. Optis, M. Rossol, A. Rybchuk, S. Redfern, J. K. Lundquist, and D. Rosencrans. 2021. “2023 National Offshore Wind Data Set (NOW-23).” [dataset]. <https://dx.doi.org/10.25984/1821404>.
- Bodini, N., Optis, M., Redfern, S., Rosencrans, D., Rybchuk, A., Lundquist, J. K., Pronk, V., Castagneri, S., Purkayastha, A., Draxl, C., Krishnamurthy, R., Young, E., Roberts, B., Rosenlieb, E., and Musial, W.: The 2023 National Offshore Wind data set (NOW-23), *Earth Syst. Sci. Data Discuss.* [preprint], <https://doi.org/10.5194/essd-2023-490>, in review, 2023.
- [BOEM] Bureau of Ocean Energy Management. Notice. 2021. “Call for Information and Nominations-Commercial Leasing for Wind Power Development on the Outer Continental Shelf in the Gulf of Mexico.” *Federal Register* 86 FR 60283 (Nov. 1, 2021): 60283–60287. <https://www.federalregister.gov/documents/2021/11/01/2021-23800/call-for-information-and-nominations-commercial-leasing-for-wind-power-development-on-the-outer>.
- BOEM. 2022. “BOEM Designates Two Wind Energy Areas in Gulf of Mexico.” <https://www.boem.gov/newsroom/press-releases/boem-designates-two-wind-energy-areas-gulf-mexico>.
- BOEM. 2023. “Proposed Sale Notice for Commercial Leasing for Wind Power Development on the Outer Continental Shelf in the Gulf of Mexico (GOMW-1).” *Federal Register* 88 FR 11939 (February): 11939–53. <https://www.federalregister.gov/documents/2023/02/24/2023-03842/proposed-sale-notice-for-commercial-leasing-for-wind-power-development-on-the-outer-continental>.

Borrmann, R., K. Rehfeldt, A. Wallasch, and S. Lüers. 2018. *Capacity Densities of European Offshore Wind Farms*. Varel, Germany: Deutsche WindGuard GmbH. Report No. SP18004A1. [BalticLINES\\_CapacityDensityStudy\\_June2018-1.pdf](https://www.vasab.org/BalticLINES_CapacityDensityStudy_June2018-1.pdf) (vasab.org).

Cole, Wesley, J. Vincent Carag, Maxwell Brown, Patrick Brown, Stuart Cohen, Kelly Eurek, Will Frazier, et al. 2021. *2021 Standard Scenarios Report: A U.S. Electricity Sector Outlook*. Golden, CO: National Renewable Energy Laboratory. NREL/TP-6A40-80641. <https://www.nrel.gov/docs/fy22osti/80641.pdf>.

Crown Estate Scotland and ARUP. 2020. “Ports for Offshore Wind, the Net Zero Opportunity Scotland.” <https://www.arup.com/perspectives/publications/research/section/ports-for-offshore-wind-a-review-of-the-net-zero-opportunity-for-ports-in-scotland>.

Draxl, Caroline, Andrew Clifton, Bri-Mathias Hodge, and Jim McCaa. 2015. “The Wind Integration National Dataset (WIND) Toolkit.” *Applied Energy* 151: 355–366. <https://doi.org/10.1016/j.apenergy.2015.03.121>.

Duffy, Patrick, Gabriel R. Zuckerman, Travis Williams, Alicia Key, Luis A. Martínez- Tossas, Owen Roberts, Nina Choquette, Jaemo Yang, Haiku Sky, and Nate Blair. 2022. *Wind Energy Costs in Puerto Rico Through 2035*. Golden, CO: National Renewable Energy Laboratory. NREL/TP-5000-83434. <https://www.nrel.gov/docs/fy22osti/83434.pdf>.

[EIA] U.S. Energy Information Administration. 2021. “U.S. Energy Atlas.” <https://atlas.eia.gov/>.

EIA. 2023a. “Power Plants.” U.S. Energy Atlas. <https://atlas.eia.gov/datasets/eia::power-plants/about>. Updated Sept. 20, 2023.

EIA. 2023b. “State Profiles and Energy Estimates” Updated for 2021. [https://www.eia.gov/state/\[ERCOT\]](https://www.eia.gov/state/[ERCOT]) Electric Reliability Council of Texas. 2023. “Load Forecast.” Accessed May 11, 2023. <https://www.ercot.com/gridinfo/load/forecast>.

ESRI 2022. Cluster and Outlier Analysis (Anselin Local Moran’s I) (Spatial Statistics)—ArcGIS Pro Documentation, n.d.). <https://pro.arcgis.com/en/pro-app/3.1/tool-reference/spatial-statistics/cluster-and-outlier-analysis-anselin-local-moran-s.htm> , accessed 2023.

Fleming, Paul, David Dunn, Patrick Duffy, Christopher Bay, Matthew Churchfield, Rebecca Barthelmie, and Sara Pryor. 2023. *Final Report – D5 Wind Farm Control and Layout Optimization for U.S. Offshore Wind Farms*. Golden, CO: National Renewable Energy Laboratory. NREL/TP-5000-85454. [https://nationaloffshorewind.org/wp-content/uploads/NREL-147506\\_Final\\_Report.pdf](https://nationaloffshorewind.org/wp-content/uploads/NREL-147506_Final_Report.pdf).

Frank, Kimberly B., Nathan C. Howe, Theodore J. Paradise, Felisa E. Sanchez, Chimera N. Thompson, and Ankur K. Tohan. 2023. “BOEM Offshore Wind Lease Update: Gulf of Mexico Auction Produces Lackluster Results, Not Likely Repeated in Future Oregon and Mid-Atlantic Lease Areas Auctions.” K&L Gates. <https://www.klgates.com/BOEM-Offshore-Wind-Lease-Update-Gulf-of-Mexico-Auction-Produces-Lackluster-Results-Not-Likely-Repeated-in-Future-Oregon-and-Mid-Atlantic-Lease-Areas-Auctions-9-5-2023>.

Gaertner, Evan, Jennifer Rinker, Latha Sethuraman, Frederik Zahle, Benjamin Anderson, Garrett Barter, Nikhar Abbas, et al. 2020. *Definition of the IEA Wind 15-Megawatt Offshore Reference Wind Turbine*. Golden, CO: National Renewable Energy Laboratory. NREL/TP-5000-75698. <https://www.nrel.gov/docs/fy20osti/75698.pdf>.

Gatzert, Nadine, and Thomas Kosub. 2016. “Risks and Risk Management of Renewable Energy Projects: The Case of Onshore and Offshore Wind Parks.” *Renewable and Sustainable Energy Reviews* 60(July): 982–998. <https://doi.org/10.1016/j.rser.2016.01.103>.

General Electric. 2013. “System and Method for Providing Yaw Backup to a Wind Farm.” European Patent Application 13192884.8. November 14, 2013. <https://patentimages.storage.googleapis.com/4c/82/0c/1edd12df0b174f/EP2738382A2.pdf>.

General Electric. No date. “Haliade-X Offshore Typhoon Certification.” General Electric Renewable Energy. Accessed May 9, 2023. <https://www.ge.com/renewableenergy/wind-energy/offshore-wind/haliade-x-typhoon-certification>.

Hallowell, Spencer T., Andrew T. Myers, Sanjay R. Arwade, Weichiang Pang, Prashant Rawal, Eric M. Hines, Jerome F. Hajjar, et al. 2018. “Hurricane Risk Assessment of Offshore Wind Turbines.” *Renewable Energy* 125(September): 234–249. <https://doi.org/10.1016/j.renene.2018.02.090>.

Hasager, C. B., P. Vincent, R. Husson, A. Mouche, M. Badger, A. Peña, P. Volker, et al. 2015. “Comparing Satellite SAR and Wind Farm Wake Models.” *Journal of Physics: Conference Series* 625(June): 012035. <https://doi.org/10.1088/1742-6596/625/1/012035>.

Hersbach, H., B. Bell, P. Berrisford, S. Hirahara, A. Horányi, J. Muñoz-Sabater, J. Nicolas, et al. 2020. “The ERA5 Global Reanalysis.” *Quarterly Journal of the Royal Meteorological Society* 146(730): 1999–2049. <https://doi.org/10.1002/qj.3803>.

[HIFLD] Homeland Infrastructure Foundation-Level Data. *Geospatial Management Office*. <https://hifld-geoplatform.opendata.arcgis.com/datasets/geoplatform::electric-substations/about>. Accessed April 2023.

[IEC] International Electrotechnical Commission. 2019a. Standard: IEC 61400-1:2019 Edition 4, “Wind turbines—Part 1: Design requirements.” Available at: [https://www.iec.ch/dyn/www/f?p=103:23:27965083281002::::FSP\\_ORG\\_ID](https://www.iec.ch/dyn/www/f?p=103:23:27965083281002::::FSP_ORG_ID).

IEC. 2019b. Standard: IEC 61400-3-1:2019 , “Wind Energy Generation Systems - Part 3-1: “Design Requirements for Fixed Offshore Wind Turbines.” Available at: <https://webstore.iec.ch/publication/29360>.

Intergovernmental Panel on Climate Change. 2021. *Climate Change 2021: The Physical Science Basis: Working Group I Contribution to the Sixth Assessment Report of the Intergovernmental Panel on Climate Change*. Cambridge, UK: Cambridge University Press. doi:10.1017/9781009157896.

Jenkinson, O. 2023. “Floating MingYang Offshore Wind Turbine Set To Power Chinese Oil and Gas Field.” *Windpower Monthly*. Accessed May 9, 2023.

<https://www.windpowermonthly.com/article/1817910/floating-mingyang-offshore-wind-turbine-set-power-chinese-oil-gas-field>.

Jha, A., D. Dolan, T. Gur, S. Soyoz, and C. Alpdogan. 2009. *Comparison of API & IEC Standards for Offshore Wind Turbine Applications in the U.S. Atlantic Ocean: Phase II*. Golden, CO: National Renewable Energy Laboratory. NREL/SR-5000-49688.

<http://www.nrel.gov/docs/fy13osti/49688.pdf>.

Jonkman, J., and M. Sprague. 2021. OpenFAST Documentation Release v3. 0.0. Golden, CO: National Renewable Energy Laboratory.

Kim, E., and L. Manuel. 2014. “Hurricane-Induced Loads on Offshore Wind Turbines With Considerations for Nacelle Yaw and Blade Pitch Control.” *Wind Engineering* 38(4): 413–423.

<https://doi.org/10.1260/0309-524X.38.4.41>.

King, J., P. Fleming, R. King, L. A. Martínez-Tossas, C. J. Bay, R. Mudafort, and E. Simley. 2021. “Control-Oriented Model for Secondary Effects of Wake Steering.” *Wind Energy Science* 6(3): 701–714.

<https://doi.org/10.5194/wes-6-701-2021>.

Liu, J., A. Elgamal, K. Mackie, and A. Shamsabadi. 2012. “A Framework for Performance-Based Earthquake Engineering of Bridge-Abutment Systems.” *Proceedings GeoCongress 2012: State of the Art and Practice in Geotechnical Engineering*.

<https://ascelibrary.org/doi/10.1061/9780784412121.173>.

Lopez, Anthony, Rebecca Green, Travis Williams, Eric Lantz, Grant Buster, and Billy Roberts. 2022. “Offshore Wind Energy Technical Potential for the Contiguous United States.” Golden, CO: National Renewable Energy Laboratory. NREL/PR-6A20-83650.

<https://doi.org/10.2172/1882929>.

Lundquist, J. K., K. K. DuVivier, D. Kaffine, and J. M. Tomaszewski. 2019. “Costs and Consequences of Wind Turbine Wake Effects Arising From Uncoordinated Wind Energy Development.” *Nature Energy* 4(January): 26–34.

<https://doi.org/10.1038/s41560-018-0281-2>.

Maclaurin, Galen, Caroline Draxl, Bri-Mathias Hodge, and Michael Rossol. 2014. “Wind Integration National Dataset (WIND) Toolkit.” *Department of Energy Open Energy Data Initiative*. Golden, CO: National Renewable Energy Laboratory

Mahdy, M., and A. S. Bahaj. 2018. “Multi Criteria Decision Analysis for Offshore Wind Energy Potential in Egypt.” *Renewable Energy* 118: 278–289.

<https://doi.org/10.1016/j.renene.2017.11.021>.

Mangat, Naunidh; Gerrit Jan van Zinderen; Lars Falbe Hansen; Fernando Sevilla. 2022. “Optimal offshore wind turbine size and standardisation study”, DNV Services UK Ltd. May 2022.

[https://topsectorenergie.nl/documents/334/20220519\\_RAP\\_DNV\\_Optimal\\_Offshore\\_Wind\\_Turbine\\_Size\\_and\\_Standardisation\\_F.pdf](https://topsectorenergie.nl/documents/334/20220519_RAP_DNV_Optimal_Offshore_Wind_Turbine_Size_and_Standardisation_F.pdf).

[MISO] Midcontinent Independent System Operator. 2023. “Market Reports – Historical Regional Forecast and Actual Load.” Accessed May 12, 2023. [https://www.misoenergy.org/markets-and-operations/real-time--market-data/market-reports/#nt=/MarketReportType:Summary/MarketReportName:Historical%20Regional%20Forecast%20and%20Actual%20Load%20\(xls\)](https://www.misoenergy.org/markets-and-operations/real-time--market-data/market-reports/#nt=/MarketReportType:Summary/MarketReportName:Historical%20Regional%20Forecast%20and%20Actual%20Load%20(xls)).

Monsoon Wind. No date. “Asean’s Largest Wind Power Project.” Accessed May 4, 2023. <https://www.monsoonwindasia.com/>.

Morris Jr., J.A., J. K. MacKay, J. A. Jossart, L. C. Wickliffe, A. L. Randall, G. E. Bath, M. B. Balling, B. M. Jensen, and K. L. Riley. 2021. “An Aquaculture Opportunity Area Atlas for the Southern California Bight.” Beaufort, NC: National Oceanic and Atmospheric Administration. NOAA Technical Memorandum NOS NCCOS 298. <https://doi.org/10.25923/tmx9-ex26>.

Mudd, Lauren, and Peter Vickery. *Gulf of Mexico Offshore Wind Energy Hurricane Risk Assessment*. Golden, CO: Contractor Report: National Renewable Energy Laboratory. <https://nrel.gov/docs/fy24osti/88211.pdf>.

Murcia, Juan Pablo. 2017. “Uncertainty Quantification in Wind Farm Flow Models.” Ph.D. dissertation. DTU Wind Energy. <https://orbit.dtu.dk/en/publications/uncertainty-quantification-in-wind-farm-flow-models>.

Musial, W., and T. Greco. 2020. “Feasibility of Ocean-Based Renewable Energy in the Gulf of Mexico.” *Marine Technology Society Journal* 54(6): 9–23. <https://doi.org/10.4031/MTSJ.54.6.3>.

Musial, W., S. Tegen, R. Driscoll, P. Spitsen, O. Roberts, L. Kilcher, G. Scott, and P. Beiter. 2020a. *Survey and Assessment of the Ocean Renewable Resources in the US Gulf of Mexico*. New Orleans, LA: Bureau of Ocean Energy Management. Contract No.: M17PG00012. Report No.: OCS Study BOEM 2020-017. [https://espis.boem.gov/final%20reports/BOEM\\_2020-017.pdf](https://espis.boem.gov/final%20reports/BOEM_2020-017.pdf).

Musial, Walter, Philipp Beiter, Jeremy Stefek, George Scott, Donna Heimiller, Tyler Stehly, Suzanne Tegen, Owen Roberts, Tessa Greco, and David Keyser. 2020b. *Offshore Wind in the US Gulf of Mexico: Regional Economic Modeling and Site-Specific Analyses*. New Orleans, LA: Bureau of Ocean Energy Management. Contract No.: M17PG00012. Report No.: OCS Study BOEM 2020-018BOEM 2020-018. [https://espis.boem.gov/final%20reports/BOEM\\_2020-018.pdf](https://espis.boem.gov/final%20reports/BOEM_2020-018.pdf).

Musial, Walter, Paul Spitsen, Patrick Duffy, Philipp Beiter, Matt Shields, Daniel Mulas Hernando, Rob Hammond, Melinda Marquis, Jennifer King, and Sathish Sriharan. 2023. “Offshore Wind Market Report: 2023 Edition.” DOE/GO-102023-6059. Washington, D.C.: U.S. Department of Energy Office of Energy Efficiency & Renewable Energy. <https://www.energy.gov/sites/default/files/2023-09/doe-offshore-wind-market-report-2023-edition.pdf>.

National Oceanic and Atmospheric Administration. 2012. “NOAA Provides Easy Access to Historical Hurricane Tracks” <https://2010-2014.commerce.gov/blog/2012/08/13/noaa-provides-easy-access-historical-hurricane-tracks.html>

National Offshore Wind Research and Development Consortium. n.d.. “Long-Term Availability and Bankability of Offshore Wind Through Hurricane Risk Assessment and Mitigation.” <https://nationaloffshorewind.org/projects/long-term-availability-and-bankability-of-offshore-wind-through-hurricane-risk-assessment-and-mitigation/>.

National Renewable Energy Laboratory. 2022. FLORIS version 3.2.1. <https://github.com/NREL/floris>.

Nygaard, Nicolai Gayle, Søren Trads Steen, Lina Poulsen, and Jesper Grønnegaard Pedersen. 2020. “Modelling Cluster Wakes and Wind Farm Blockage.” *Journal of Physics: Conference Series* 1618(6): 062072. <https://doi.org/10.1088/1742-6596/1618/6/062072>.

Nygaard, N. G., L. Poulsen, E. Svensson, and J. G. Pedersen. 2022. “Large-Scale Benchmarking of Wake Models for Offshore Wind Farms.” *Journal of Physics: Conference Series* 2265(2): 022008. <https://doi.org/10.1088/1742-6596/2265/2/022008>.

Ocean Wind 1. No date. “Ocean Wind 1, An Ørsted and PSEG Project.” Accessed May 9, 2023. <https://oceanwindone.com/about-the-project>.

Parkison, Sara B., and Willett Kempton. 2022. “Marshaling Ports Required to Meet US Policy Targets for Offshore Wind Power.” *Energy Policy* 163(April): 112817. <https://doi.org/10.1016/j.enpol.2022.112817>.

Porter, Aaron, and Shane Phillips. 2016. *Determining the Infrastructure Needs to Support Offshore Floating Wind and Marine Hydrokinetic Facilities on the Pacific West Coast and Hawaii*. U.S. Department of the Interior, Bureau of Ocean Energy Management, Pacific OCS Region, Camarillo, CA. OCS Study BOEM 2016-011. <https://www.boem.gov/sites/default/files/environmental-stewardship/Environmental-Studies/Pacific-Region/Studies/BOEM-2016-011.pdf>.

Pryor, Sara C., Rebecca J. Barthelmie, and Tristan J. Shepherd. 2021. “Wind Power Production from Very Large Offshore Wind Farms.” *Joule* 5(10): 2663–2686. <https://doi.org/10.1016/j.joule.2021.09.002>.

Randall, A. L., J. A. Jossart, T. Matthews, M. Steen, I. Boube, S. Stradley, R. Del Rio, et al. No date. *A Wind Energy Area Siting Analysis for the Gulf of Mexico Call Area*. Accessed May 3, 2023. Available at: <https://www.boem.gov/sites/default/files/documents/renewable-energy/state-activities/GOM-WEA-Modeling-Report-Combined.pdf>.

Reguero, Borja G., Michael W. Beck, David Schmid, Daniel Stadtmüller, Justus Raeppe, Stefan Schüssele, and Kerstin Pflieger. 2020. “Financing Coastal Resilience by Combining Nature-Based Risk Reduction with Insurance.” *Ecological Economics* 169(March): 106487. <https://doi.org/10.1016/j.ecolecon.2019.106487>.

Revolution Wind. 2023. “Gulf Coast Region Playing Leading Role in Buildout of U.S. Offshore Wind Industry, Including Work on First-Ever American-Built Offshore Wind Service Vessel.” <https://revolution-wind.com/news/2023/04/gulf-coast-region-playing-leading-role-in-buildout-of-us-offshore-wind-industry>.

Riley, K. L., L. C. Wickliffe, J. A. Jossart, J. K. MacKay, A. L. Randall, G. E. Bath, M. B. Balling, B. M. Jensen, and J. A. Morris, Jr. 2021. “An Aquaculture Opportunity Area Atlas for the U.S. Gulf of Mexico.” Beaufort, NC: National Oceanic and Atmospheric Administration. NOAA Technical Memorandum NOS NCCOS 299. <https://doi.org/10.25923/8cb3-3r66>.

Rodríguez-Rodríguez, D., D. A. Malak, T. Soukissian, and A. Sánchez-Espinosa. 2016. “Achieving Blue Growth Through Maritime Spatial Planning: Offshore Wind Energy Optimization and Biodiversity Conservation in Spain.” *Marine Policy* 73: 8–14. <https://doi.org/10.1016/j.marpol.2016.07.022>.

Sanchez Gomez, M., J. K. Lundquist, G. Deskos, S. R. Arwade, A. T. Myers, and J. F. Hajjar. 2023. “Wind Fields in Category 1–3 Tropical Cyclones Are Not Fully Represented in Wind Turbine Design Standards.” *JGR Atmospheres* 128(5): e2023JD039233. <https://doi.org/10.1029/2023JD039233>.

Schneemann, Jörg, Andreas Rott, Martin Dörenkämper, Gerald Steinfeld, and Martin Kühn. 2020. “Cluster Wakes Impact on a Far-Distant Offshore Wind Farm’s Power.” *Wind Energy Science* 5(1): 29–49. <https://doi.org/10.5194/wes-5-29-2020>.

Shaw, T. A., M. Baldwin, E. A. Barnes, R. Caballero, C. I. Garfinkel, Y. T. Hwang, C. Li, et al. 2016. “Storm Track Processes and the Opposing Influences of Climate Change.” *Nature Geoscience* 9(9): 656–664. <https://doi.org/10.1038/ngeo2783>.

Shields, Matt, Jeremy Stefek, Frank Oteri, Sabina Maniak, Matilda Kreider, Elizabeth Gill, Ross Gould, Courtney Malvik, Sam Tirone, and Eric Hines. 2023. *A Supply Chain Road Map for Offshore Wind Energy in the United States*. Golden, CO: National Renewable Energy Laboratory. NREL/TP-5000-84710. <https://www.nrel.gov/docs/fy23osti/84710.pdf>.

Skamarock, C., B. Klemp, J. Dudhia, O. Gill, Z. Liu, J. Berner, W. Wang, G. Powers, G. Duda, D. Barker, and X. Huang. 2021. *A Description of the Advanced Research WRF Model Version 4.3*. Boulder, CO: National Center for Atmospheric Research. NCAR/TN-556+STR. <https://doi.org/10.5065/1dfh-6p97>.

State of Louisiana. 2022. *Louisiana Climate Action Plan - Climate Initiatives Task Force Recommendations to the Governor*. [https://gov.louisiana.gov/assets/docs/CCI-Task-force/CAP/Climate\\_Action\\_Plan\\_FINAL\\_3.pdf](https://gov.louisiana.gov/assets/docs/CCI-Task-force/CAP/Climate_Action_Plan_FINAL_3.pdf).

Swiss Re. 2020. “Managing Offshore Wind Project Risk in Nat Cat-Prone APAC.” October 19, 2020. <https://corporatesolutions.swissre.com/insights/knowledge/managing-offshore-wind-project-risk-in-nat-cat-prone-APAC.html>.

Trowbridge, Matthew, Jennifer Lim, and Ashley Knipe. 2023. “Alternative Port Assessment to Support Offshore Wind: Final Assessment Report.” Oakland, CA: Moffatt & Nichol. <https://efiling.energy.ca.gov/GetDocument.aspx?DocumentContentId=83268&tn=248750>.

Vickery, P.J., D. Wadhera, L. A. Twisdale, and F. M. Lavelle. 2009. “United States Hurricane Wind Speed Risk and Uncertainty.” *Journal of Structural Engineering* 135(3): 301–320. [https://doi.org/10.1061/\(ASCE\)0733-9445\(2009\)135:3\(301\)](https://doi.org/10.1061/(ASCE)0733-9445(2009)135:3(301)).

Vineyard Wind 1. No date. “Nation’s first commercial-scale offshore wind project.” Vineyard Wind. Accessed May 9, 2023. <https://www.vineyardwind.com/vineyardwind-1>.

Walker, Keith, Neil Adams, Brian Gribben, Breanne Gellatly, Nicolai Gayle Nygaard, Andrew Henderson, Miriam Marchante Jiménez, et al. 2016. “An Evaluation of the Predictive Accuracy of Wake Effects Models for Offshore Wind Farms.” *Wind Energy* 19(5): 979–996. <https://doi.org/10.1002/we.1871>.

Wilkie, David, and Carmine Galasso. 2020. “A Probabilistic Framework for Offshore Wind Turbine Loss Assessment.” *Renewable Energy* 147(March): 1772–1783. <https://doi.org/10.1016/j.renene.2019.09.043>.

Wiser, Ryan, Mark Bolinger, Ben Hoen, Dev Millstein, Joe Rand, Galen Barbose, Naïm Darghouth, Will Gorman, Seongeun Jeong, Eric O’Shaughnessy, and Ben Paulos. 2023. *Land-Based Wind Market Report: 2023 Edition*. U.S. Department of Energy Office of Energy Efficiency and Renewable Energy. <https://www.energy.gov/eere/wind/articles/land-based-wind-market-report-2023-edition>.